Field Relations, Crystallization, and Petrology of Reversely Zoned Granitic Plutons in the Bottle Lake Complex, Maine

U.S. GEOLOGICAL SURVEY PROFESSIONAL PAPER 1320

Field Relations, Crystallization, and Petrology of Reversely Zoned Granitic Plutons in the Bottle Lake Complex, Maine

By Robert A. Ayuso

U.S. GEOLOGICAL SURVEY PROFESSIONAL PAPER **1320**

UNITED STATES GOVERNMENT PRINTING OFFICE, WASHINGTON: 1984

DEPARTMENT OF THE INTERIOR

WILLIAM P. CLARK, *Secretary*

U.S. GEOLOGICAL SURVEY

Dallas L. Peck, *Director*

Library of Congress Cataloging in Publication Data

Ayuso, Robert A.
Field relations, crystallization, and petrology of reversely zoned granitic plutons in the Bottle Lake Complex, Maine.

(Geological Survey professional paper ; 1320)
Bibliography: p.
1. Batholiths—Maine. 2. Granite—Maine. I. Title. II. Series.
QE461.A888 1984 552'.3 84-600000

**For sale by the Distribution Branch, U.S. Geological Survey,
604 South Pickett Street, Alexandria, VA 22304**

CONTENTS

ILLUSTRATIONS

TABLES

LIST OF GEOGRAPHIC LOCALITIES SHOWN ON PLATE 1

A	Almanac Mountain
B	Whitney Cove Mountains
C	Passadumkeag Mountain
D	Duck Mountain
E	Getchell Mountain
F	Topsfield facies
G	Tomah Mountain
H	Farrow Mountain
I	East Musquash Mountain
J	North Branch of Vickery Brook
K	Mount Delight
L	Pineo Mountains
M	Sysladobsis Lake Area
N	Whitney Cove
O	Pork Barrel Lake
P	Upper Sysladobsis Lake
Q	No. 3 Pond
R	Lombard Mountain
S	Bowers Mountain
T	Moose Mountain
U	Chain Lakes
V	Pug Lake
W	McLellan Cove
X	Chamberlain Ridge
Y	Hasty Cove
Z	Orie Lake
AA	Junior Lake
BB	Farm Cove
CC	East Musquash Lake
DD	Mud Cove

FIELD RELATIONS, CRYSTALLIZATION, AND PETROLOGY OF REVERSELY ZONED GRANITIC PLUTONS IN THE BOTTLE LAKE COMPLEX, MAINE

By ROBERT A. AYUSO

ABSTRACT

The Bottle Lake Complex is a composite batholith of Middle Devonian age that intrudes the core of the Merrimack synclinorium in east-central Maine. The batholith consists of the Whitney Cove and Passadumkeag River plutons. Both are granites and are petrographically and geochemically reversely zoned, having more mafic cores than rims. Primary sphene, magnetite, and abundant mafic xenoliths are characteristic of these plutons. The abundance and composition of amphibole, biotite, and plagioclase indicate that the most mafic rocks are concentrated in the core facies.

The bulk composition of granites in the Bottle Lake Complex is also reversely zoned, from high SiO_2 in the rim facies (71–77 weight percent) to low SiO_2 in the core facies (67–72 percent). Higher contents of Al_2O_3 (14–16.5), Fe_2O_3 (2.5–5.4), MgO (0.6–1.3), and TiO_2 (0.3–0.8) are characteristic of the core facies, compared to the abundance of Al_2O_3 (12.0–14.5), Fe_2O_3 (1.4–3.0), MgO (0–0.8), and TiO_2 (0.1–0.5) in the rim facies. Reverse zonation is also evident in the generally higher strontium, niobium, yttrium, and zirconium of the more mafic granites in the interior. Mafic xenoliths show more dispersed major and trace element variations compared to the host granites. Calculated biotite stabilities coupled with the granite minimum melting curve suggest that emplacement conditions were as follows: P=1–1.8 kbar, t=720–780°C, and f_{O_2} slightly higher than the Ni–NiO but lower than hematite-magnetite buffer equilibrium curve.

Reversely zoned plutons in the Bottle Lake Complex result from remobilization (resurgence) of the more mafic lower layers and of the accumulated and scavenged crystal mush into the upper, more felsic parts of the plutons modified by fractional crystallization (plagioclase, biotite, amphibole, apatite, zircon, magnetite-ilmenite). In the initial stages of evolution, each pluton was a convecting and chemically stratified system with more mafic granitic magma at the base. Periodic influxes of more mafic granitic magma resulted in mixing of liquids and redistribution of minerals. Surges of more mafic granitic magmas or venting of the magma chamber may have triggered the remobilization of the lower layers into the upper, more felsic layers. Mafic xenoliths and their host granites are not related by fractionation and probably represent foreign blocks obtained at depth.

Granite magmas in the Bottle Lake Complex were emplaced consecutively and were obtained from a compositionally variable source. The trend in isotopic composition becomes more radiogenic for strontium, lead, and oxygen from the Passadumkeag River to the Whitney Cove pluton. A volcaniclastic source (graywacke) that progressively became more continental in character accounts for the range of isotopic compositions in the Bottle Lake Complex. Although multiple injection of granite magmas occurred in the batholith, each pluton represents a closed geochemical system. Significant input of lead from reservoirs similar to the oceanic mantle, lower continental crust (granulite), or upper continental crust as represented by the metasediments are ruled out by the isotopic tracers.

INTRODUCTION

The granitic rocks of the Bottle Lake Complex provide an excellent environment for studying the field relations, petrography, and compositional distinctions within a composite batholith emplaced during the Acadian orogeny. The Bottle Lake Complex belongs to a group of Paleozoic intrusives forming a discontinuous trend that extends from coastal to north-central Maine (fig. 1). Plate 1 is a geologic map of the Bottle Lake Complex; letter symbols in parentheses are used herein to designate locations shown on the map.

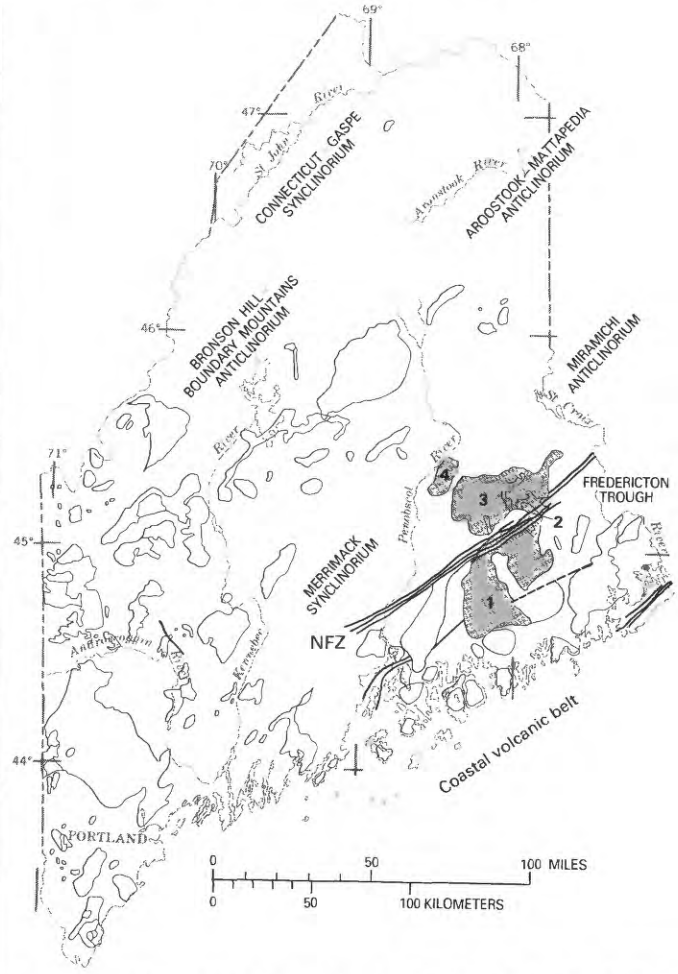

FIGURE 1.—Map of Maine showing the location of the Bottle Lake Complex and other plutons in the area. (1) Lead Mountain pluton; (2) Wabassus Quartz Monzonite; (3) Bottle Lake Complex, (4) Center Pond pluton. Traces of the Norumbega Fault Zone (NFZ) are also shown (modified from Louiselle and Ayuso, 1980).

Detailed mapping and routine petrographic studies show that each pluton within the Bottle Lake Complex exhibits reverse zonation. This feature contrasts with typical mineralogic and geochemical zoning trends in calc-alkaline plutons in which higher color index and more mafic rocks from the outer rim surround felsic rocks in the interior (see Pitcher, 1979a, b).

This report presents the results of detailed mapping, petrographic, and mineral chemistry studies of the Bottle Lake Complex. A brief summary of the results obtained from geochronologic (Rb–Sr, U–Pb), isotopic (common Pb), and geochemical (major and trace element abundances) studies (Ayuso, 1982) is also included because it supplements the field observations. Such observations place strong constraints on the sequence of intrusion, magmatic evolution accounting for the reverse zonation, and nature of the granitic sources within a Middle Devonian composite body.

METHODS OF STUDY

Because of limited access into the area, most of the field work consisted of pace-and-compass traverses to hilltops either from logging roads or from lakeshores. Hilltops are shallowly covered by glacial debris, soil, and vegetation, and outcrops are common. Outcrops along lakeshores are also common. In general, leucocratic granites are most exposed, and granites containing abundant mafic minerals have fewer exposures because they weather and disaggregate more readily. The mafic mineral-rich rocks are concentrated on the western lobe of the Bottle Lake Complex. Rocks of lower color index (lighter colored) are predominantly in the eastern lobe of the Bottle Lake Complex and form numerous outcrops.

Modal analyses of 150 granite samples (Ayuso, 1979, 1982) stained by the method of Boone and Wheeler (1968) were made in order to distinguish between plagioclase, quartz, alkali feldspar, and total mafic minerals (biotite, hornblende, sphene, allanite, and so on). Mafic minerals were later apportioned by examination of thin sections. Routine point counting consisted of selecting up to three slabs per sample with minimum dimensions of 20×20 cm and counting 1,000–2,000 points using mainly a 0.3×0.3-cm grid. This spacing was adequate for most rocks, especially the equidimensional granites. However, some of the slabs were smaller than statistically permissible for very coarse-grained rocks. The best estimate of the uncertainty in the modal analyses is ±2 percent using the method of Van der Plas and Tobi (1965).

Mineral compositions were determined using an automated ARL nine-channel electron microprobe with an operating voltage of 15 kilovolts, 0.150 nanoampere emission current, and 2- to 10-micrometer spot size. Silicate and oxide minerals were employed as standards, which were checked against the composition of known silicates. Corrections were made by the method of Bence and Albee (1968). Seventy samples were analyzed for feldspar, biotite, amphibole, oxide minerals, sulfides, apatite, allanite, and sphene. A minimum of 10 analyses were made in the essential minerals of each sample to detect variations within and between grains. Opaque and accessory phases were similarly analyzed in selected samples. The maximum compositional variation estimated by microprobe analyses is given by the standard deviation. For biotite, the results show the following maximum weight percent deviations: SiO_2 (0.6), Al_2O_3 (0.3), FeO (0.7), MgO (0.4), MnO (0.02), TiO_2 (0.1), CaO (0.1), Na_2O (0.1), K_2O (0.3), F (0.4), and Cl (0.03). Plagioclase cores and rims, averaged separately, show similar deviations: SiO_2 (0.4), Al_2O_3 (0.4), CaO (0.15), Na_2O (0.3), and K_2O (0.2). Finally, the typical variations in magnetite and ilmenite are as follows: magnetite, FeO (0.50), TiO_2 (0.15), and MnO (0.10); ilmenite, FeO (0.7), TiO_2 (0.6), and MnO (0.5).

Twenty alkali feldspar concentrates were homogenized (sanidinized) and analyzed by X-ray powder diffraction techniques (Wright, 1968) to estimate their bulk composition and structural state.

Analytical procedures of the X-ray fluorescence study followed the method of Norrish and Hutton (1969). Details and techniques concerning the geochronology and isotopic work on the Bottle Lake Complex are given in Ayuso and Arth (1983) and Ayuso (1982). Locations from which samples were used in this study are shown on plate 1.

ACKNOWLEDGMENTS

I am grateful to my assistants, S. T. Johnson and F. Bunky Wehr for their dedication. Special thanks are extended to D. R. Wones, who introduced me to the problems of granite petrogenesis and the geology of Maine. I am indebted to A. K. Sinha, whose steady criticism and pursuit of analytical excellence encouraged me throughout the study, and I thank M. C. Loiselle for helping during data collection and reduction and contributing in many stimulating discussions. I am especially grateful to my colleagues at Virginia Polytechnic Institute and State University: N. K. Foley, B. Hanan, J. D. Myers, and M. X. Wells for their encouragement and help. Many of the ideas expressed in this paper resulted from fruitful discussions with my colleagues at the Geological Survey. Comments of D. R. Wones, A. K. Sinha, D. A. Hewitt, F. D. Bloss, J. G. Arth, R. A. Bailey, W. F. Cannon, B. R. Lipin, R. L. Smith, and D. B. Stewart greatly improved the presentation and scientific content of the report.

PREVIOUS WORK

The area of this report is included within a reconnaissance map by Larrabee and others (1965), who established the extent of the granitic plutons and attempted a regional correlation of the stratigraphy of the country rocks. Contacts between the plutons and country rocks are generally better defined for the northern contact based on aeromagnetic (Doyle and others, 1961; Boucot and others, 1964) and geologic studies (Larrabee and others, 1965; Ayuso, 1979; Ayuso and Wones, 1980) than for the more inaccessible and swampy terrane of the southern contact.

Building on the pioneering effort by Larrabee and his coworkers, Ludman (1978a, b; 1981) presented a better understanding of the metamorphic rocks in the region concentrating on the area to the northeast and east of the Bottle Lake Complex. Detailed field work was done by Olson (1972), and reconnaissance mapping was done by Cole (1961) to the southwest and north of the Bottle Lake Complex, respectively.

Recent work in the area has indicated anomalously high contents of molybdenum, arsenic, tungsten, and bismuth in stream sediment samples near the granite-country rock contact near Tomah Mountain (G) (Nowlan and Hessin, 1972; Post and others, 1967). In conjunction with those reports, molybdenite in granite bedrock was also reported. Subsequent work by Otton and others (1980) indicated that uranium and thorium were also present in anomalously high concentrations in stream sediment samples and concluded that U-Mo mineralization was likely as a result of vein or contact-metasomatic processes. Not enough observations were made, however, to properly evaluate the economic potential of the Tomah Mountain (G) area.

PHYSICAL SETTING

The Bottle Lake Complex is located between the towns of Topsfield and Lincoln in one of the popular recreational areas of east-central Maine. The region is characterized by low relief, numerous lakes and swamps, and abundant glacial debris (fig. 2). Several hills are about 500 m high, for example, Almanac Mountain (A), Whitney Cove Mountains (B), Passadumkeag Mountain (C), Duck Mountain (D), and Getchell Mountain (E) (pl. 1). The Madagascal and the Passadumkeag Rivers are the major streams that dominate the drainage patterns in the area and connect extensive swamps (for example, 1000 Acre Heath). Mining and prospecting are notably absent in the region despite the concentration of pegmatites in several areas, the enrichment of sulfide minerals in the contact aureole between State Route 6 and the northern contact of the plutons (Doyle and others, 1961; Kleinkopf, 1960), and the potential for U-Mo mineralization near Tomah Mountain.

METAMORPHIC ROCKS

The Bottle Lake Complex intrudes greenschist facies metamorphic rocks of the Merrimack synclinorium. Country rocks are consistently low in metamorphic grade and show great differences in lithology and age (Larrabee and others, 1965; Olson, 1972; Ludman, 1978b). The age span represented by these rocks extends from Cambrian(?) to Devonian with diverse lithologies consisting of almost monomineralic sandstones to andesitic volcanics (Ludman, 1978b). Metasedimentary units generally show primary sedimentary features but have few fossils and are difficult to correlate regionally. Many faults occur between and within the metavolcanic and metasedimentary sections. All of these faults, however, are cut by the Bottle Lake Complex.

The oldest rocks intruded by the Bottle Lake Complex are Cambrian(?) to Ordovician(?) green and maroon slates, argillaceous quartzo-feldspathic sandstones, and quartz-granule conglomerates. Larrabee and others (1965) suggested the age on the basis of the similarity to the upper Proterozoic and Lower Cambrian(?) Grand Pitch Formation and to parts of the Ordovician Tetagouche Group in New Brunswick. Most units are thick bedded and exhibit penetrative cleavage and an early episode of isoclinal folding probably of pre-Acadian orogeny in age (Ludman, 1978b). This early folding episode was recognized only within these rocks.

FIGURE 2.—View from Almanac Mountain looking southeast toward the Bottle Lake Complex. Distance to the far hills, Whitney Cove Mountains, is about 15 km.

Mineral assemblages show zoning as a function of distance from the granite-country rock contact. Detailed traverses at right angles away from the pluton show zones of garnet, cordierite, and biotite hornfels. About 1 km from the contact, chlorite- and white-mica-bearing argillaceous quartzo-feldspathic sandstones are typical country-rock lithologies.

All of the rocks have tourmaline, epidote, calcite, sphene, and opaque minerals, as well as two feldspars. Albite (showing checkerboard texture) and alkali feldspar are subordinate in abundance to quartz and suggest that the source was igneous in character.

The Ordovician(?) or Silurian(?) metavolcanic and metasedimentary rocks form a band to the west of the Cambrian(?) and Ordovician(?) section. In addition, Ludman (1978a) also mapped a thinner but similar section south of East Musquash Lake (CC) and north of the Bottle Lake Complex in the Scraggly Lake and Waite quadrangles respectively (pl. 1). Volcanic rocks exposed south of East Musquash Lake (CC) consist of hornblende-bearing andesite interbedded with minor sedimentary and volcaniclastic sandstones (Ludman, 1978a), while pelitic to quartzose rocks showing graded and fine-scale bedding characerize the tourmaline-bearing metasedimentary rocks. Contact metamorphism is also evident in these rocks as noted by Cole (1961) and is indicated by the presence of garnet, cordierite, tremolite, and biotite as a function of distance from the plutonic contact. Garnet-cordierite hornfels are formed closest to the pluton and change to tremolite-epidote-biotite schists away from the contact.

Contiguous to the granite-country rock contact, felsic pods, which mineralogically consist of two feldspars and of muscovite, quartz, garnet, allanite and biotite, are sometimes present. These pods are irregularly shaped, small (10–20 cm), and consistently show similar mineralogy and cuneiform textures. Traces of relict and retrograded aluminosilicate(?) minerals and muscovite are concentrated within alkali feldspar. In contrast to the felsic pods, the host country rock consists of finer grained, garnet-cordierite hornfels which also contain white mica and biotite.

Silurian and Lower Devonian(?) rocks are designated as the Vassalboro Formation (Osberg, 1968) and are the most abundant country rocks intruded by the granites (pl. 1). Ruitenberg and Ludman (1978), Ludman (1978b), and Wones (1979) suggest that the Vassalboro Formation is correlative to the Flume Ridge Formation (as used by Ludman and Westerman, 1977) to the southeast, the Kellyland Formation to the northeast, and the Bucksport Formation (as used by Wing, 1959) to the southwest of the Bottle Lake Complex.

The Vassalboro is generally characterized in this area by calcareous siltstones interbedded with pelitic sediments. Changes in bedding style, calcareous nature, color, and grain size are common in hornfels around the plutonic rocks. In the vicinity of the northern contact, near No. 3 Pond (Q) in the Winn quadrangle, the Vassalboro is a pin-striped, shaly, slightly rusty, and intensely jointed rock. The stripes are generally centimeter-sized dark and light banks of contrasting mineralogy. Biotite-rich stripes are dark purple and alternate with light-colored stripes consisting of calcite and quartz. Throughout the rock, the assemblage diopside, amphibole, epidote, and quartz coexists with biotite and calcite. Contact metamorphism in these rocks occurs as garnet-cordierite-biotite hornfels formed close to the contact.

OTHER GRANITIC ROCKS IN THE REGION

At least three other Paleozoic granitic plutons in addition to the Bottle Lake complex are exposed in the area: the Center Pond pluton, the Lead Mountain pluton, and the Wabassus Quartz Monzonite (fig. 1; pl. 1). A brief summary of their characteristics is as follows. The Center Pond pluton was first studied by Larrabee and others (1965), but a more complete description is given in Scambos (1980). Field characteristics are given in Scambos (1980) and are summarized by Ayuso and Wones (1980), who noted the general similarity between the Passadumkeag River and Center Pond plutons. Although the Center Pond pluton is one of the smallest granites in this area (fig. 1), together with the Bottle Lake Complex it exhibits a characteristic mineral assemblage (from amphibole- to biotite-rich) as well as bulk compositional variations (from quartz diorite and quartz monzonite to granite) which may be used to distinguish granitic plutons intruding this part of the Merrimack synclinorium (Ayuso and others, 1980). As found in the Passadumkeag River pluton, the Center Pond pluton is cut by a right-lateral, northeast-trending fault zone.

The Lead Mountain pluton is a large (1,000 km^2), composite body in which granite is the predominant rock type. Exposures of this pluton are found directly south of the Bottle Lake Complex, within fault-bounded blocks, and as a large granitic mass extending south toward the Atlantic coast (fig. 1). Recent mapping suggests that the pluton has an extensive lithological range from amphibole- and biotite-bearing granite to biotite and muscovite granites. Petrographic contrast (abundance of mafic minerals, ratio of magnetite to ilmenite, rock type variation) between the Bottle Lake Complex and the Lead Mountain pluton, which lie on either side of the Norumbega fault, argue against correlation of the two granites.

The Wabassus Quartz Monzonite was first studied by Larrabee and others (1965) and is exposed only within

the blocks bounded by the Norumbega fault system (pl. 1) (Ayuso and Wones, 1980). Petrographic correlation with the Bottle Lake Complex or with the Lead Mountain pluton is not supported because the Wabassus is finer grained, more felsic, and texturally different from the other nearby plutons. Preliminary observations suggest that biotite is the predominant mafic phase. This rock is commonly exposed in intensely sheared and deformed outcrops that show only traces of the original mafic mineralogy and felsic assemblage.

THE BOTTLE LAKE COMPLEX

The granitic plutons of the Bottle Lake Complex are exposed in an area of about 1,100 km^2 in the Waite, Scraggly Lake, Springfield, Winn, Wabassus Lake, Nicatous Lake, and Saponac 15-minute quadrangles (pl. 1). The outline of the Bottle Lake Complex consists of two overlapping, subcircular intrusives arranged along an east-west trend, escept for the northeast extension of the eastern intrusive—the Topsfield facies (F).

The Bottle Lake Complex consists of the Passadumkeag River and Whitney Cove plutons. The Topsfield facies (F), which extends north of Mount Delight (K), is considered part of the Whitney Cove pluton because of the absence of sharp contacts between it and typical Whitney Cove rocks and because of similarity in petrographic characteristics. The two plutons are readily distinguished from each other by differences in mafic mineralogy (especially the ratio of biotite to amphibole), abundance of pegmatites and aplites, and abundance and types of inclusions (Ayuso, 1979).

The intrusives in the Bottle Lake Complex are characterized by generally coarse-grained granitic rocks that consist of two feldspars, biotite and quartz, primary sphene, magnetite, ilmenite, zircon, apatite, allanite, and pyrite. Hornblende is abundant only in the Passadumkeag River pluton, where it occurs primarily in rocks of high color index also containing numerous mafic xenoliths (fig. 3).

Larabee and others (1965) made no petrographic distinctions between the granitic rocks of the Bottle Lake Complex, except for the possibility of an internal contact between the Topsfield facies and the main mass of the Whitney Cove pluton. Petrographic variation in the granites was ascribed to secondary processes, principally to different degrees of country-rock assimilation.

The Bottle Lake Complex is probably of Middle Devonian age, and its component plutons may differ only slightly in age. Field observations show that the Whitney Cove pluton is cut by the Norumbega fault zone that disturbed Pennsylvanian sediments in southern New Brunswick (Wones and Stewart, 1976) but is younger than the Silurian to lower Devonian(?) country rocks it intrudes. Such structural and stratigraphic controls suggest that the Whitney Cove pluton must be older than Pennsylvanian and younger than Early Devonian.

Previous geochronologic work on the Whitney Cove pluton by Faul and others (1963) indicated ages of 377 and 379 m.y., according to the International Union of Geological Sciences (IUGS) constants (Steiger and Jager, 1977), by the K–Ar method. This finding is in good agreement with a linear whole-rock Rb–Sr isochron which resulted in an age of 379±10 (Ayuso and Arth, 1983). Zartman and Gallego (1979) suggested a zircon Pb–Pb age of 404±4 m.y. for a sample from the Topsfield facies, broadly in agreement with the range of 397 to 404 m.y. obtained by Ayuso (1982) on zircon samples from the main mass of the Whitney Cove pluton. Discordant zircons from the Whitney Cove pluton suggested a Concordia intercept age of 399±16 m.y., roughly similar to the Pb–Pb ages.

Samples from the Passadumkeag River pluton were not dated by the K–Ar method, but a linear whole-rock Rb–Sr isochron consisting of xenolith-poor samples yielded an age of 381±8 m.y. (Ayuso and Arth, 1983). U–Pb analyses of discordant zircons resulted in Concordia intercept ages of 388±10 m.y. for samples containing at least trace amounts of mafic xenoliths, while zircons from a large mafic xenolith gave ages of 415 and 117 m.y. The range of Pb–Pb ages in the Passadumkeag River pluton is from 374 to 406 m.y., while a range from 382 to 402 m.y. characterizes the mafic xenolith.

The presence of distinct zircon populations in samples from the Bottle Lake Complex noted by Ayuso (1982) does not support a straightforward interpretation of the U–Pb results. The youngest Pb–Pb age (374 m.y.) was obtained on a zircon fraction containing

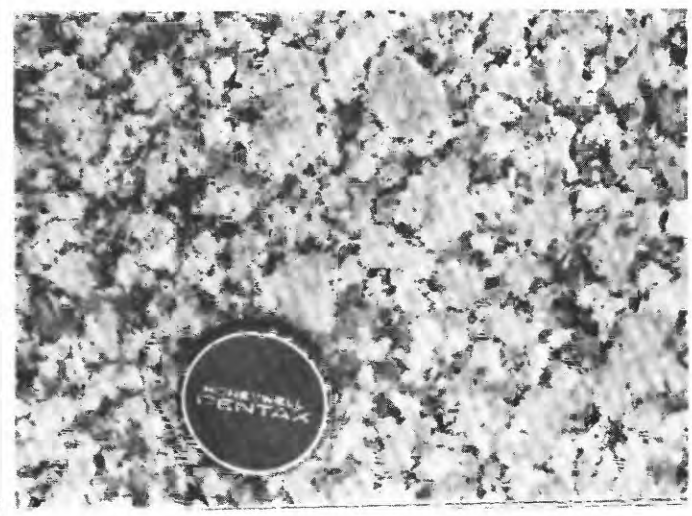

FIGURE 3.—Photograph showing the massive texture and coarse grain size prevalent in the Passadumkeag River pluton.

the least amount of the zircon type abundant in the mafic xenolith. Although the results from the whole-rock Rb–Sr and zircon U–Pb methods cannot be resolved because of analytical uncertainty, Ayuso and Arth (1983) suggest that the ages might reflect the inherited lead from older, discordant zircons of the mafic xenoliths that contaminated the newly developed zircons of the granitic magmas. Thus, although the Concordia intercept ages of the Passadumkeag River pluton suggest that it is younger than the Whitney Cove pluton, the crystallization ages obtained by the whole-rock Rb–Sr method are nearly the same for both plutons. Additional support for a slightly older age of the Whitney Cove pluton is given because the Passadumkeag River pluton is not cut by the fault zone that transects the Whitney Cove pluton and because rock types characteristic of the Passadumkeag River pluton intrude rocks typical of the Whitney Cove pluton.

THE WHITNEY COVE PLUTON

FIELD RELATIONS

The Whitney Cove pluton covers an area of 400 km^2 and is characteristically granitic in mineralogy (IUGS classification of Streickeisen, 1973). It is easily recognized in the field because of its relatively low abundance of ferromagnesian minerals and its lack of amphibole. Other typical features include abundance of aplites and pegmatites and scarcity of mafic xenoliths. Three units are included in this pluton: the Topsfield facies, the rim facies, and the core facies (pl. 1).

THE TOPSFIELD FACIES

The geologic map of the Whitney Cove pluton does not show a contact between the Topsfield and the rim facies because of the gradual petrographic change between the two. The best exposures of the Topsfield facies are on Tomah Mountain (G), Farrow Mountain (H), and East Musquash Mountain (I) (pl. 1). These mountains form a scarp along the western and northern boundaries of the Topsfield facies.

As Larrabee and others (1965) noted, granitic rocks exposed directly to the south of the mountains near the North Branch of Vickery Brook (J) progressively become more similar to the gray, coarser grained rocks typical of the rim facies exposed on Mount Delight (K).

The Topsfield facies (F) is characterized by severe shearing and jointing. Most outcrops consist of intensely weathered granitic rocks ranging in color from moderate pink (5R 7/4) to moderate red (5R 5/4), according to the Rock-Color Chart of the Geological Society of America (Goddard and others, 1948 (1951)). Grain size is medium to coarse and the color index is generally less than 5. Pink alkali feldspar and plagioclase are phenocrysts in a matrix of felsic minerals and biotite. Zircon, apatite, allanite, opaque oxides (magnetite), and pyrite are not abundant. Most rocks exhibit aggregates of epidote, chlorite, and opaque oxides instead of primary biotite. Feldspars are commonly replaced by sericite and epidote.

THE RIM FACIES

Despite the similarity in mineralogy across the pluton, the most distinctive feature that separates the two facies is the characteristic seriate texture of the rim. The rim facies of the Whitney Cove pluton typically consists of grayish-pink (5R 8/2) to moderate-pink (5R 7/4) rocks. They are medium to coarse grained. Hypidiomorphic and seriate textures are developed on rocks of low color index (fig. 4).

Two feldspars are present as phenocrysts, with alkali feldspar phenocrysts larger (up to 3.5 cm) and more abundant than plagioclase. Euhedral quartz phenocrysts (up to 1 cm) and distinctive pseudohexagonal biotite books are characteristic of the pluton as a whole. Matrix minerals include two feldspars, quartz, biotite, allanite, sphene, apatite, and zircon. The opaque phases consist of magnetite, ilmenite, and pyrite.

Magnificent outcrops are exposed in the Pineo Mountains (L) and in the Sysladobsis Lake area (M). Many of the outcrops contain aplites, pegmatites, granophyres, and quartz veins. Felsic dikes are variable in attitude and thickness and exhibit a tendency to subdivide and crisscross within individual outcrops.

Modal mineral analyses indicate that the rim facies is uniformly granitic in mineralogy (table 1). The average mineral content of alkali feldspar (40.2 percent), plagioclase (27.5 percent), quartz (28.1 percent), and the sum of the mafic minerals (biotite, opaque minerals, accessory minerals) (4.2 percent) attest to the felsic nature of this rock (Ayuso, 1979). Biotite is the predominant mafic phase, and the total abundance of the accessories and opaque minerals is characteristically less than 1 percent (figs. 4–5). Chlorite, epidote, and sericite have formed by alteration of biotite and plagioclase.

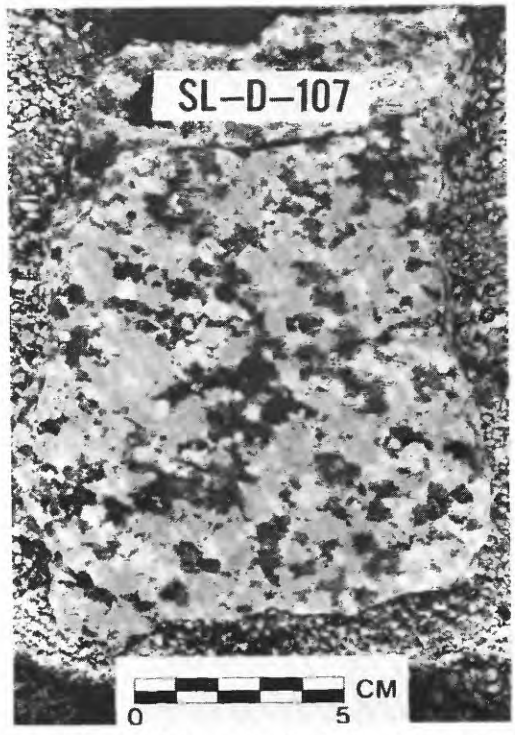

FIGURE 4.—Stained slab from the rim facies of the Whitney Cove pluton. Dark-gray areas are biotite, quartz, and accessory minerals. Alkali feldspar is light gray, and plagioclase is white.

THE CORE FACIES

The core facies of the Whitney Cove pluton is best exposed along the shores of Whitney Cove (N) in the Wabassus Lake and Scraggly Lake quadrangles (pl. 1). Contacts between the core and rim facies are mostly gradational and poorly exposed. Large outcrops showing both rock types are exposed near Pork Barrel Lake (O). Distinction between the two facies strongly depends on the development of the typically porphyritic texture of the core rocks (fig. 6).

Other characteristics of the core facies include the formation of a fine-grained matrix and the grayish-pink (5R 8/2) to grayish-orange-pink (10R 8/2) color. Large country-rock and quartz dioritic xenoliths are rare, but ovoidal clusters of fine-grained mafic minerals are more common. These clusters are small (up to 5 cm), widely disseminated, and consist principally of biotite with variable amounts of accessory minerals and plagioclase. The core facies typically has biotite as the predominant mafic phase in fine-grained clusters in the matrix and within the feldspars. Fine-grained biotite and feldspars impart a distinctive appearance to this facies.

Despite the overlap in modal abundances across the pluton, the core facies is distinguished from the rim facies by its enrichment in plagioclase and depletion in alkali-feldspar and quartz (fig. 5). Modal examination of stained slabs (table 1) and thin sections indicates the following average mineralogy: alkali feldspar, 33.9 percent; plagioclase, 35.8 percent; quartz, 25.6 percent; total mafic minerals including the opaque and accessory suites, 4.7 percent. The modal analyses show that the core facies is generally enriched in mafic minerals compared to the rim.

PETROGRAPHY AND MINERAL COMPOSITIONS

The Whitney Cove pluton contains accessory phases, oxides, and sulfides as subhedral to euhedral grains mainly within biotite or near small clusters formed by plagioclase and biotite. Apatite is an example of a mineral that appears optically homogeneous but which is chemically heterogeneous (for example, F and MnO, table 2). Heterogeneity is exhibited even within individual grains.

Allanite is common as large (up to 1.5 mm), euhedral, and optically and compositionally zoned grains intergrown with biotite and oxide minerals. Higher contents of titanium, iron, and in some cases flourine and calcium

TABLE 1.—*Average modal composition of plutons in the Bottle Lake Complex, Maine*
[Range is shown in parentheses]

Mineral	Whitney Cove pluton		Passadumkeag River pluton	
	Rim	Core	Rim	Core
Quartz	28.1 (20–48)	25.6 (20–31)	24.1 (22–30)	19.4 (13–29)
Plagioclase	27.5 (21–42)	35.8 (24–50)	30.0 (20–41)	37.6 (26–52)
Alkali feldspar	40.2 (29–55)	33.9 (24–53)	39.2 (28–50)	33.0 (20–46)
Biotite	4.2 (1–6)	4.7 (1–12)	4.6 (1–9)	5.8 (1–12)
Amphibole	0	0	2.1 (0–8)	4.2 (1–9)
Others (sphene, apatite, magnetite, ilmenite, zircon, allanite)	<0.5	<0.5	<0.5	<0.5

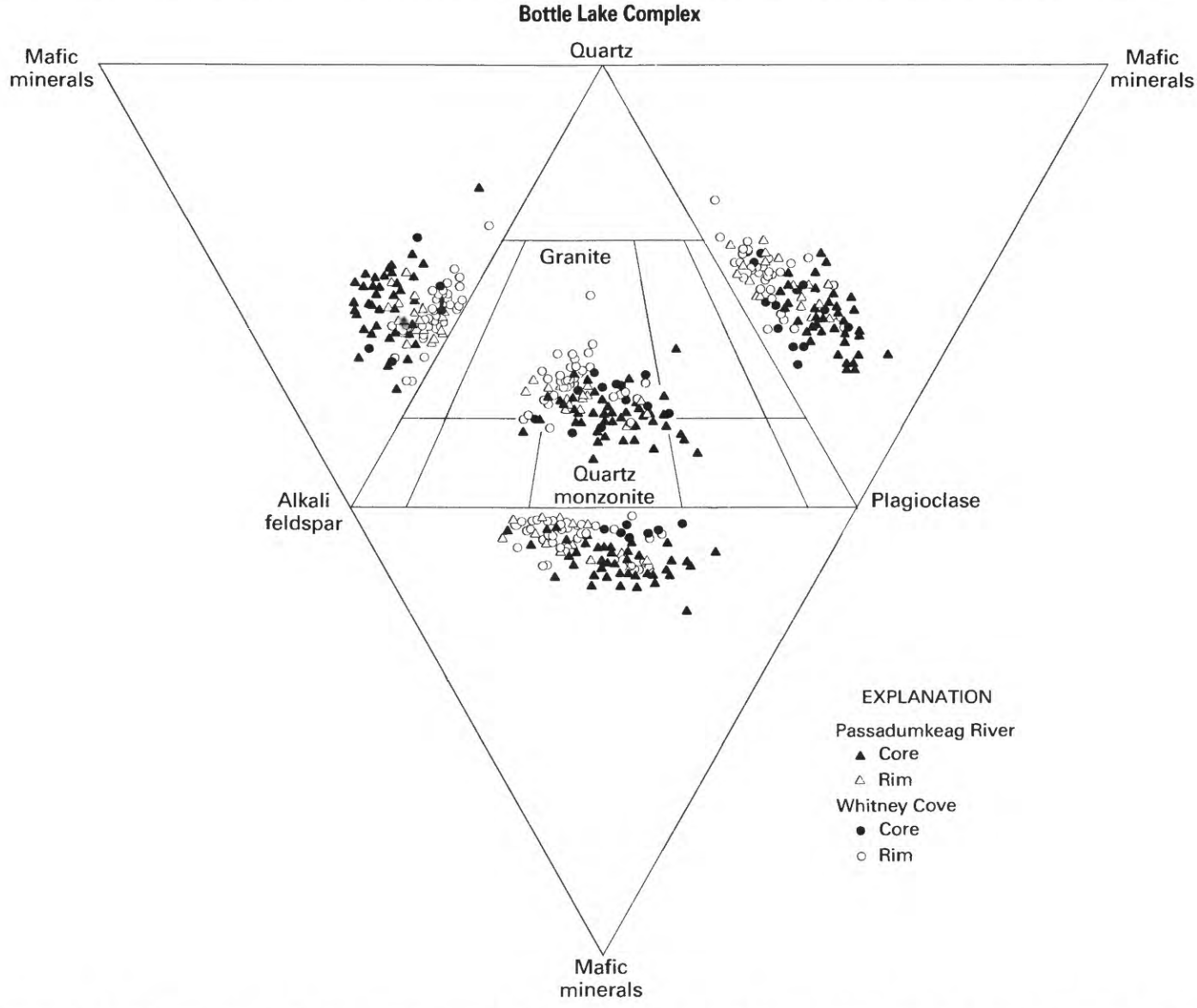

FIGURE 5.—Modal composition of the plutons of the Bottle Lake Complex. The four modal components illustrated are quartz, plagioclase, alkali feldspar, and the sum of the mafic minerals. Modal classification shown is from Streickeisen (1973).

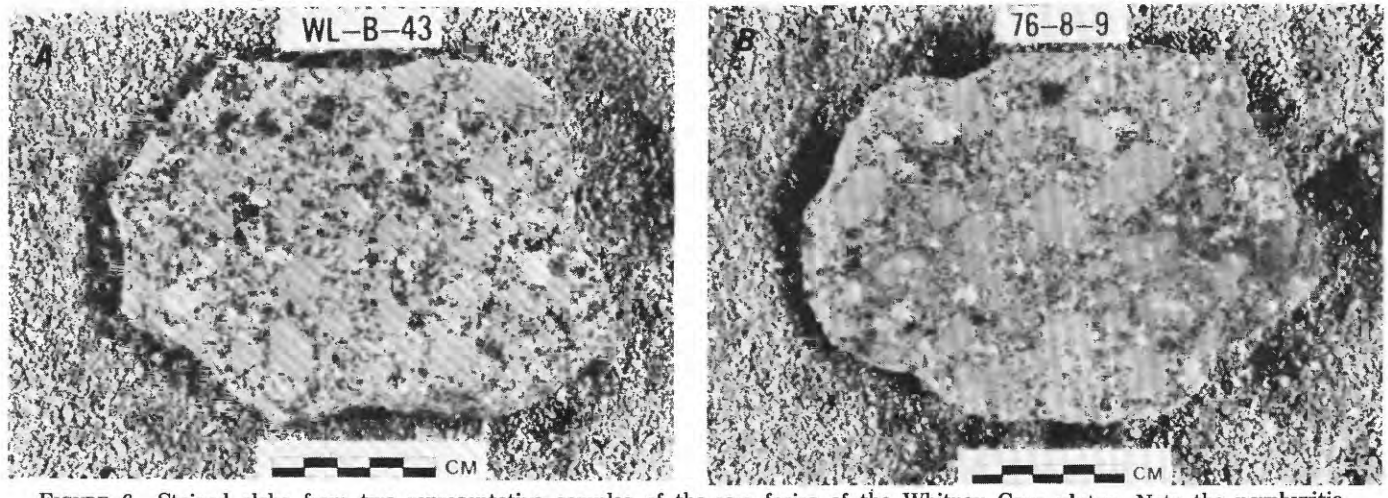

FIGURE 6.—Stained slabs from two representative samples of the core facies of the Whitney Cove pluton. Note the porphyritic character of this rock and the euhedral shapes of the alkali feldspar (light gray) and subhedral plagioclase (white).

are characteristic in the cores of allanite compared to lower phosphorus in the rims (table 2). Sphene occurs as large primary grains (up to 4 mm) and as a product of biotite breakdown. No clear and consistent trend exists in the abundance or in the mineral chemistry of any accessory phase across the Whitney Cove pluton (table 2).

Magnetite and ilmenite form subhedral grains within biotite, plagioclase, and allanite. Intergrowths between biotite and magnetite are also common as are the anhedral concentrations of magnetite along biotite lamellae. Magnetite abundances show no trend across the pluton, and compositionally they contain less than 1 weight percent TiO_2 (table 3). Rounded pyrite grains are found preferentially within magnetite grains. Granular ilmenite forms individual grains, coexists with magnetite, and also forms domains (Buddington and Lindsley, 1964) within it. Reequilibration of ilmenite at low temperature (Czamanske and Mihalik, 1972) is indicated by its manganiferous compositions (3.0 to 13.0 weight percent) (table 4). A trend is evident toward lower manganese in ilmenites of the rim facies of the pluton.

BIOTITE

Comparison of the chemical composition of biotite from the core and rim facies of the Whitney Cove pluton suggests that important contrasts exist within the granite (table 5). Biotite from the core facies is for the most part lower in the ratio of Fe/(Fe+Mg) (0.48–0.58) compared to the rim facies (0.52–0.71) (fig. 7; table 5). The total Fe content of biotite from core to rim facies is positively correlated with SiO_2 content of the rock (fig. 8). The core facies generally contains biotites with the lowest manganese content (fig. 7; table 5). Results indicate that despite the absence of a strong gradient in abundance of biotite from rim to core facies, biotite shows compositional zoning in Fe/(Fe+Mg) ratios which readily facilitates distinguishing between the marginal and the interior portions of the pluton (fig. 7; table 5).

The expected enrichment of titanium in early biotite and its correlation with higher phlogopite content (Robert, 1976; Czamanske and Wones, 1973) is not well developed in the Whitney Cove pluton (fig. 7). Biotites in the core facies contain about 0.19 to 0.23 Ti (atoms per 11 oxygens) and overlap with the range of 0.18 to 0.23 found in the rim facies (fig. 7; table 5). Corrosion and resorption of titanium-rich biotite suggest that early-crystallized biotites partially equilibrated with more felsic melt. The dispersal of titanium content is also evident in figure 8, where biotite composition is plotted against the silica content of the rock. Despite the clear distinction in the two facies for SiO_2, biotites have similar titanium abundance and show no progressive or systematic gradient from the margin toward the interior rocks (table 5).

Biotite from the Whitney Cove pluton shows no direct correlation between titanium and the silicon content (fig. 8) or between titanium and the mole fraction of iron in the octahedral layer (fig. 9). Similarly, no direct correlation exists between titanium content and the total abundance of the octahedral cations. However, the value for Fe/3 increases as a function of titanium within individual facies. Thus, biotite from the core facies has lower values for Fe/3 than those of the rim facies. At a given value of titanium, biotites from the core facies tend to be lower in Fe/3. (fig. 9).

Aluminum in octahedral coordination (Al^{VI}) is characteristically widely dispersed with increasing Fe/(Fe+Mg) ratios (fig. 7). Both the core and rim facies display a great deal of compositional scatter for Al^{VI} as well as for aluminum in tetrahedral coordination (Al^{IV}) (fig. 7). Al^{IV}, however, suggests a general increase as a function of the Fe/(Fe+Mg) ratio, so that higher Al^{IV} values for the rim facies in some cases are correlated with higher Fe/(Fe+Mg) ratios. The wide range in Al^{VI} content and in the Fe/(Fe+Mg) ratios in the Whitney Cove pluton suggests that these biotites record different conditions during their crystallization. In figure 10, the biotites from the core facies with the lowest Fe/(Fe+Mg) ratios tend to have higher abundance of Al^{VI} and coexist with the most calcic plagioclase. No correlations are evident between total aluminum and the alkali content of biotite in the pluton or between the sum of Al^{VI} and Ti with the ratio of Fe/(Fe+Mg). Total aluminum, Al^{IV}, and Al^{VI} in these biotites also lack meaningful correlations with the silica content of the rock.

Results for other constituents in biotites from the Whitney Cove pluton are summarized as follows:

- The iron content and the Fe/(Fe+Mg) ratio of biotite show the only systematic changes within the pluton. The iron content is directly related to the silica content of the rock (fig. 8). Higher iron in biotite is evident in rocks from the rim facies (table 5). Czamanske and others (1981) found decreasing or constant Fe/(Fe+Mg) ratios with increasing SiO_2 of the magnetite series granites in the Japanese batholith. According to Czamanske and others (1981), oxidation during magmatic differentiation resulted in such a trend. The generally decreasing Fe/(Fe+Mg) ratio in biotite toward the interior of the Whitney Cove pluton is generally correlated with decreasing SiO_2 of the rock (fig. 8), and thus suggests that oxidation during differentiation cannot account for the change in Fe/(Fe+Mg) ratios of the biotites.
- The potassium abundance in biotite shows no gradient between the core and rim facies (fig. 8).

TABLE 2.—*Representative electron microprobe analyses of allanite,*

[Values are weight percent. Total iron as FeO; for allanite, cols. 1-3 are from the Passadumkeag River pluton; cols. 4 and 5 are from the Whitney Cove pluton; for apatite, cols. 6-15 are

Column	1	2	3	4	5	6	7	8	9	10	11	12	13	14
Mineral	Allanite					Apatite								
Sample number	24C	25C	88R	49C	93R	20C	25C	29C	75C	89C	105C	10R	12R	27R
SiO_2	28.82	25.56	22.32	31.37	29.87	0.18	0.79	0.88	0.35	1.00	0.55	0.47	1.08	0.47
TiO_2	3.39	3.68	5.09	2.62	2.40	.06	.12	.06	.06	.00	.04	.00	.10	.07
Al_2O_3	16.98	12.48	15.08	12.52	11.27	.00	.00	.00	.00	.00	.00	.00	.00	.01
FeO	16.21	14.51	24.99	18.03	16.96	.50	.75	.61	.38	.97	.24	.64	.66	.26
MnO	.33	.44	.25	.43	.45	.08	.09	.10	.12	.20	.09	.17	.13	.12
MgO	.58	.50	.25	.92	1.31	.11	.12	.14	.04	.10	.12	.08	.11	.12
CaO	5.97	5.94	3.31	5.83	8.52	54.16	53.18	53.58	54.17	52.50	53.86	55.27	54.22	54.73
Na_2O	.12	.24	.44	.07	.10	.00	.00	.00	.00	.00	.00	.00	.00	.00
K_2O	.04	.07	.10	.03	.06	.10	.14	.08	.09	.00	.07	.00	.17	.05
BaO	.06	.13	.00	.06	.00	.00	.08	.00	.03	.00	.13	.06	.07	.13
P_2O_5	.53	.60	.00	.06	.00	40.66	40.09	40.28	39.58	41.14	40.25	38.96	40.23	39.68
SrO	.00	.00	.00	.00	.00	.00	.00	.00	.00	.00	.00	.00	.00	.00
F	.43	.49	.00	.27	.00	4.03	4.44	3.72	4.41	3.70	4.42	3.63	3.45	4.21
Cl	.02	.08	.00	.03	.00	.00	.01	.01	.01	.04	.01	.02	.00	.00
Total	73.48	64.72	71.83	72.26	70.94	99.88	99.81	99.46	99.24	99.65	99.78	99.30	100.22	99.85

- Manganese contents in biotites show a scattered but broadly increasing trend toward higher Mn content with increasing Fe/(Fe+Mg) (fig. 7); however, there is significant scatter for the felsic rim facies.
- Although fluorine is always present in biotite, it shows no obvious trend when plotted against the Fe/(Fe+Mg) ratio or the silica content of the rock (not shown).
- Sodium, chlorine, phosphorus, barium, and strontium in biotite show no gradients across the pluton. Generally, these elements fall below the microprobe detectability limit, or they exhibit random variations (table 5).

PLAGIOCLASE

Plagioclase was the first feldspar to crystallize in the Whitney Cove pluton. Several petrographic types are evident including plagioclase (1) as phenocrysts, (2) in the groundmass, (3) in clusters with biotite, and (4) concentrated along the edges of other felsic minerals.

Phenocrysts have distinct textures (kind and number of inclusions, associated contiguous mineralogy, resorption features), and optical characteristics (zoning, twinning), even though they show the same range in composition. At least two groups of phenocrysts are present. One group has a mottled appearance ("restite" according to White and Chappell, 1977), is characteristically blotchy in extinction, and consists of cores enclosing many inclusions with thin, optically continuous rims. These phenocrysts are generally associated with clusters of biotite and contrast with the other phenocryst group which is distributed throughout the rock, has a more regular optical and chemical zoning, has wider rims, and tends to show more euhedral habits. A gradient exists toward calcic-rich plagioclase from rim (An_{20}) to core (An_{55}) facies of the Whitney Cove pluton. The composition of plagioclase (table 6) across the pluton (fig. 10) agrees with the core to rim facies zoning suggested by the composition of biotite (table 5).

In general, phenocryst cores and mottled plagioclase grains overlap in composition and are distinctly more calcic than plagioclase in the matrix. Within any single specimen, however, average core compositions of the two textural types may differ by up to 10 mol percent anorthite. Inclusions of plagioclase in alkali feldspar are typically at least as calcic as the phenocryst cores, exhibit similar compositional ranges, and are characteristically rimmed by a band of sodic plagioclase. The most calcic grains are sometimes found as inclusions in other phases. They differ by about 3-5 mol percent anorthite from the most calcic phenocryst cores of nearby rocks.

Plagioclase cores are slightly zoned. Most zoning trends are in the normal fashion with a progressive decrease in calcium from core to rim generally becoming more albitic by about 5 mol percent anorthite. Strontium concentrations are highest in the cores (up to 0.3 weight percent) but fall below the microprobe detectability limit in the rims. Barium, phosphorous, and other oxides were generaly undetectable. Iron was consistently present (up to 0.3 weight percent) in many

apatite, and sphene from the Bottle Lake Complex, Maine

from the Passadumkeag River; cols. 16–26 are from the Whitney Cove; for sphene, cols. 27–31 are from the Passadumkeag River pluton; R and C represent rim and core facies, respectively]

15	16	17	18	19	20	21	22	23	24	25	26	27	28	29	30	31
Apatite												Sphene				
80R	37C	52R	53C	92C	58R	54R	57R	85R	94R	104R	107R	13C	22C	84C	105C	35R
0.67	0.42	0.50	0.41	1.85	0.32	0.52	0.44	0.65	0.59	0.46	0.59	29.86	30.61	31.12	30.95	30.18
.00	.00	.00	.00	.00	.00	.00	.00	.03	.00	.00	.00	34.35	32.25	33.24	33.80	31.69
.00	.00	.00	.00	.00	.00	.00	.00	.00	.00	.00	.00	2.06	2.78	2.13	2.05	2.67
.91	.39	.82	.61	1.58	.31	.64	.45	.40	.57	.68	.58	2.05	2.11	2.00	2.21	1.88
.14	.43	.13	.15	.19	.20	.16	.26	.22	.14	.27	.18	.19	.19	.17	.22	.26
.11	.10	.12	.07	.39	.06	.06	.08	.11	.10	.06	.10	.07	.13	.08	.11	.07
52.94	53.37	54.46	54.81	52.22	54.99	53.61	54.06	53.84	54.13	53.99	54.43	28.25	26.48	27.25	27.13	27.83
.04	.11	.00	.00	.00	.00	.00	.00	.00	.00	.00	.00	.02	.05	.03	.06	.05
.01	.03	.00	.00	.00	.00	.00	.00	.06	.00	.00	.00	.01	.02	.01	.02	.03
.00	.01	.03	.09	.02	.07	.08	.03	.06	.00	.06	.03	.02	.13	.10	.09	0
41.11	41.23	39.51	39.50	41.07	40.54	40.24	39.06	40.42	41.87	40.71	39.81	.04	.04	.03	.04	0
.04	.01	.00	.00	.00	.00	.00	.00	.00	.00	.00	.00	.04	.05	.04	0	0
3.90	4.15	3.35	3.56	3.57	3.58	3.40	3.68	4.10	3.34	3.91	3.65	.84	.87	.67	.80	0
.02	.02	.02	.01	.02	.02	.01	.01	.00	.01	.01	.02	.02	.01	.01	.01	0
99.89	100.27	98.94	99.21	100.91	100.09	98.72	98.07	99.89	100.75	100.15	99.39	97.82	95.72	96.88	97.49	94.66

phenocryst cores and rims. However, no compositional trend was evident.

The composition of plagioclase in contact with large, euhedral biotite is typically calcic, normally within the compositional range of the phenocryst cores. In contrast, the composition of plagioclase touching matrix quartz is characteristically sodic (An_{13}–An_{19}), typical of phenocryst rims and matrix plagioclase. The compositional range typical of granulated plagioclase in the mafic mineral-poor mortar (granular) texture is An_2 to An_{14}.

Groundmass plagioclase forms subhedral grains up to about 0.5 cm with an average composition of An_{20}. Clusters of ferromagnesian minerals and plagioclase consist of large, stubby, mottled phenocrysts, and finer grained plagioclase which is compositionally similar to the groundmass. The most sodic plagioclase (An_2) is found in the fine-grained matrix of the aplites and in the grains forming selvages (mortar texture) around other felsic minerals.

QUARTZ

Quartz forms inclusions near the rims of plagioclase phenocrysts and euhedral grains within alkali feldspar. It is also present as subhedral to euhedral grains in the matrix suggesting that it crystallized before alkali feldspar. Within the core of the pluton, quartz forms euhedral phenocrysts that in places coalesce to form clusters. Undulose extinction is a characteristic feature except near the faults where much of the quartz is completely annealed.

ALKALI FELDSPAR

Alkali feldspar encloses all other phases, indicating that it crystallized late in the sequence. Microcline twins are commonly developed in the pluton, and these generally are embayed by perthite patches. Rapakivi (viborgite) texture is usually evident in most exposures. Alkali feldspar ranges in composition from Or_{85} to Or_{98}, and its structural state resembles maximum microcline according to the scheme of Wright (1968) and Wright and Stewart (1968). Compositional zoning was not detected, although the composition of the albitic rims in the rapakivi texture ranged from almost pure Ab to Ab_{89}–An_{11}. No gradients are evident across the pluton, probably because the consistently high orthoclase content is indicative of substantial deuteric alteration. Alkali feldspar, however, was also out of equilibrium prior to the deuteric stage as indicated by the corroded and embayed alkali feldspar cores, by the intricate and irregular intergrowths of alkali feldspar and biotite, and by the irregular widths of the albite rims in the rapakivi texture. Edges shared by alkali feldspar and plagioclase show myrmekitic textures in which growth proceeded at the expense of plagioclase. Granophyre textures are for the most part constrained to between contiguous alkali feldspar grains.

SEQUENCE OF CRYSTALLIZATION

In accordance with the above observations, figure 11 presents a generalized crystallization sequence of the Whitney Cove pluton. Crystallization was initiated by

TABLE 3.—*Representative electron microprobe analyses of structural formulae of magnetite from the Bottle*

[Calculated per four oxygen atoms; total iron as FeO; cols. 1-12 are from the Passadumkeag River pluton; cols. 13-20 are from the Whitney Cove pluton; R and

Column	1	2	3	4	5	6	7	8	9	10	11	12	13
Sample number	5C	13C	17C	28C	36C	78C	8R	12R	23R	74R	80R	109R	44C
							Weight percent						
SiO_2	0.16	0.15	0.13	0.15	0.08	0.16	0.13	0.18	0.19	0.12	0.04	0.12	0.05
TiO_2	.14	.11	.25	.15	.22	.75	.21	.28	.07	.18	.17	.25	.25
Al_2O_3	.03	.09	.03	.13	.08	.01	.03	.03	.03	.06	.05	.05	.10
FeO	91.47	89.65	91.31	90.91	91.49	89.67	91.48	90.68	89.04	90.87	90.40	90.65	91.46
MnO	.17	.14	.12	.18	.19	.16	.12	.19	.15	.17	.15	.21	.25
MgO	.00	.01	.00	.00	.05	.00	.04	.06	.00	.01	.07	.01	.01
CaO	.11	.16	.14	.15	.15	.16	.14	.12	.12	.13	.13	.11	.20
Na_2O	.00	.00	.00	.01	.02	.01	.00	.00	.01	.00	.00	.00	.00
K_2O	.05	.05	.06	.05	.06	.07	.08	.04	.05	.06	.05	.06	.07
BaO	.11	.09	.10	.12	.28	.05	.10	.09	.06	.03	.17	.11	.22
Total	92.24	90.45	92.14	91.85	92.62	91.04	92.33	91.67	89.62	91.63	91.23	91.57	92.61
							Number of atoms						
Si	0.006	0.006	0.005	0.006	0.003	0.006	0.005	0.007	0.004	0.005	0.002	0.005	0.002
Ti	.004	.003	.007	.004	.007	.022	.006	.008	.002	.005	.005	.007	.007
Al	.001	.004	.001	.006	.003	.001	.001	.001	.001	.003	.002	.007	.005
Fe	2.964	2.961	2.961	2.955	2.953	2.928	2.960	2.959	2.974	2.962	2.965	2.957	2.953
Mn	.006	.005	.004	.006	.007	.005	.004	.006	.005	.006	.005	.007	.008
Mg	.000	.000	.000	.000	.002	.000	.002	.004	.000	.000	.004	.000	.001
Ca	.005	.007	.006	.006	.007	.007	.006	.005	.005	.005	.006	.005	.008
Na	.000	.000	.000	.001	.000	.001	.000	.000	.001	.000	.000	.000	.000
K	.003	.003	.003	.003	.002	.004	.004	.002	.003	.003	.003	.003	.003
Ba	.002	.001	.002	.002	.005	.001	.002	.001	.001	.001	.003	.002	.003

TABLE 4.—*Representative electron microprobe analyses and structural formulae of ilmenite from the Bottle*

[Structural formlae calculated for three oxygen atoms; total iron as FeO; R and C represent rim and core facies, respectively; cols. 1-15 are from the Passadumkeag

Column	1	2	3	4	5	6	7	8	9	10	11	12	13
Sample number	3C	4C	5C	17C	26C	28C	78R	111C	8R	12R	23R	74R	80R
							Weight percent						
SiO_2	0.07	0.12	0.05	0.09	0.10	0.08	0.10	0.06	0.10	0.13	0.11	0.11	0.06
TiO_2	51.10	49.54	50.43	51.37	49.37	50.31	49.74	50.07	48.68	51.27	50.44	49.43	50.88
Al_2O_3	.00	.00	.00	.00	.00	.00	.00	.00	.00	.00	.00	.00	.00
FeO	43.86	44.49	42.63	43.32	44.70	42.75	44.75	40.21	45.46	41.94	43.45	41.35	39.38
MnO	4.27	4.41	5.64	4.94	3.90	6.91	4.41	8.47	5.06	5.44	5.82	7.95	8.37
MgO	.03	.08	.03	.03	.04	.03	.04	.02	.08	.08	.05	.02	.06
CaO	.11	.09	.12	.13	.15	.11	.16	.10	.15	.10	.18	.12	.12
Na_2O	.00	.01	.02	.00	.01	.00	.00	.01	.00	.00	.01	.01	.00
K_2O	.04	.03	.05	.07	.04	.06	.05	.05	.04	.04	.04	.05	.03
BaO	.23	.24	.26	.27	.23	.21	.20	.21	.15	.25	.22	.24	.25
Total	99.71	99.01	99.23	100.22	98.54	100.46	99.45	99.20	99.72	99.25	100.32	99.28	99.15
							Number of atoms						
Si	0.002	0.003	0.001	0.003	0.003	0.002	0.003	0.002	0.003	0.003	0.003	0.003	0.001
Ti	.980	.963	.974	.980	.965	.964	.963	.969	.945	.985	.967	.960	.981
Al	.000	.000	.000	.000	.000	.000	.000	.000	.000	.000	.000	.000	.000
Fe	.936	.961	.916	.920	.971	.911	.963	.865	.982	.896	.926	.893	.844
Mn	.092	.096	.123	.106	.086	.149	.096	.185	.111	.118	.126	.174	.182
Mg	.015	.003	.001	.002	.002	.001	.002	.001	.003	.003	.002	.001	.002
Ca	.003	.003	.003	.004	.005	.003	.004	.003	.004	.003	.005	.003	.003
Na	.000	.000	.001	.000	.001	.000	.000	.001	.000	.000	.001	.001	.000
K	.001	.001	.001	.003	.001	.002	.002	.002	.001	.001	.001	.001	.001
Ba	.003	.002	.003	.003	.002	.002	.002	.002	.002	.003	.002	.002	.003

Lake Complex, Maine
C represent rim and core facies, respectively]

14	15	16	17	18	19	20
52C	92C	43R	53R	57R	107R	108R
0.06	0.18	0.19	0.25	0.33	0.33	0.10
.17	.62	.29	.12	.49	.28	.14
.12	.01	.00	.07	.21	.21	.00
91.10	91.16	89.65	90.81	89.46	88.57	90.71
.23	.32	.15	.12	.21	.30	.22
.00	.07	.00	.08	.08	.02	.02
.14	.13	.12	.14	.14	.12	.13
.00	.00	.01	.01	.00	.01	.00
.05	.04	.05	.05	.06	.05	.06
.24	.07	.03	.06	.24	.19	.11
92.11	92.60	90.49	91.71	91.22	90.08	91.49
0.002	0.007	0.008	0.010	0.013	0.013	0.004
.005	.018	.009	.004	.014	.008	.004
.006	.001	.000	.004	.010	.010	.000
2.959	2.928	2.956	2.952	2.909	2.922	2.967
.008	.010	.005	.004	.007	.010	.007
.000	.004	.000	.005	.005	.001	.001
.006	.005	.005	.006	.006	.005	.005
.000	.000	.005	.001	.000	.001	.000
.003	.002	.003	.003	.003	.003	.003
.004	.001	.001	.001	.004	.003	.002

Lake Complex, Maine
River pluton; cols. 16-21 are from the Whitney Cove pluton]

14	15	16	17	18	19	20	21
109R	114R	44C	92C	43R	53R	93R	108R
0.06	0.06	0.02	0.14	0.11	0.20	0.28	.08
49.98	47.56	48.96	48.71	51.91	49.07	52.12	51.28
.00	.01	.02	.00	.00	.00	.02	.00
42.19	44.15	42.26	36.20	35.32	38.38	35.51	40.83
6.14	7.11	8.11	13.37	10.46	10.92	10.15	7.61
.03	.04	.03	.06	.00	.08	.02	.10
.10	.26	.26	.23	.14	.17	.30	.14
.00	.01	.00	.00	.00	.00	.02	.01
.04	.05	.05	.05	.04	.05	.04	.06
.22	.49	.46	.28	.26	.25	.26	.24
98.76	99.74	100.17	99.04	98.24	99.12	98.72	100.35
0.002	0.002	0.001	0.004	0.003	0.005	0.017	.002
.971	.932	.949	.950	.999	.954	.998	.977
.000	.000	.001	.000	.000	.000	.001	.000
.912	0.962	0.911	0.785	0.762	0.830	0.756	.865
.134	.132	.177	.293	.227	.239	.219	.163
.001	.001	.001	.002	.000	.004	.001	.004
.003	.007	.007	.006	.004	.005	.009	.004
.000	.000	.000	.000	.000	.000	.001	.001
.001	.002	.002	.002	.001	.002	.001	.002
.003	.005	.005	.003	.003	.003	.003	.002

precipitation of the accessory phases generally in this order: zircon plus apatite, followed by oxides plus sulfides, and by allanite plus sphene. Biotite was the next phase to crystallize followed by plagioclase, quartz, and alkali feldspar.

SUMMARY OF THE BULK CHEMISTRY

The preceding sections demonstrated that the Whitney Cove pluton was zoned mineralogically, texturally, and in the composition of its constituent minerals (Ayuso and others, 1982a). This zoning is also evident in the bulk composition of the granites from the rim and core facies (table 7). A summary of the geochemical characteristics follows in this section.

The general gradient from core to rim facies occurs with decreasing CaO, MgO, Fe_2O_3, TiO_2, Al_2O_3, and P_2O_5 as SiO_2 increases from 67.0 to 77.0 weight percent (fig. 12). These marked differences across the pluton take place at a uniform total alkali element abundance. Normative compositions are corundum-poor for the pluton as a whole (table 7), but the sum of normative felsic minerals is highest in the rim facies.

The most important observation derived from the bulk compositional change in the Whitney Cove pluton is that with the exception of the K_2O content, there is remarkable compositional colinearity from the margins to the interior (fig. 12). Compared to the mafic xenolith suite, the Whitney Cove pluton is more silicic. Rocks from near the trace of the major fault cutting the pluton generally also plot within the variation shown by the granite as a whole.

Preliminary trace element determinations (U, Th, Pb, Rb, Sr, Y, Sc, Cr, Ta, Hf, Cs, Ba, Zr, and the rare earth elements) show irregular gradients within the pluton, except for the strong and consistent variations in zirconium, strontium, and niobium (table 7). These three elements support the distinction between each facies and the geochemical zonation from core to rim. Higher abundances of strontium, zirconium, and niobium are concentrated in the interior of the Whitney Cove pluton. Rubidium shows no definite trend from core to rim facies. Barium and yttrium are somewhat lower in the most siliceous rocks but do not clearly separate the two facies.

The process of fractional crystallization was evaluated using the least-squares computer program of Wright and Doherty (1970) for the major elements and the program developed by J. G. Arth (U.S. Geological Survey) for the trace elements in order to identify and quantify a fractionating assemblage capable of yielding the observed petrographic and bulk compositional variations. Ayuso (1982) suggested that crystallization

TABLE 5.—*Representative electron microprobe analyses and structural formulae of biotate from the Whitney Cove pluton*

[Calculated per 11 oxygen atoms; total iron as FeO; R and C represent rim and core facies, respectively; nd, not determined]

Column	1	2	3	4	5	6	7	8	9	10	11	12	13	14	15	16
Sample number	37C	44C	49C	51C	52C	58C	92C	41R	53R	54R	57R	85R	94R	104R	106R	107R
								Weight percent								
SiO_2	36.66	37.05	36.88	36.90	37.65	37.57	37.20	35.51	37.98	37.15	37.23	38.16	36.78	35.94	36.85	37.81
TiO_2	3.37	3.32	4.11	3.87	3.85	3.79	4.07	3.94	3.57	3.77	3.12	3.90	3.85	3.16	3.50	3.40
Al_2O_3	14.92	14.92	14.34	14.05	14.42	14.14	14.05	13.31	14.01	13.93	15.23	14.47	13.28	14.70	13.95	13.93
FeO	20.18	18.72	21.89	20.78	21.10	21.89	21.04	26.02	20.94	23.67	23.52	20.99	24.42	24.62	21.04	20.93
MnO	.63	.43	.59	.53	.60	.61	.63	.65	.63	.64	.72	.55	.52	.77	.55	.62
MgO	9.48	11.28	8.94	9.92	9.49	9.72	9.67	6.25	10.29	8.31	7.61	10.84	7.91	7.74	9.95	10.40
CaO	.05	.07	.05	.10	.13	.08	.04	.04	.09	.08	.06	.00	.04	.04	.04	.06
Na_2O	.18	.09	.10	.14	.09	.11	.11	.08	.08	.17	.10	.00	.11	.21	.11	.07
K_2O	9.36	9.42	9.59	9.18	9.15	9.45	9.44	9.26	9.73	9.40	9.43	9.91	9.28	9.35	9.28	9.55
BaO	.22	.23	.29	.36	.18	.19	.33	.20	.23	.20	.29	.25	.23	.36	.25	.17
P_2O_5	.00	.00	.00	.00	.00	.00	.00	.00	.00	.00	.00	.00	.00	.00	.00	.00
SrO	.00	.00	.00	.00	.00	nd	.00	nd	.00	.00	.00	.00	.00	.00	.00	.00
F	1.81	1.25	1.51	1.43	.59	1.17	1.28	1.10	1.38	.99	.91	1.20	1.58	3.50	1.60	1.38
Cl	.09	.04	.06	.06	.06	.05	.06	.10	.09	.11	.09	.07	.10	.08	.07	.09
Total	96.95	96.82	98.35	97.32	97.31	98.77	97.92	96.46	99.02	98.42	98.31	100.34	98.10	100.47	97.19	98.41
								Number of atoms								
Si	2.77	2.78	2.77	2.79	2.84	2.81	2.80	2.79	2.82	2.81	2.81	2.79	2.81	2.68	2.79	2.82
Ti	.19	.19	.23	.22	.22	.21	.23	.23	.20	.21	.18	.21	.22	.18	.20	.19
Al	1.33	1.32	1.27	1.25	1.28	1.24	1.25	1.23	1.23	1.24	1.36	1.25	1.19	1.29	1.24	1.23
Fe	1.28	1.17	1.38	1.31	1.33	1.37	1.32	1.71	1.30	1.50	1.49	1.28	1.56	1.54	1.33	1.31
Mn	.04	.03	.04	.03	.04	.04	.04	.04	.04	.04	.05	.03	.03	.05	.04	.04
Mg	1.07	1.26	1.00	1.12	1.07	1.08	1.08	.73	1.14	.94	.86	1.18	.90	.96	1.12	1.16
Ca	.00	.01	.00	.01	.01	.01	.00	.00	.01	.01	.01	.00	.00	.00	.00	.01
Na	.03	.01	.01	.02	.01	.02	.02	.01	.01	.03	.01	.00	.02	.03	.02	.01
K	.90	.90	.92	.88	.88	.90	.91	.93	.92	.91	.91	.93	.90	.89	.91	.92
Ba	.01	.01	.01	.01	.01	.01	.01	.01	.01	.01	.01	.01	.01	.01	.01	.01
P	.00	.00	.00	.00	.00	.00	.00	.00	.00	.00	.00	.00	.00	.00	.00	.00
Sr	.00	.00	.00	.00	.00	nd	.00	nd	.00	.00	.00	.00	.00	.00	.00	.00
F	.43	.30	.36	.34	.14	.28	.30	.27	.32	.24	.22	.28	.38	.83	.39	.33
Cl	.01	.01	.01	.01	.01	.01	.01	.01	.01	.01	.01	.01	.01	.01	.01	.01
Fe/(Fe+Mg)	.54	.48	.58	.54	.55	.56	.55	.70	.53	.61	.63	.52	.63	.62	.54	.53

of 19 percent of the liquid in equilibrium with 13 percent plagioclase, 5 percent biotite, 0.5 percent apatite, and 0.5 percent magnetite-ilmenite accounted for some of the bulk chemical variation from representative rocks from the core and rim facies. The overall bulk chemical and petrographic variation of the internal subdivisions fo the Whitney Cove pluton, however, cannot be explained by fractionation. In addition, the occurrence of more mafic granitic rocks in the interior of the pluton may be suggested to reflect processes other than fractional crystallization.

THE PASSADUMKEAG RIVER PLUTON

FIELD RELATIONS

The Passadumkeag River pluton is exposed in an area of about 700 km^2. It consists of rock types ranging in mineralogy from granite to quartz monzonite and shows an obvious change toward darker (more mafic-mineral-rich) rocks toward the interior. Euhedral, black hornblende is a distinctive feature of the pluton as is a high abundance of mafic xenoliths. The Passadumkeag River pluton consists of the rim and core facies (pl. 1).

THE RIM FACIES

Rocks forming the rim facies are grayish pink (5R 8/2) to grayish-orange pink (10R 8/2). They are typically granitic in mineralogy (IUGS classification of Streickeisen, 1973) and show textures ranging from porphyritic to equidimensional. The outcrop pattern of this facies suggests that it is variable in width. Near the area north of Upper Sysladobsis Lake (P) (Springfield quadrangle), the rim facies is widest, but to the west, in the area near No. 3 Pond (Q) (Winn quadrangle), it is absent (pl. 1).

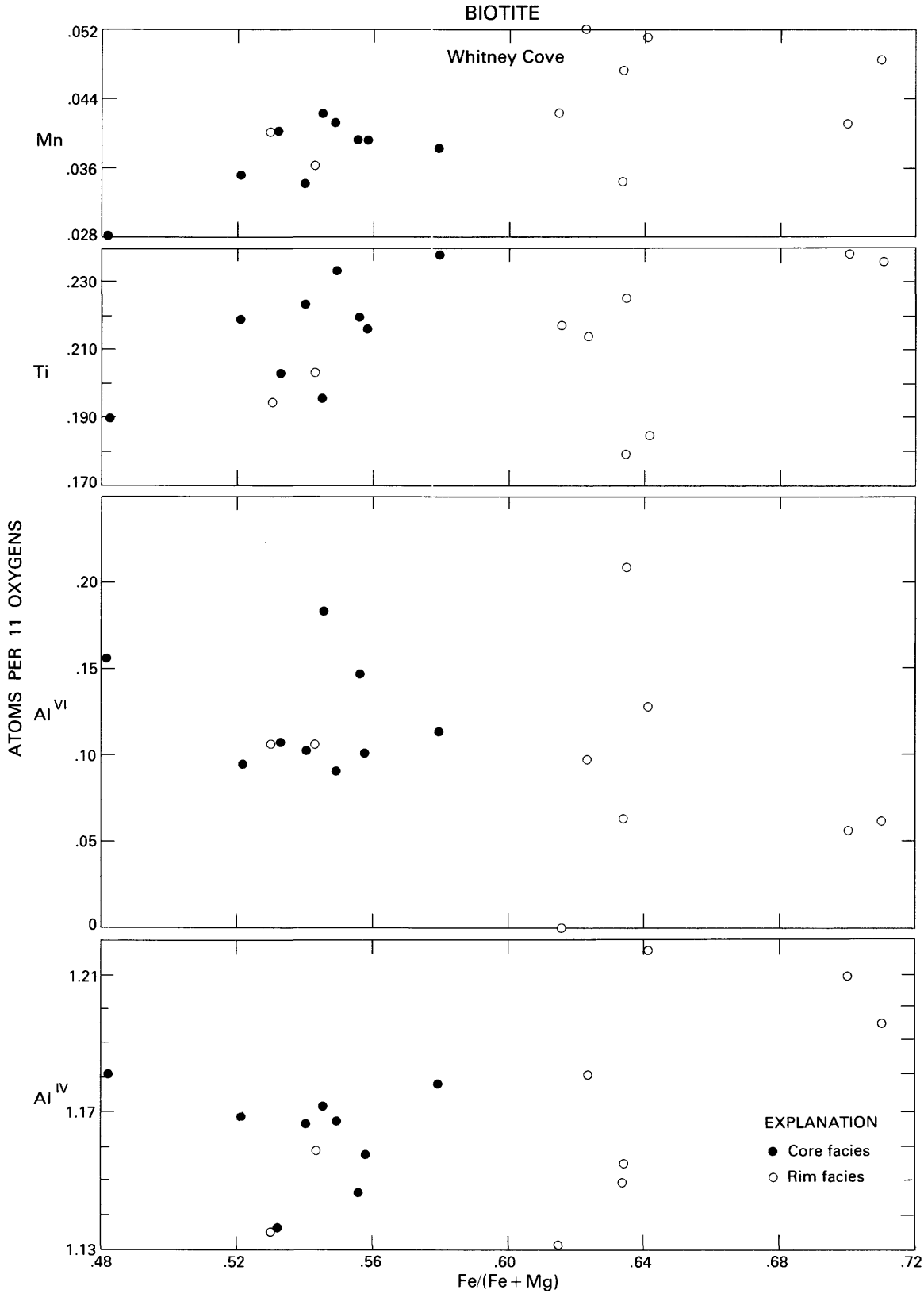

FIGURE 7.—Compositions of biotite in the Whitney Cove pluton as a function of Fe/(Fe+Mg). Each symbol represents the average obtained on at least 10 grains per sample. Note the different Fe/(Fe+Mg) ratios of biotite from each facies of the pluton. See table 5 for specific titanium and manganese values.

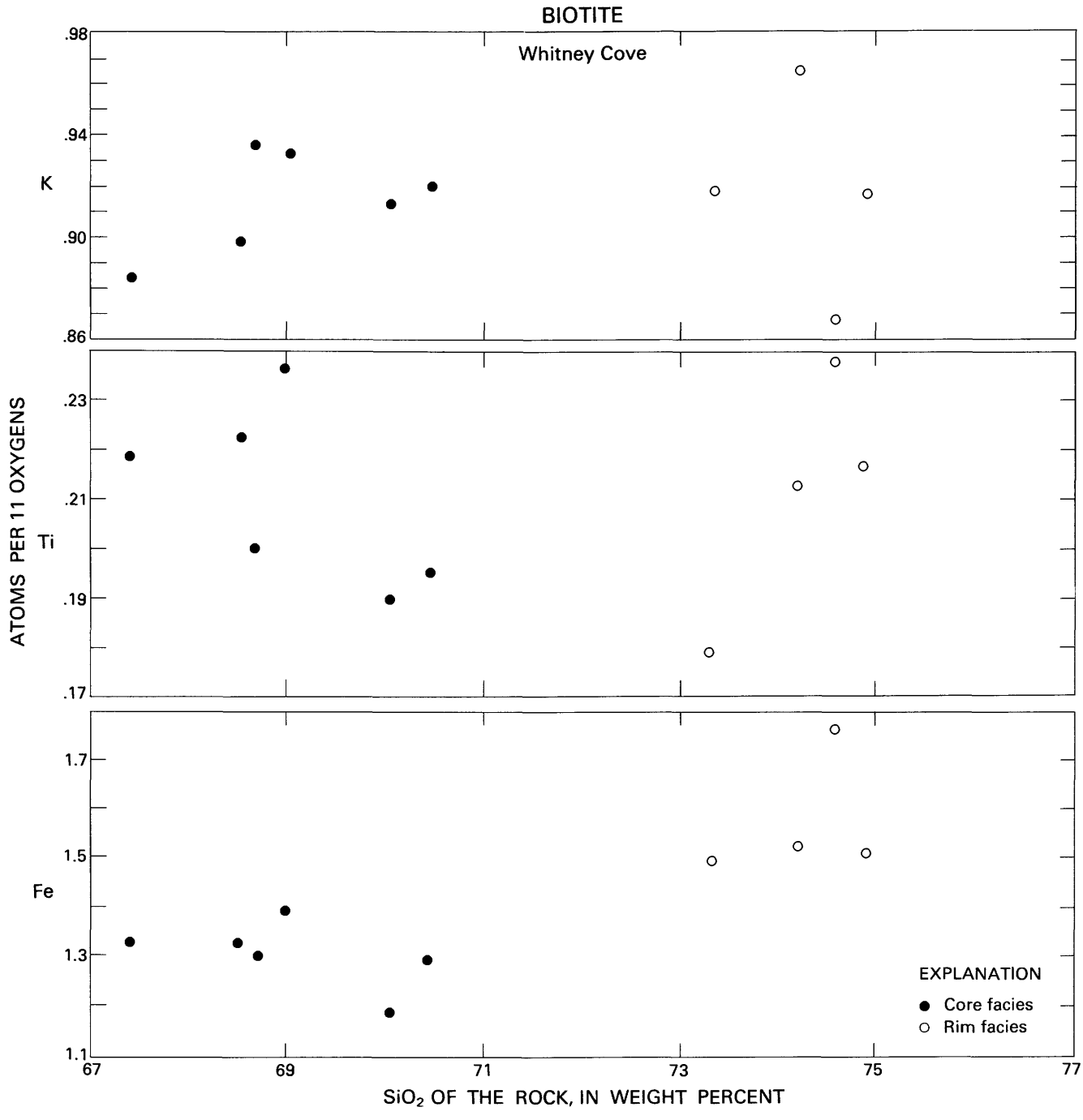

FIGURE 8.—Compositions of biotite in the Whitney Cove pluton as a function of SiO_2 content of the whole rock. Note the higher iron content of biotite with increasing silica content.

Detailed mapping and subdivision of this facies into different types is also possible using the abundance of amphibole, total ferromagnesian mineral content, and development of seriate, equidimensional and porphyritic textures (Ayuso, 1979; Ayuso and Wones, 1980). Many of these lithologic types (fig. 13) are evident in the Springfield and Scraggly Lake quadrangles which contrast with the predominantly amphibole-poor, equidimensional rocks developed elsewhere in the rim facies, for example, in the Nicatous Lake quadrangle.

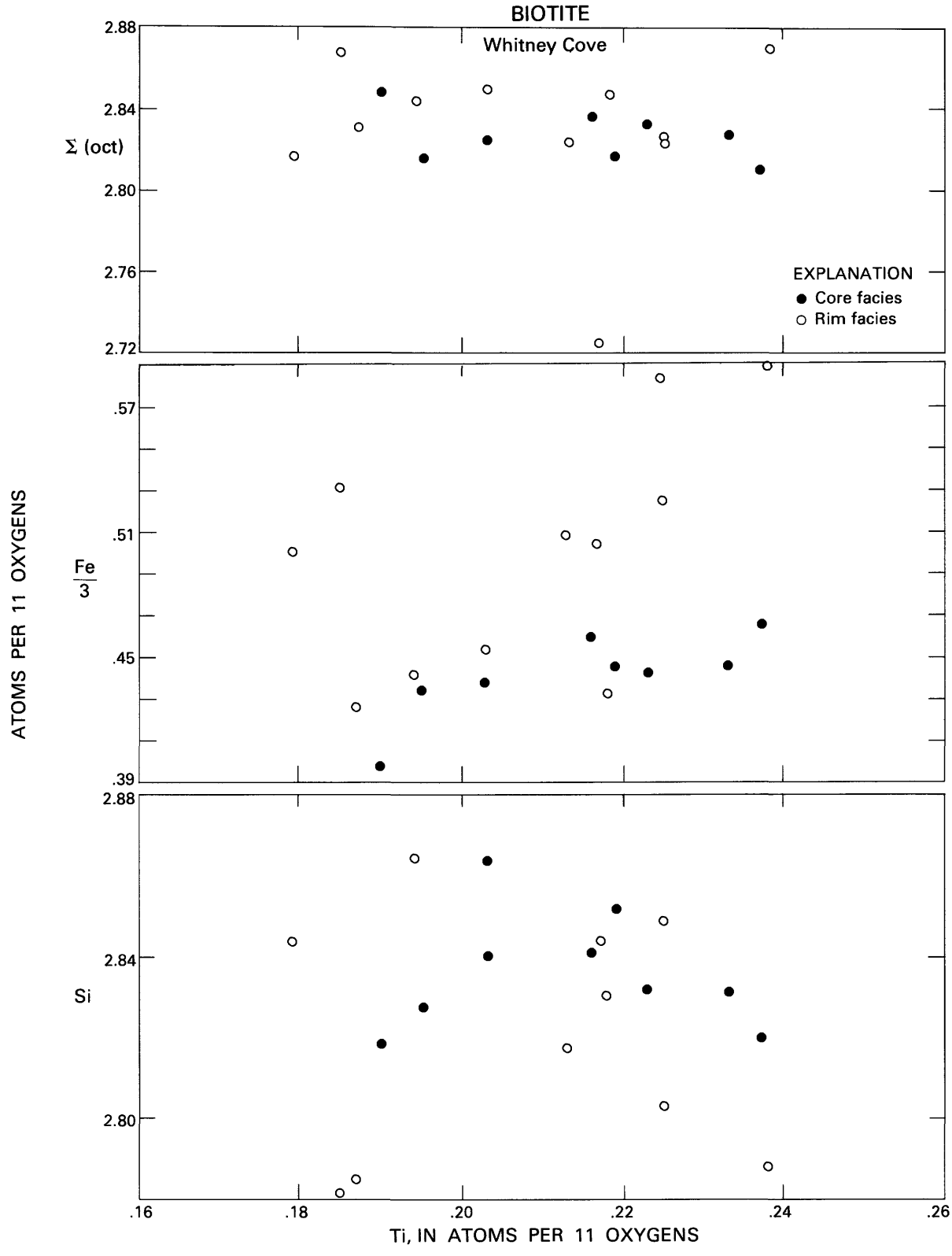

FIGURE 9.—Compositions of biotite in the Whitney Cove pluton showing the absence of clear correlations between different components as a function of titanium content of the biotite. Fe/3 in the rim facies is generally higher than for biotite in the core facies. See table 5 for specific silicon and titanium content.

TABLE 6.—*Representative electron microprobe analyses and structural formulae of plagioclase*

[Calculated per eight oxygen atoms; total iron as FeO; R and C represent rim and core facies, respectively;

Column	1	2	3	4	5	6	7	8	9	10	11	12	13
Sample number	37C	44C	49C	51C	52C	58C	92C	41R	43R	53R	54R	85R	93R
								Weight percent					
SiO_2	59.65	61.46	63.04	55.88	63.80	61.40	57.87	64.06	65.07	64.04	63.83	63.79	63.73
TiO_2	.00	.00	.00	.00	.00	.00	.00	.00	.00	.00	.00	.00	.00
Al_2O_3	25.45	24.47	23.08	28.30	22.65	24.40	26.31	22.66	22.09	22.64	22.84	23.06	22.67
FeO	.11	.17	.15	.29	.15	.14	.41	.10	.06	.17	.13	.10	.09
MnO	.01	.00	.02	.03	.01	.00	.00	.01	.01	.01	.00	.02	.00
MgO	.02	.01	.02	.09	.02	.01	.02	.01	.01	.02	.02	.01	.00
CaO	7.15	5.45	4.59	9.98	4.00	5.41	8.11	3.94	2.81	4.57	4.19	3.86	3.69
Na_2O	7.27	8.25	8.81	5.45	9.04	8.12	6.65	9.05	9.71	8.72	8.85	8.98	9.54
K_2O	.25	.37	.29	.24	.29	.14	.14	.36	.28	.59	.30	.20	.25
SrO	nd	nd	nd	nd	nd	.00	.12	nd	nd	nd	nd	nd	.07
Total	99.91	100.18	100.00	100.28	99.96	99.62	99.63	100.19	100.03	100.76	100.16	100.02	100.04
								Number of atoms					
Si	2.66	2.73	2.79	2.51	2.82	2.73	2.61	2.82	2.81	2.82	2.81	2.81	2.82
Ti	.00	.00	.00	.00	.00	.00	.00	.00	.00	.00	.00	.00	.00
Al	1.34	1.28	1.21	1.50	1.18	1.28	1.40	1.18	1.15	1.17	1.19	1.20	1.18
Fe	.00	.01	.01	.01	.01	.01	.01	.00	.00	.01	.01	.00	.00
Mn	.00	.00	.00	.00	.00	.00	.00	.00	.00	.00	.00	.00	.00
Mg	.00	.00	.00	.01	.00	.00	.00	.00	.00	.00	.00	.00	.00
Ca	.34	.26	.22	.48	.19	.26	.39	.19	.13	.22	.20	.18	.18
Na	.63	.71	.76	.47	.77	.70	.58	.77	.83	.74	.76	.77	.82
K	.01	.02	.02	.01	.02	.01	.01	.02	.02	.02	.02	.01	.01
Sr	nd	nd	nd	nd	nd	.00	.00	nd	nd	nd	nd	nd	.00
								Feldspar components, mol percent					
An	35	26	22	50	19	27	40	19	14	22	20	19	17
Ab	64	72	76	49	79	72	59	79	85	76	78	80	81
Or	1	2	2	1	2	1	1	2	2	2	2	1	1

Additional petrographic heterogeneity in the rim facies is expressed by the progressive changes in fabric and mineralogy away from the granite-country rock contact. Rarely, porphyritic rocks are associated with aplites and tourmaline-bearing pegmatites at the contact, but within a few meters toward the interior they become medium-grained and equidimensional granites (fig. 13). Many of these changes are evident in the area of Getchell Mountain (E) and near Almanac Mountain (A) in the Springfield quadrangle.

Forceful intrusion of the pluton is indicated by sharp contacts exposed north of No. 3 Pond (Q). Lit-par-lit disaggregation of country rock by aplites and pegmatites, however, is a common contact phenomenon and is exemplified by outcrops west of Getchell Mountain (E) where the band of porphyritic rocks developed at the contact is poor in mafic minerals and pinkish gray (5YR 8/1) to grayish-orange pink (10R 8/2) in color. Amphibole is the most important mafic mineral in the pluton as a whole but is typically uncommon near the contact; it increases in abundance and grain size, however, toward the interior of the pluton. Similar increases in the abundance of the accessory and varietal minerals are also evident. Mafic xenoliths are absent at the contact, and their change in abundance and size parallels that of amphibole.

Although porphyritic rocks are generally massive, some of the seriate granites are foliated parallel to the contact. Preferred orientation of the feldspars, biotite and quartz argues for a granitic magma already saturated with respect to these phases during intrusion at this level. Exposures of foliated granites are common to the west of Lombard Mountain (R) and south of Bowers Mountain (S) in the Springfield and Scraggly Lake quadrangles, respectively.

Other typical changes occurring within the rim facies as a function of distance from the country rock include the general decrease in schlieren, amorphous felsic inclusions, and country-rock xenoliths. All of these, except for the felsic inclusions, are alined with their apparent long dimensions horizontal and parallel to the contact. Many of the felsic masses show textures and mineralogy similar to the porphyritic band developed at the contact with the country rock.

The average modal composition of the rim facies is as follows: alkali feldspar, 39.2 percent; plagioclase, 30.0

in the Whitney Cove pluton

nd, not determined]

14	15	16	17	18
94R	104R	106R	107R	108R
62.31	65.00	63.83	62.74	63.47
.00	.00	.00	.00	.01
24.04	22.13	23.01	23.50	22.85
.14	.10	.10	.14	.15
.00	.01	.01	.00	.02
.01	.01	.01	.02	.01
4.60	3.52	4.26	4.68	4.44
8.59	9.12	9.03	8.65	9.01
.46	.35	.25	.23	.16
nd	nd	nd	nd	nd
100.15	100.24	100.51	99.97	100.11
2.76	2.86	2.81	2.78	2.80
.00	.00	.00	.00	.00
1.25	1.15	1.19	1.23	1.19
.01	.00	.00	.01	.01
.00	.00	.00	.00	.00
.00	.00	.00	.00	.00
.22	.17	.20	.22	.21
.74	.78	.77	.74	.77
.03	.02	.02	.01	.01
nd	nd	nd	nd	nd
22	17	20	23	21
75	81	78	76	78
3	2	2	1	1

percent; quartz, 24.1 percent; biotite, 4.6 percent; and amphibole, 2.1 percent. The sum of opaque minerals and accessories accounts for significantly less than 1 percent of the mode. The trend in modal abundances within the Passadumkeag River pluton is clearly toward an interior facies rich in plagioclase and mafic minerals (fig. 5; table 1).

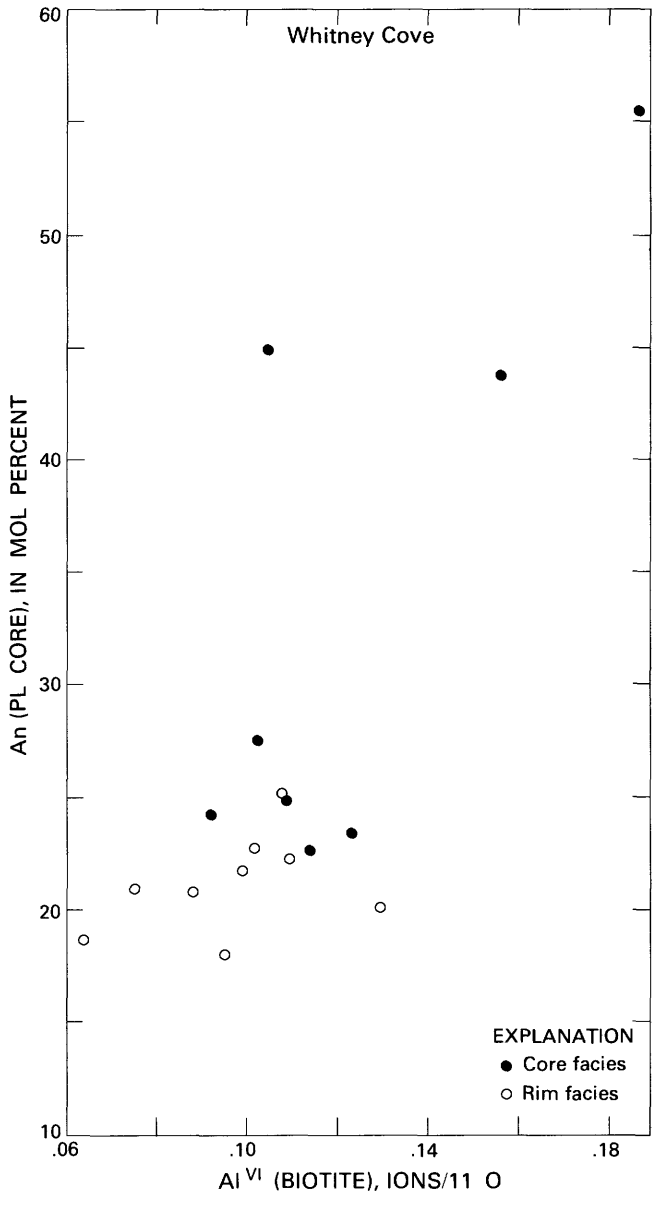

FIGURE 10.—The normative anorthite (An) content of plagioclase cores plotted as a functon of the Al^{VI} content of biotite in the Whitney Cove pluton. Higher anorthite component in plagioclase coexists with biotite containing the highest Al^{VI} in the core facies. Rim facies have plagioclase with lower anorthite contents and biotite with lower Al^{VI}.

THE CORE FACIES

Granitic rocks representative of the core facies are coarse grained, very pale orange (10YR 8/2) to yellowish gray (5Y 8/1) in color, and contain numerous mafic xenoliths (fig. 14) and characteristic euhedral, black amphibole prisms (Ayuso, 1979). Plagioclase content attains its highest value in this facies resulting in rocks properly termed quartz monzonite. The change between facies is in places abrupt, as in the area west of Upper Sysladobsis Lake (P), but is commonly unexposed and of unknown nature (pl. 1).

The rocks are predominantly porphyritic to seriate and display euhedral alkali feldspar with rapakivi texture (fig. 15). Plagioclase and amphibole are phenocrysts in a matrix of mafic and felsic minerals. The average modal composition of this facies is as follows: plagioclase, 37.6 percent; alkali feldspar, 33.0 percent; quartz, 19.4 percent; biotite, 5.8 percent; amphibole, 4.2 percent; the sum of the accessory and opaque suites is less than 1 percent (table 1). The core contains about twice the total mafic mineral content of the rim. Additionally, reverse modal zonation is displayed by the antipathetic

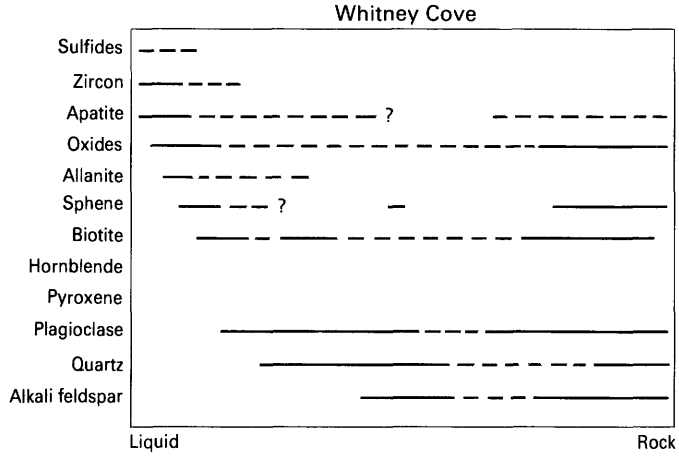

FIGURE 11.—Generalized order of crystallization in the Whitney Cove pluton. Plagioclase, quartz, and alkali feldspar crystallized after the accessory and mafic minerals.

correlation between the sum of alkali feldspar plus quartz and that of total mafic mineral content plus plagioclase. Typical outcrops are exposed west of Sysladobsis Lake (M), on Moose Mountain (T), and around the Chain Lakes (U).

The most distinctive feature of the rocks within the core facies is their heterogeneity in the regional sense. This heterogeneity results in the absence of smooth and linear trends in the modal abundances across the pluton. Typical core facies rocks consist of randomly distributed, fine-grained quartz-dioritic clusters, rich in mafic minerals interspersed with clusters made almost exclusively of feldspathic minerals. Similarly, the entire lithological diversity of mafic xenoliths is sometimes exemplified in individual outcrops by a great range in size, shape, and mineralogy. Xenoliths range in size from the small (5–10 cm), ovoidal, fine-grained, and randomly

TABLE 7.—*Representative major and trace element analyses and norm composition of the Whitney Cove pluton*

[R and C refer to rim and core facies, respectively; total iron as Fe_2O_3; LOI, loss on ignition]

Column	1	2	3	4	5	6	7	8	9	10
Sample number	38R	39R	41R	47R	37C	50C	51C	52C	58C	60C
Weight percent										
SiO_2	73.18	74.30	74.58	73.46	70.45	70.51	68.51	67.40	69.50	71.97
TiO_2	.34	.20	.26	.30	.47	.49	.54	.64	.48	.37
Al_2O_3	13.94	13.25	13.44	13.60	14.70	14.30	15.00	15.20	14.64	13.61
Fe_2O_3	2.11	1.78	1.84	2.40	2.93	3.07	3.27	3.97	2.93	2.42
MnO	.05	.04	.04	.05	.10	.07	.06	.08	.06	.06
MgO	.37	.34	.28	.42	.77	.81	.92	1.02	.83	.54
CaO	1.30	1.06	1.07	1.29	1.91	2.10	2.24	2.32	2.16	1.60
Na_2O	3.23	2.97	3.08	1.32	3.23	3.57	3.44	3.66	3.45	3.37
K_2O	4.94	5.14	5.18	4.80	4.41	4.41	4.65	4.31	4.75	4.82
P_2O_5	.13	.09	.05	.08	.15	.15	.18	.22	.17	.15
LOI	.48	.44	.16	.49	.44	.92	1.21	1.58	.80	.51
Total	100.07	99.61	99.98	100.21	99.56	100.40	100.02	100.58	99.73	99.57
Norm										
Q	32.49	34.97	34.28	32.55	30.10	27.67	24.42	23.97	26.63	31.95
C	1.23	1.09	.94	.79	1.51	.18	.42	.82	.44	.87
Or	29.17	30.49	30.62	28.31	26.18	26.19	27.77	25.77	28.38	28.83
Ab	27.31	25.23	26.07	28.03	27.45	30.45	30.70	31.42	28.84	26.72
An	5.60	4.69	4.78	5.87	8.53	9.49	10.04	10.19	9.71	7.04
En	.92	.85	.70	1.04	1.93	2.03	2.32	2.57	2.09	1.36
Hm	2.11	1.79	1.84	2.40	2.94	3.09	3.30	4.02	2.96	2.45
Il	.11	.09	.09	.11	.22	.15	.13	.17	.13	.13
Tn	.00	.00	.00	.00	.00	.00	.00	.00	.00	.00
Ru	.28	.16	.22	.24	.36	.41	.48	.56	.42	.31
Ap	.31	.21	.12	.19	.36	.36	.43	.53	.41	.36
Trace elements in ppm										
Rb	165	160	197	148	193	158	164	171	152	186
Sr	183	158	113	148	280	236	289	276	264	237
Y	27	37	35	29	22	38	38	44	33	36
Ba	527	564	352	424	755	509	703	527	584	497
Zr	195	164	162	159	177	203	227	281	195	185
Nb	17	16	17	10	20	24	25	26	20	19

oriented masses of biotite and plagioclase common throughout the Passadumkeag River pluton, to banded biotite-rich aggregates and to large (up to 1 m), disc-shaped and prominently porphyritic quartz-diorite rocks.

PETROGRAHY AND MINERAL COMPOSITIONS

Compositonal variation of the constituent phases within the Passadumkeag River pluton exceeds the analytical uncertainty, supports the modal heterogeneity, and argues for distinct chemical differences even within each facies. The core facies of this pluton probably contains more accessories than the rim facies, especially as inclusions within mafic minerals and close to the mafic xenoliths. Zircon and apatite were the earliest phases to crystallize. Apatite in the Passadumkeag River pluton shows larger variations in fluorine (from 1.6 to 4.4 weight percent) and manganese (from the limit of detectability to 0.24 weight percent) than in the Whitney Cove pluton (table 2). Allanite (table 2) tends to form euhedral and smaller grains than in the Whitney Cove pluton, and these are also optically and compositionally zoned from core to rim. Primary sphene presents euhedral sides to all phases except apatite and zircon, while secondary sphene is generally anhedral and replaces amphibole and biotite. Representative analyses of sphene are given in table 1.

Magnetite and ilmenite are generally enclosed in mafic minerals, occur as secondary reaction products in biotite and amphibole, and are scattered in the matrix. Rounded pyrite grains are rare and appear to concentrate within magnetite. Magnetite contains less than 1.0 weight percent TiO_2 and shows no differences between facies (table 3). Manganese in ilmenite is lower than in the Whitney Cove pluton but ranges up to 8.5 weight percent and suggests reequilibration at low temperature (table 4).

Clinopyroxene(?) is an extremely rare phase in the Passadumkeag River pluton. It is found only in one sample of the core facies as very fine-grained inclusions within plagioclase phenocrysts. Although the phenocrysts also enclose amphibole, no reaction rims between amphibole with the generally subhedral, monoclinic, and optically unzoned clinopyroxenes are evident.

AMPHIBOLE

Amphibole is heterogeneously distributed in this granite. Near the granite-country rock contact, amphibole is absent. In a few areas within the core facies, amphibole and biotite are subequal in abundance, but more commonly, amphibole is subordinate to biotite. Two varieties of amphibole, a phenocryst and a matrix component, are present in the Passadumkeag River pluton. Amphibole phenocrysts (up to 0.7 cm) are black prisms, invariably euhedral to all other silicates except biotite. Although amphibole generally precedes biotite in the crystallization sequence, inclusions of unalined biotite plates within amphibole suggest a stage of coprecipitation of these two phases. Crystallization of biotite prior to amphibole agrees with the suggestion of Wones and Dodge (1977) that in potassium-rich magmas, exemplified by the Bottle Lake Complex, a magmatic stage with low water activity promotes crystallization of biotite before amphibole.

In accordance to the classification of Leake (1978), the amphiboles belong to the calcic group and range from edenite and edenitic hornblende to ferro-edenites and ferro-edenitic hornblende. The Fe/(Fe+Mg) ratios range from about 0.51 to 0.75 (table 8) without a distinct trend in the pluton from rim to core facies (fig. 16). A gap in the Fe/(Fe+Mg) ratio occurs at about 0.64 to 0.66, probably as an artifact of sampling. Manganese displays a roughly increasing trend with higher Fe/(Fe+Mg) ratios (fig. 16). The change in the total abundance in the A-site, and of potassium in the A-site, lacks a consistent trend in more iron-rich amphibole. Fluorine is positively correlated with the silica content of the rock (not shown), and is in agreement with the change found in coexisting biotites. This relatively systematic change in fluorine content was not evident in biotite from the Whitney Cove pluton (table 5). The abundances of calcium, sodium, and titanium in amphibole are also typically scattered and show no distinctive gradient in the Passadumkeag River pluton (fig. 16). The total aluminum variation in amphibole shows a broadly increasing trend with Fe/(Fe+Mg) ratio. However, Al^{IV} shows no correlation with increasing Fe/(Fe+Mg) ratios (table 8), in contrast with the scattered but positively correlated change for Al^{VI}.

The change in Fe/(Fe+Mg) ratio of amphibole is not clearly correlated with the silica content of the rock (fig. 17) or with silicon in tetrahedral coordination (Si^{IV}) of the amphibole (table 8). At a given Fe/(Fe+Mg) ratio, the amphiboles in the Passadumkeag River pluton are higher in Si^{IV} than amphiboles from the Eagle Peak pluton (Noyes, 1978) and the Sierra Nevada batholith (Dodge and others, 1968). In contrast to the drastic decrease in Fe/(Fe+Mg) ratios of progressively more siliceous magnetite-series granitic rocks found by Czamanske and others (1981), amphiboles from the Passadumkeag River pluton are dispersed but do not show a decrease in Fe/(Fe+Mg) ratios in more siliceous rocks (table 8). This observation strongly argues against

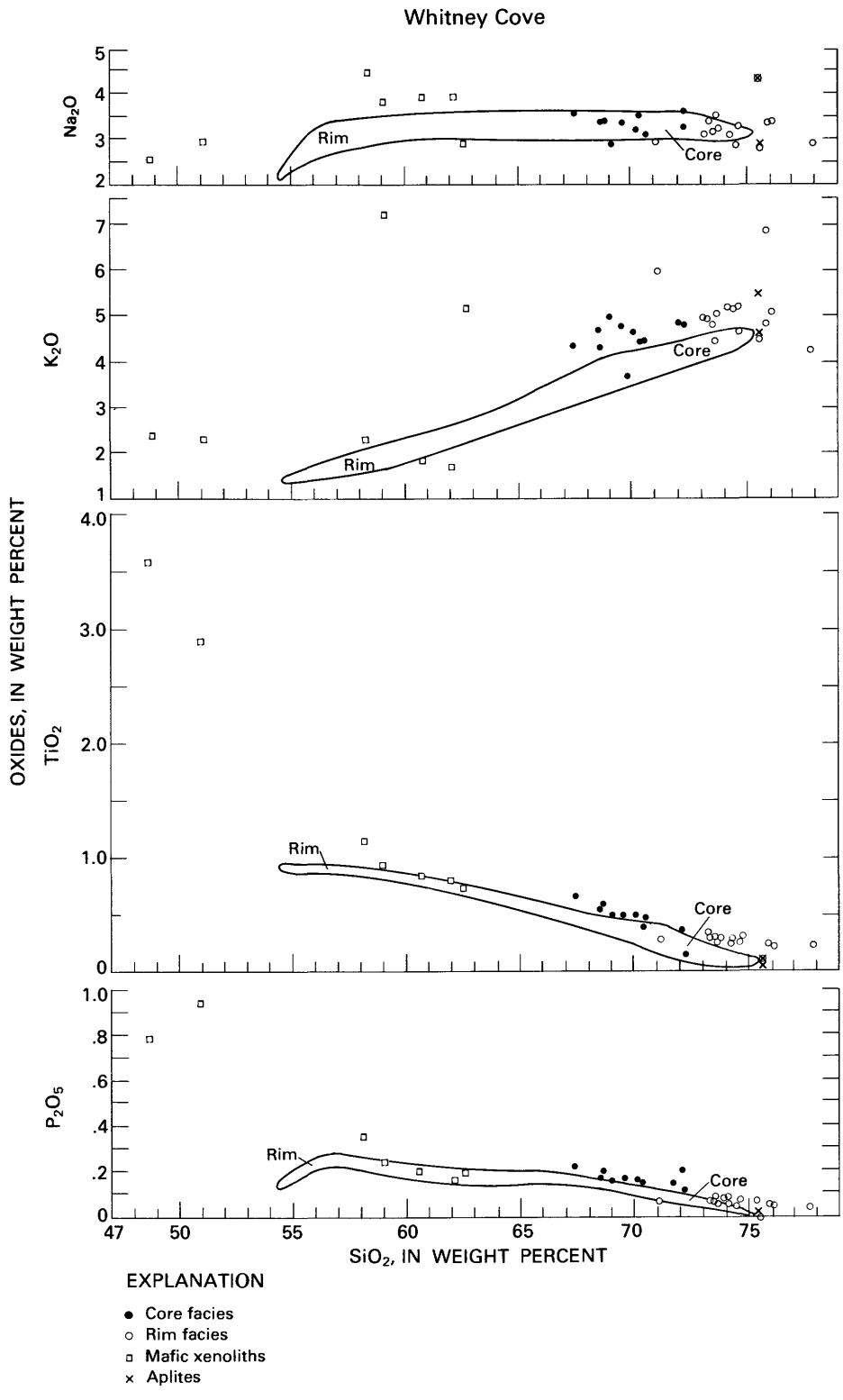

FIGURE 12.—Variation diagrams of the Whitney Cove pluton showing the core and rim facies. The composition of the mafic xenoliths from the Passadumkeag River pluton and aplites are also plotted. Note the correlation of the oxides with the silica content of the rock, the absence of significant gaps in the trend, and the more silicieous character of the rim facies. Samples from the rim facies are lower in Al_2O_3, Fe_2O_3, MgO, TiO_2, and CaO than the core facies. This compositional zoning of rocks from a single pluton is opposite to the arrangement in concentric and normally zoned plutons.

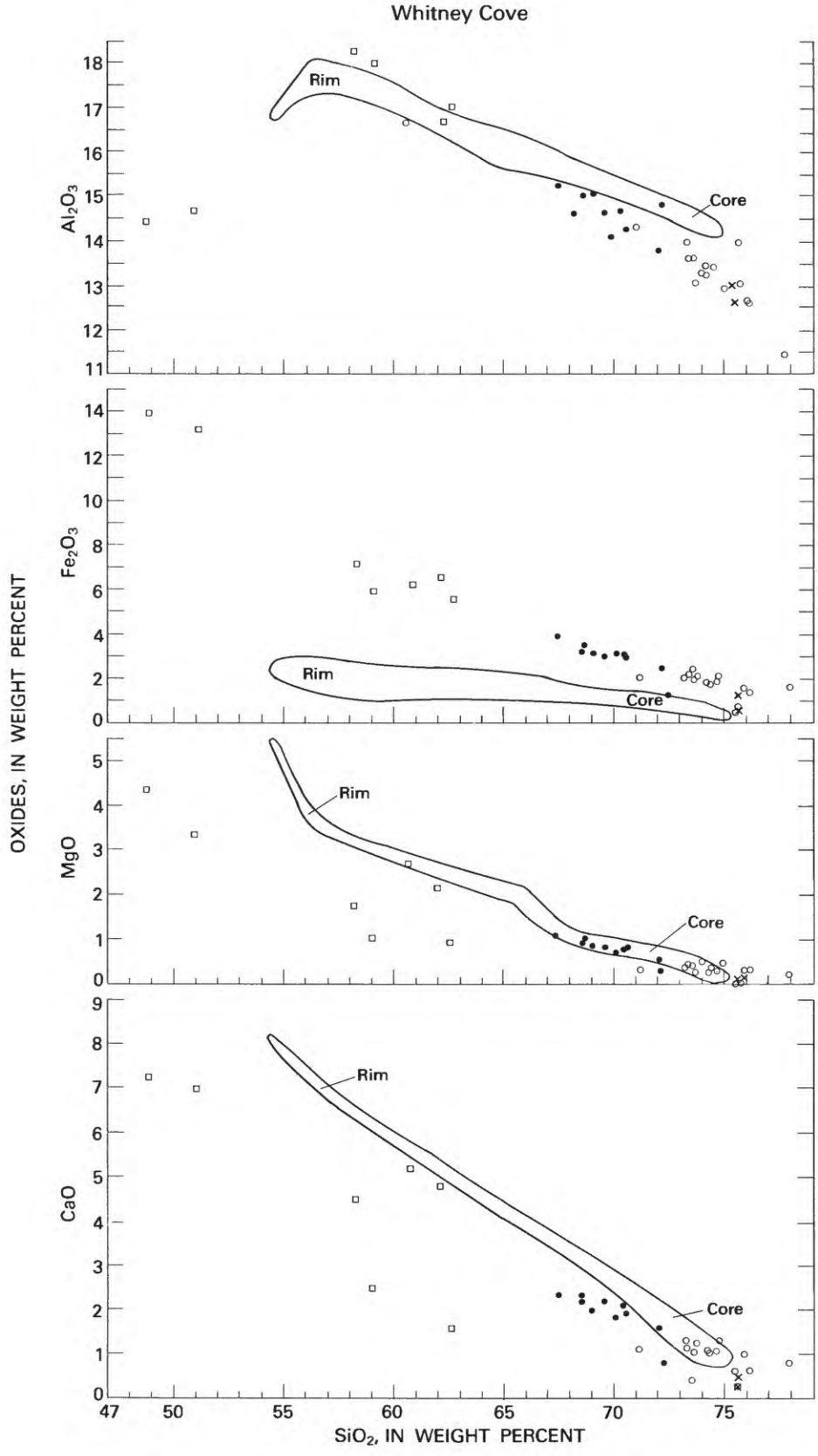
Whitney Cove
OXIDES, IN WEIGHT PERCENT
Al_2O_3
Fe_2O_3
MgO
CaO
Rim
Core
SiO_2, IN WEIGHT PERCENT
47
50
55
60
65
70
75

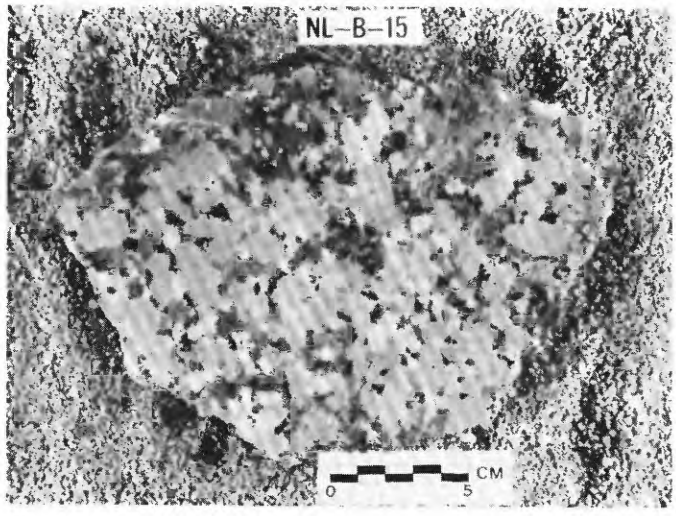

FIGURE 13.—Stained slab of a characteristic sample from the rim facies of the Passadumkeag River pluton. Note the alkali feldspar (light gray) and plagioclase (white) form subhedral crystals and surround areas rich in mafic minerals (dark gray).

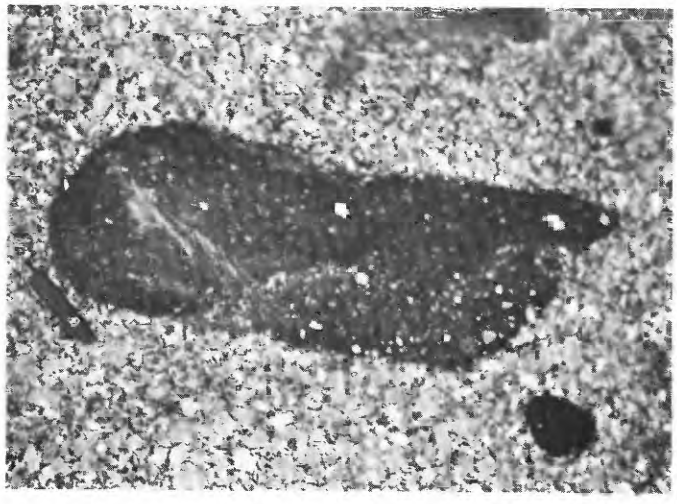

FIGURE 14.—A typical outcrop of the core facies of the Passadumkeag River pluton. Mafic xenoliths have a large range in size in the core facies (knife is 7 cm long). Reaction bands are typically absent at the contact between the host granite and the mafic xenoliths. Note the grain size and the textural contrast between the xenolith and its host.

significant oxidation during magmatic differentiation during the evolution of the Passadumkeag River pluton.

The absence of gradual compositional changes in amphiboles from the Passadumkeag River pluton suggests that during amphibole crystallization substantial chemical heterogeneity existed in the pluton. Also, amphibole compositions argue against the existence of a systematic change in the silica activity of the rocks as represented by the core and rim facies.

Amphiboles from the rim facies range widely in titanium contents, from about 0.13 to 0.19 (atoms per 23 oxygens) in rocks with a minimum content of 70 weight percent SiO_2 in the rock. They are in contrast to amphibole from the core facies which attains abundances up to 0.23 but with a range in SiO_2 content from about 65 to 72 weight percent (fig. 17). Higher fluorine abundances in amphibole are correlated with higher SiO_2 content of the rock. Total aluminum, manganese, potassium (fig. 17), Al^{IV}, and Al^{VI} are in contrast to this relation because they typically lack meaningful gradients with the SiO_2 content of the rock. Total aluminum, however, generally increases with the Fe/(Fe+Mg) ratio, while Al^{VI} is uncorrelated with the anorthite component in coexisting plagioclase (fig. 18) from samples of the rim and core facies. Plagioclase from the core facies has a higher anorthite content than plagioclase in the rim facies at a given value of Al^{VI} in the amphibole.

Substitutions in amphibole involving Al^{IV} for the sum of the total of the A-site occupancy $+Al^{VI}+2(Ti)$ were suggested by Czamanske and Wones (1973) and Robinson (1971) to dominate the evolution of amphibole compositions. Czamanske and Wones (1973) and Czamanske and others (1981) noted the slight deficiency of Al^{IV} in granites from Finnmarka and Japan, respectively. Similar deficiencies in aluminum were found in the amphiboles from the Passadumkeag River pluton.

Other substitutions including the coupling of Al^{IV} for titanium are not evident in the amphiboles of the Passadumkeag River pluton, although there is a tendency for $Al^{VI}+Ti$ to increase with Fe/(Fe+Mg). The change in

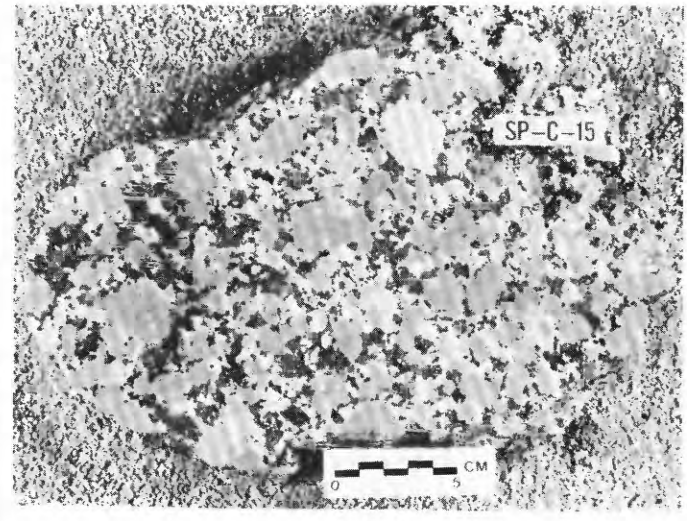

FIGURE 15.—Stained slab of a sample from the core facies of the Passadumkeag River pluton. Plagioclase (white) forms subhedral crystals subequal in size to alkali feldspar (light gray). Note the relative enrichment of plagioclase in this sample compared to that seen in figure 13.

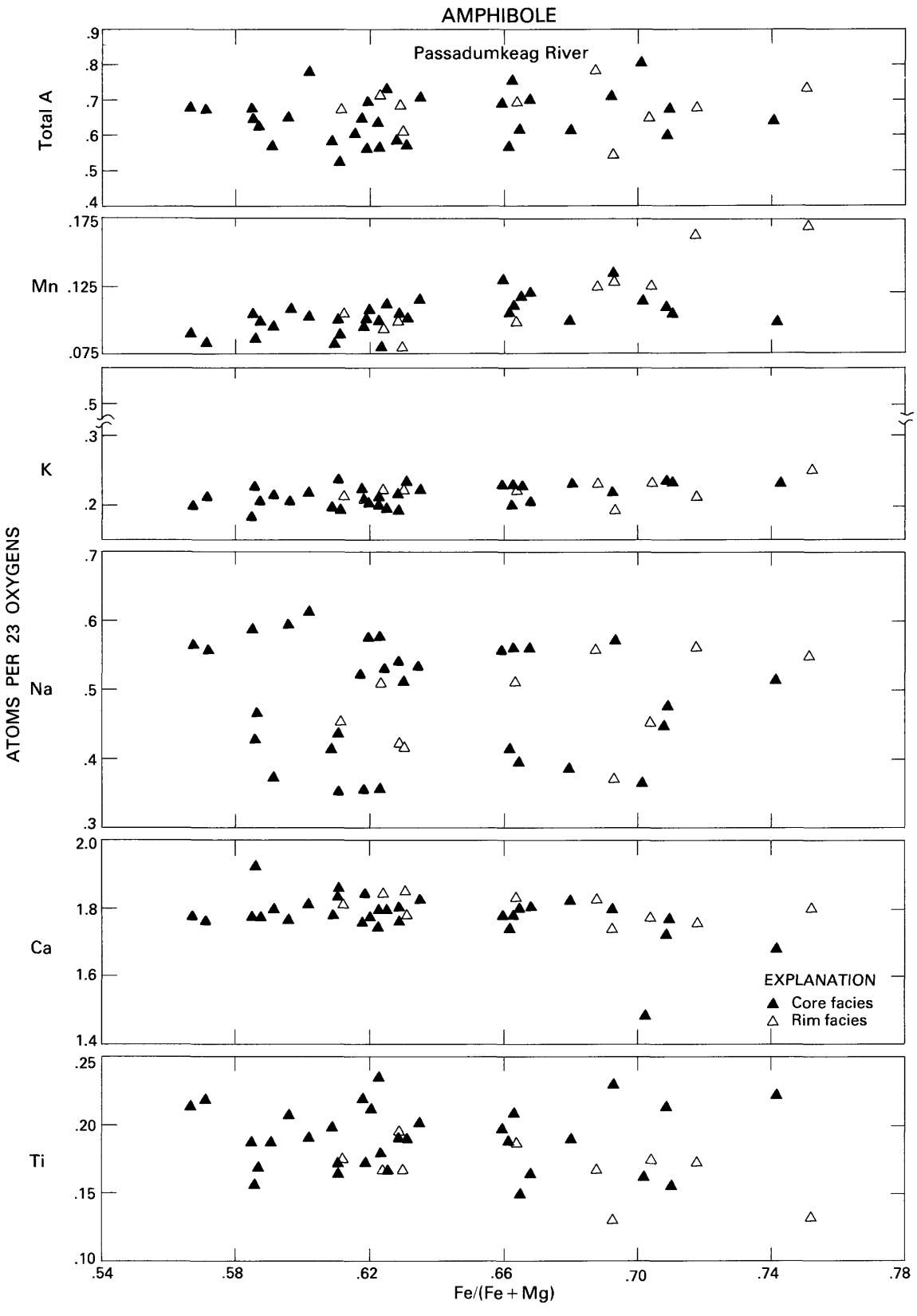

FIGURE 16.—Compositions of amphibole in the Passadumkeag River pluton as a function of Fe/(Fe+Mg). Each symbol represents the average obtained on at least 10 grains per sample. Note the absence of clearly defined trends with increasing Fe/(Fe+Mg) ratio. Only manganese shows a broad positive correlation with Fe/(Fe+Mg) in the amphibole. The content of titanium, sodium and the total in the A-site shows large scatter. The compositions of amphibole in the core and rim facies are generally not significantly different. A gap in Fe/(Fe+Mg) ratios from about 0.64 to 0.66 is probably an artifact of sampling. See table 8 for specific values.

TABLE 8.—*Representative electron microprobe analyses and*

[Calculated for 23 oxygen atoms using the scheme of Czamanske and Wones (1973).

Column	1	2	3	4	5	6	7	8	9	10	11	12	13	14	15
Sample number	4C	9C	13C	17C	21C	24C	25C	26C	29C	31C	36C	75C	78C	79C	84C
							Weight percent								
SiO_2	44.56	44.46	43.48	43.76	41.85	42.83	42.62	42.74	44.08	44.44	43.99	43.91	42.28	42.70	43.63
Al_2O_3	8.62	8.66	7.61	7.81	10.10	8.20	8.48	8.28	7.78	8.22	8.28	8.35	7.66	8.45	8.01
TiO_2	1.68	1.66	1.77	1.85	1.39	1.96	1.88	1.72	1.71	1.66	1.91	1.68	1.60	1.37	1.62
FeO	22.77	21.51	21.11	20.46	25.63	24.28	26.06	22.25	21.39	22.89	22.04	22.41	21.34	25.22	23.59
MnO	.78	.74	.81	.69	.87	.92	.73	.86	.70	.70	.72	.79	.76	.79	.80
MgO	7.49	8.37	8.02	8.77	6.10	6.04	5.10	7.18	8.35	7.49	7.75	7.39	7.93	5.46	6.75
CaO	10.93	11.05	10.60	10.72	8.89	10.78	10.00	10.89	10.58	10.85	10.73	10.92	10.65	10.50	10.47
Na_2O	1.38	1.25	1.96	1.89	1.23	1.90	1.69	1.76	1.81	1.77	1.76	1.38	2.01	1.89	1.38
K_2O	1.12	1.12	1.03	1.00	2.71	1.11	1.16	1.13	.87	.98	1.14	1.02	1.08	1.05	1.00
BaO	.05	.04	.01	.00	.06	.02	.07	.01	nd	.00	.13	.05	.02	.00	.05
F	.41	.37	.55	.48	.71	.33	.58	.38	.51	.37	.40	.31	.60	.61	.35
Cl	.16	.16	.11	.11	.15	.14	.29	.14	.11	.15	.20	.17	.12	.13	.12
P_2O_5	.00	.01	.02	.01	.01	.02	.01	.02	.20	.02	.00	.02	.01	.01	.01
SrO	.01	.02	.01	.01	.00	.01	.04	.00	.00	.00	.00	.00	.02	.00	.01
Total	99.96	99.47	97.09	97.56	99.70	98.54	98.71	97.36	98.09	99.54	99.05	98.40	96.08	98.18	97.79
							Number of atoms								
Si	6.763	6.744	6.787	6.760	6.526	6.686	6.705	6.693	6.846	6.777	6.742	6.770	6.711	6.722	6.801
Al	1.237	1.256	1.213	1.240	1.474	1.314	1.295	1.307	1.154	1.223	1.258	1.230	1.289	1.278	1.199
(TET)	8.000	8.000	8.000	8.000	8.000	8.000	8.000	8.000	8.000	8.000	8.000	8.000	8.000	8.000	8.000
Al	.304	.293	.188	.183	.393	.195	.277	.221	.247	.254	.238	.287	.143	.290	.272
Fe	2.811	2.626	2.738	2.583	3.025	3.170	3.304	2.902	2.655	2.853	2.772	2.813	2.792	3.268	2.971
Mg	1.694	1.892	1.866	1.019	1.419	1.405	1.196	1.675	1.902	1.703	1.770	1.707	1.875	1.280	1.568
Ti	.191	.189	.208	.215	.163	.230	.223	.202	.196	.190	.220	.193	.190	.162	.189
Mn	.000	.000	.000	.000	.000	.000	.000	.000	.000	.000	.000	.000	.000	.000	.000
(M_1-M_3)	5.000	5.000	5.000	5.000	5.000	5.000	5.000	5.000	5.000	5.000	5.000	5.000	5.000	5.000	5.000
Ca	1.777	1.796	1.773	1.774	1.483	1.802	1.685	1.827	1.732	1.722	1.762	1.802	1.812	1.772	1.749
Mn	.100	.095	.107	.090	.115	.131	.097	.115	.090	.091	.093	.102	.102	.106	.105
Fe	.080	.103	.018	.061	.318	.000	.123	.013	.078	.067	.055	.067	.040	.069	.105
Na	.043	.006	.102	.075	.084	.067	.095	.045	.100	.120	.090	.029	.046	.069	.041
(M_4)	2.000	2.000	2.000	2.000	2.000	2.000	2.000	2.000	2.000	2.000	2.000	2.000	2.000	2.000	2.000
Na	.364	.361	.492	.492	.459	.508	.419	.489	.435	.403	.434	.393	.572	.509	.374
K	.216	.216	.206	.198	.543	.221	.233	.226	.169	.191	.222	.197	.219	.210	.199
Ba	.003	.002	.001	.000	.004	.001	.005	.001	.000	.000	.008	.003	.001	.000	.003
(A)	.583	.579	.699	.690	1.006	.730	.657	.716	.604	.594	.664	.593	.792	.719	.576
Fe/(Fe+Mg)	.631	.591	.596	.567	.702	.693	.742	.635	.509	.632	.615	.629	.602	.722	.662

the sum of Al^{IV} and Al^{VI} as a function of Al^{IV} is consistent with the change found in the Japanese granites studied by Czamanske and others (1981). However, perhaps a result of the limited compositional variation in this pluton compared to the Japanese granites, amphiboles from the Passadumkeag River pluton form an array along a steeper slope.

BIOTITE

Biotite is the predominant mafic mineral in the Passadumkeag River pluton. Several textural types are present including phenocrysts, groundmass, and biotite forming fine-grained clusters with other mafic minerals and plagioclase. Comparison of biotite compositions across the pluton from rim to core facies characteristically shows major overlap (table 9). The Passadumkeag River pluton is characterized by biotites with Fe/(Fe+Mg) ratios ranging from about 0.57 to 0.80 (table 9) and lacking a distinctive trend in titanium between biotites from the core and rim facies (fig. 19). However, in spite of the overlap, at a given Fe/(Fe+Mg) ratio, biotites from many of the samples from the core facies usually have higher titanium than those in the rim facies. Plotted against the Fe/(Fe+Mg) ratio of the biotite, the titanium content shows no progressive gradient (fig. 19). Titanium content, however, is broadly correlated with the SiO_2 content of the rock (fig. 20), so that lower titanium in biotite occurs, in most cases, in the more silicic marginal facies of the pluton. Compared to the Whitney Cove pluton, the composition of biotite in the Passadumkeag River pluton shows a range for titanium from about 0.17 to 0.27 (atoms per 11 oxygens) (table 9), broadly in agreement with the range found in the Whitney Cove pluton. Biotite from the Passadumkeag River pluton suggests no correlations between titanium and the total abundance of the octahedral ca-

structrual formulae of amphibole from the Passadumkeag River pluton

Total iron as FeO; R and C represent rim and core facies, respectively; nd, not determined]

16	17	18	19	20	21	22	23	24	25	26	27	28	29	30	31	32
86C	89C	91C	105C	110C	112C	113C	115C	8R	10R	12R	23R	27R	35R	76R	77R	88R
Weight percent—continued																
43.27	44.52	42.77	44.23	43.37	42.92	44.57	43.67	44.06	43.73	44.25	43.00	44.15	42.28	43.69	44.00	42.89
8.49	8.10	8.29	8.24	8.44	8.50	8.03	7.26	8.07	8.27	7.04	8.69	8.15	8.62	8.12	8.66	8.92
1.41	1.42	1.81	1.50	1.69	1.75	1.89	1.43	1.52	1.61	1.11	1.39	1.50	1.10	1.54	1.46	1.49
23.56	22.04	24.78	21.30	23.13	23.52	20.77	22.81	21.93	23.66	24.78	24.79	22.69	25.66	22.43	22.53	25.02
.91	.69	.81	.75	.98	.90	.65	.85	.79	.74	1.00	1.23	.62	1.28	.70	.70	.95
6.66	7.89	6.70	8.40	6.66	6.85	8.70	7.69	7.80	6.73	6.19	5.46	7.49	4.75	7.44	7.70	5.89
10.83	11.09	10.23	10.77	10.70	10.76	10.83	10.73	11.02	10.88	10.40	10.55	11.28	10.60	10.68	11.33	10.68
1.86	1.48	1.54	1.56	1.86	1.83	1.89	1.66	1.66	1.70	1.22	1.86	1.39	1.80	1.80	1.75	1.49
1.05	1.00	1.17	1.06	1.16	1.15	1.10	.99	1.13	1.14	.98	1.07	1.14	1.24	1.10	1.14	1.18
.01	.06	.04	.03	.14	.10	.11	.11	.14	.14	.06	.03	.02	.02	.11	.00	.04
.45	.31	.51	.57	.41	.44	.45	.51	.43	.46	.66	.55	.72	.63	.47	.37	.49
.10	.11	.31	.11	.20	.20	.17	.12	.14	.17	.11	.20	.11	.07	.18	.12	.15
.02	.00	.01	.01	.00	.00	.00	.00	.00	.00	.01	.03	.09	.02	.00	.02	.00
.00	.00	.01	.00	.00	.00	.00	.00	.00	.00	.00	.03	.03	.01	.00	.02	.00
98.62	98.71	98.98	98.53	98.74	98.92	99.16	97.83	98.69	99.23	97.81	98.88	99.38	98.08	98.35	99.80	99.19
Number of Atoms—continued																
6.722	6.815	6.748	6.783	6.721	6.665	6.778	6.818	6.779	6.749	6.952	6.711	6.772	6.706	6.759	6.690	6.667
1.278	1.185	1.252	1.217	1.279	1.335	1.222	1.182	1.221	1.251	1.048	1.289	1.228	1.294	1.241	1.310	1.333
8.000	8.000	8.000	8.000	8.000	8.000	8.000	8.000	8.000	8.000	8.000	8.000	8.000	8.000	8.000	8.000	8.000
.277	.277	.284	.273	.264	.217	.216	.154	.243	.254	.256	.309	.245	.317	.239	.243	.301
3.040	2.759	3.166	2.637	2.997	2.966	2.580	2.889	2.791	3.012	3.164	3.236	2.875	3.403	2.850	2.844	3.160
1.519	1.800	1.336	1.920	1.542	1.617	1.989	1.790	1.788	1.547	1.448	1.269	1.712	1.123	1.716	1.746	1.365
.164	.164	.214	.170	.197	.200	.215	.167	.178	.187	.132	.172	.168	.131	.195	.167	.174
.000	.000	.000	.000	.000	.000	.000	.000	.000	.000	.000	.000	.000	.000	.000	.000	.000
5.000	5.000	5.000	5.000	5.000	5.000	5.000	5.000	5.000	5.000	5.000	5.000	5.000	5.000	5.000	5.000	5.000
1.803	1.819	1.723	1.770	1.778	1.797	1.764	1.795	1.817	1.815	1.751	1.765	1.854	1.801	1.771	1.845	1.778
.120	.089	.107	.097	.129	.115	.083	.112	.103	.098	.133	.149	.081	.145	.100	.090	.126
.022	.064	.092	.095	.002	.051	.062	.089	.032	.042	.093	.000	.037	.000	.052	.055	.093
.055	.028	.078	.038	.091	.037	.091	.004	.048	.045	.023	.086	.028	.054	.077	.010	.003
2.000	2.000	2.000	2.000	2.000	2.000	2.000	2.000	2.000	2.000	2.000	2.000	2.000	2.000	2.000	2.000	2.000
.505	.411	.367	.426	.468	.519	.467	.529	.449	.465	.347	.478	.387	.498	.463	.505	.447
.207	.195	.234	.208	.228	.226	.213	.197	.222	.224	.196	.213	.222	.250	.218	.222	.234
.000	.004	.003	.002	.009	.006	.007	.007	.009	.009	.004	.002	.001	.001	.007	.000	.002
.712	.610	.604	.636	.705	.751	.687	.733	.680	.698	.547	.693	.610	.749	.688	.727	.683
.668	.611	.709	.587	.660	.651	.571	.625	.612	.664	.693	.718	.630	.752	.628	.624	.704

tions, with the mole fraction of iron in octahedral coordination, or with the silica content (fig. 21).

A dispersed but positive correlation exists between the Fe/(Fe+Mg) ratio of biotite and of the rock. Despite this systematic change, however, biotite compositions cannot be used reliably to distinguish between the marginal and interior facies of the Passadumkeag River pluton (table 9). No correlation exists between the Fe/(Fe+Mg) ratio of the biotite and the silica content of the rock. The absence of a compositional gradient of biotite and the composition of the rock distinguishes biotites of the Passadumkeag River pluton from those of the Whitney Cove pluton (tables 5, 9).

The content of Fe in biotite does not show a correlation with the silica content of the rock (fig. 21), and thus despite the tendency for higher Fe at higher silica of the granite, biotites from the two facies cannot be properly distinguished. Higher fluorine contents may be evident in biotite from rocks with high silica in the Passadumkeag River pluton, although biotite from the core facies of the Whitney Cove pluton probably contains even higher fluorine content (tables 5, 9).

The abundances of potassium (fig. 20), sodium, chlorine, phosphorous, barium, and strontium are uncorrelated with either the Fe/(Fe+Mg) ratio of the biotite or with the silica content of the rock. This observation also applies to the manganese content which shows a wide and unsystematic range from core to rim facies.

The distribution of Al^{VI} in the biotite from the pluton is not correlated with the Fe/(Fe+Mg) ratio (fig. 19); it forms, however, a band roughly correlated with the anorthite component in coexisting plagioclase from the rim facies (fig. 22). Overlap between the biotites of the two facies is a characteristic feature. Increasing Al^{VI} with higher Fe/(Fe+Mg) ratios is the normal trend expected for biotite coexisting with felsic liquid (Nockolds, 1947; Czamanske and Wones, 1973).

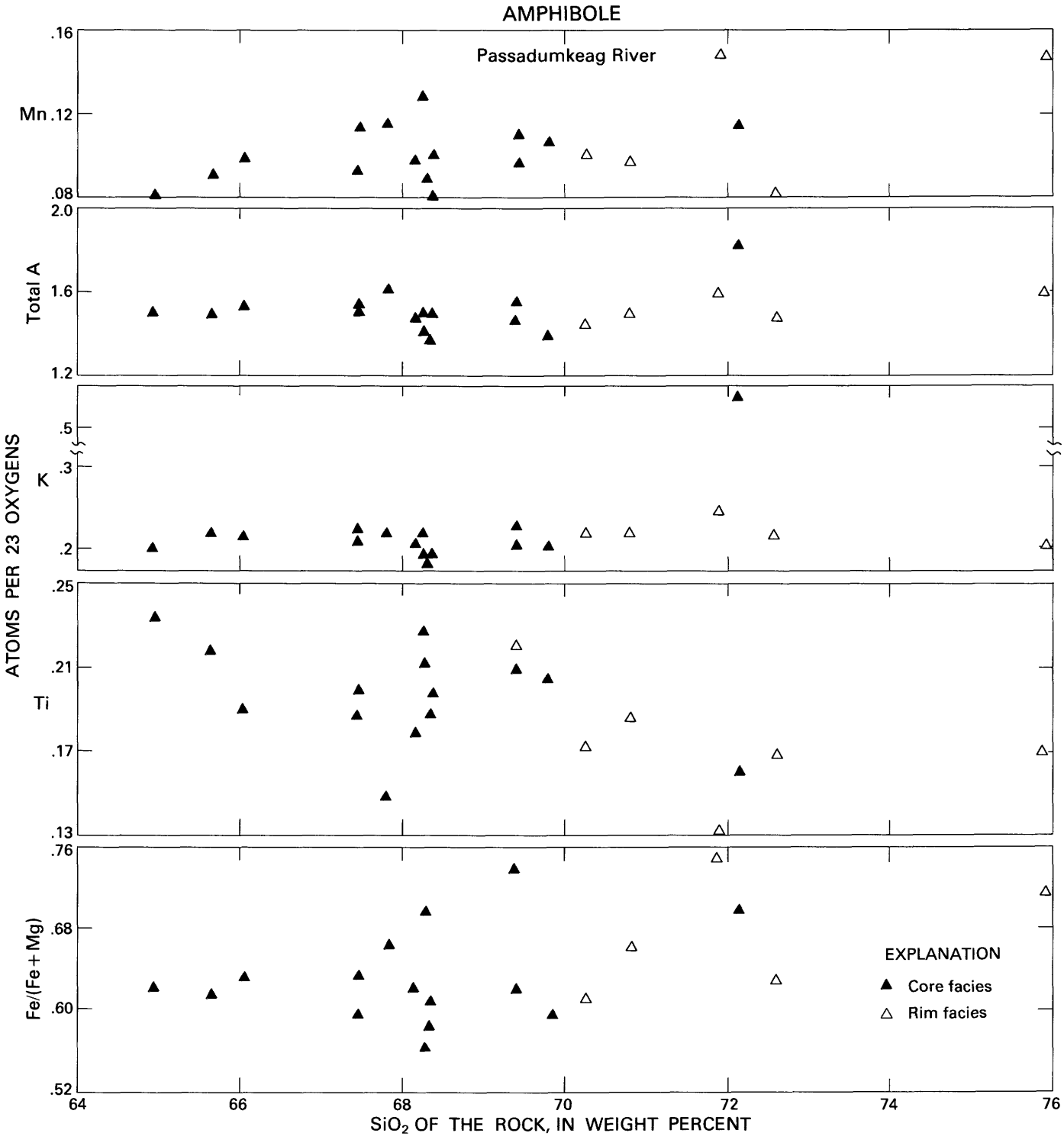

FIGURE 17.—Compositions of amphibole in the Passadumkeag River pluton as a function of the SiO_2 content (in percent) of the rock. Note the large range in amphibole compositions at a given value of silica. Clearly defined trends from core to fim facies are absent. The most silicieous rocks (rim facies) may have amphiboles with lower titanium contents than those from the core facies. The Fe/(Fe+Mg) ratio in the amphiboles shows quite a wide range and is not well correlated with the silica content of the rock. In general, however, some of the amphiboles in samples from the rim facies have compositions that are somewhat higher in Fe/(Fe+Mg) ratios than the majority of amphiboles from the core facies.

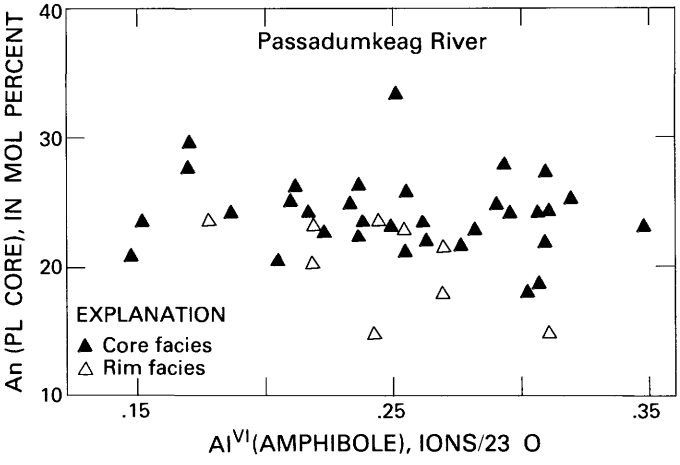

FIGURE 18.—The anorthite content (An) of plagioclase cores expressed as a function of the Al^{VI} of amphibole in the Passadumkeag River pluton. Plagioclase in the core facies has a higher An content than plagioclase in the rim facies for a given value of Al^{VI} in the coexisting amphibole. No compositional trend is evident for coexisting plagioclase and amphibole for the entire pluton, although samples from the rim facies suggest lower An contents of plagioclase in amphibole with higher values of Al^{VI}.

Results of biotite analyses for Al^{IV} form a wide band ranging from about 1.12 to 1.21 (atoms per 11 oxygens) (fig. 19). In contrast to the biotites from the core and rim facies in the Whitney Cove pluton, the most aluminous biotites from the rim facies of Passadumkeag River pluton are generally correlated with the most albitic plagioclase (fig. 22). Total aluminum shows no correlation with the total alkali content of biotite; total aluminum in biotite is roughly correlated positively with Fe/(Fe+Mg) ratio of the biotite and negatively with the silica content of the rock. The highest ratio of Fe/(Fe+Mg) and the sum of Al^{VI} and titanium occur in samples from the rim facies. However, the bulk of the pluton shows a lack of progressive variation expected from an idealized crystallization history.

INTERRELATIONS BETWEEN BIOTITE, AMPHIBOLE, AND ROCK

Both biotite and amphibole display similar ranges in Fe/(Fe+Mg) ratios, suggesting equilibrium partitioning during their crystallization (fig. 23). Samples that show the greatest deviations occur at the rim facies. The Fe/(Fe+Mg) ratios of biotite and amphibole show wide scatter above the 1:1 line at values lower than 0.64. At values higher than 0.66, amphibole tends to have slightly higher ratios than coexisting biotite (fig. 23).

In a plot of Al^{VI} for biotite and hornblende (not shown), the most aluminous hornblende is positively correlated with biotite. This systematic change suggests that hornblende is enriched in Al^{VI} at twice the rate of biotite. The variation (K_D) in $Al^{IV}/(Al^{IV}+Si)$ in biotite and amphibole in relation to the sum of Al^{VI} and titanium is very limited and lacks a positive correlation in the Passadumkeag River pluton.

The distribution of titanium between coexisting biotite and hornblende is typical of granitic systems (Czamanske and Wones, 1973; Czamanske and others, 1977), showing a slight enrichment in favor of biotite (K_D amphibole/biotite=0.9). Also, as suggested by these authors and by Greenland and others (1968), manganese is concentrated in amphibole by a factor of about 4.

PLAGIOCLASE

The textural variation shown by plagioclase is significant. Plagioclase occurs forming two petrographic groups of phenocrysts, as groundmass grains, and in fine-grained clusters with mafic minerals. The composition of plagioclase does not clearly relfect the modal zoning from the granitic rim facies toward the core (figs. 18, 22). Although plagioclase compositons of An_{46} occur within the inclusion-rich phenocrysts in the core facies, the average is An_{20-30}. In general, plagioclase in the Passadumkeag River pluton shows large compositional variability within each facies (table 10). The only distinction is that the average compositon of plagioclase cores in the rim facies is constrained to less than An_{25} whereas plagioclase in the core facies is generally more calcic. In some cases, plagioclase inclusions within alkali feldspar are the most calcic compositions within a sample. Matrix plagioclase shows a range between An_{12} to An_{28}, overlapping the composition of the plagioclase phenocrysts.

ALKALI FELDSPAR

The composition of alkali feldspar shows insignificant variations between facies. This general compositional homogeneity probably resulted form deuteric alteration and reequilibration to compositions of Or_{85-98}. Inclusions of all other phases are commonly enclosed within subhedral alkali feldspar, arguing for late crystallizaton of alkali feldspar. Euhedral faces are only observed when alkali feldspar shares faces with quartz.

Rapakivi texture is uncommon in the Passadumkeag River pluton. In contrast with the Whitney Cove pluton, however, this texture is developed in a small number of alkali feldspar phenocrysts in most outcrops.

TABLE 9.—*Representative electron microprobe analyses and*

[Calculated per 11 oxygen atoms; total iron as FeO; R and

Column	1	2	3	4	5	6	7	8	9	10	11	12	13	14	15	16
Sample number	3C	4C	5C	9C	13C	17C	20C	75C	78C	79C	82C	84C	91C	105C	21C	25C
								Weight percent								
SiO_2	36.39	36.87	35.21	36.88	36.87	36.03	36.11	36.14	35.66	36.55	36.83	35.96	36.21	36.65	37.12	35.92
TiO_2	4.07	4.23	3.56	3.38	3.71	3.91	3.72	4.08	4.01	3.08	3.39	4.00	3.22	3.63	2.94	4.59
Al_2O_3	13.57	14.00	13.47	14.42	13.43	13.14	14.00	13.86	13.03	14.13	13.82	13.72	13.89	13.45	14.29	13.49
FeO	24.77	25.14	23.98	23.04	23.33	23.13	24.80	24.65	23.69	26.82	23.66	25.76	26.59	22.76	26.35	26.68
MnO	.48	.47	.54	.47	.51	.43	.51	.48	.42	.49	.49	.43	.36	.41	.65	.33
MgO	7.67	7.89	8.33	9.27	8.87	8.74	7.76	7.60	6.79	6.79	8.65	7.41	6.75	9.46	7.22	5.70
CaO	.04	.00	.05	.00	.06	.04	.00	.08	.00	.00	.06	.00	.00	.00	.00	.00
Na_2O	.08	.00	.08	.00	.12	.09	.00	.14	.00	.00	.08	.00	.00	.00	.00	.00
K_2O	9.20	9.48	8.88	9.32	9.40	9.81	8.96	9.64	11.12	9.76	9.47	9.33	9.41	9.83	9.36	9.48
BaO	.13	.15	.09	.18	.05	.09	.10	.00	.08	.14	.04	.07	.07	.15	.08	.06
P_2O_5	.01	.00	.01	.00	.00	.01	.00	.00	.00	.00	.01	.00	.00	.00	.00	.00
SrO	.02	.00	.03	.00	.00	.01	.00	.00	.00	nd	.02	.00	.00	.00	.00	.00
F	.46	.65	.82	.62	.86	.91	.63	.00	.89	.72	.73	.49	.77	.87	1.09	.62
Cl	.08	.12	.06	.18	.58	.06	.06	.00	.07	.05	.07	.06	.41	.06	.32	.35
Total	96.97	99.00	95.11	97.76	97.79	96.40	96.65	96.67	95.76	98.53	97.32	97.23	97.68	97.27	99.42	97.22
								Number of atoms								
Si	2.81	2.79	2.77	2.80	2.81	2.79	2.80	2.81	2.82	2.81	2.82	2.79	2.80	2.80	2.81	2.80
Ti	.24	.24	.21	.19	.21	.23	.22	.24	.24	.18	.20	.23	.19	.21	.17	.27
Al	1.24	1.25	1.25	1.29	1.21	1.20	1.28	1.27	1.21	1.28	1.25	1.25	1.27	1.21	1.28	1.24
Fe	1.60	1.59	1.58	1.46	1.49	1.50	1.61	1.60	1.56	1.72	1.51	1.67	1.72	1.46	1.67	1.74
Mn	.03	.03	.04	.03	.03	.03	.03	.03	.03	.03	.03	.03	.02	.03	.04	.02
Mg	.88	.89	.98	1.05	1.01	1.01	.90	.88	.80	.78	.99	.86	.78	1.08	.81	.66
Ca	.00	.00	.00	.00	.01	.00	.00	.01	.00	.00	.01	.00	.00	.00	.00	.00
Na	.01	.00	.01	.00	.02	.01	.00	.02	.00	.00	.01	.00	.00	.00	.00	.00
K	.91	.92	.89	.90	.91	.97	.89	.96	1.12	.96	.92	.92	.93	.96	.90	.94
Ba	.00	.01	.00	.01	.00	.00	.00	.00	.00	.00	.00	.00	.00	.01	.00	.00
P	.00	.00	.00	.00	.00	.00	.00	.00	.00	.00	.00	.00	.00	.00	.00	.00
Sr	.00	.00	.00	.00	.00	.00	.00	.00	.00	.00	.00	.00	.00	.00	.00	.00
F	.11	.16	.20	.15	.21	.22	.15	.00	.22	.18	.18	.12	.19	.21	.26	.15
Cl	.01	.02	.01	.02	.07	.01	.01	.00	.01	.01	.01	.01	.01	.01	.04	.05
Fe/(Fe+Mg)	.65	.64	.62	.58	.60	.60	.64	.65	.66	.69	.60	.66	.69	.57	.67	.73

Granophyre is evident in samples close to the granite-country rock contact. These samples are commonly associated with other textures which include myrmekitic intergrowths, with development of mortar or granulated texture, and with deeply embayed and corroded rims of biotite and opaques.

QUARTZ

Quartz is concentrated in the matrix, especially within the felsic clusters. Subhedral to anhedral grains, typically showing undulatory extinction and sutured borders are characteristic of this pluton. The absence of euhedral faces of quartz in contact with all other phases except alkali feldspars indicates that quartz is one of the latest phases to precipitate.

SEQUENCE OF CRYSTALLIZATION

Petrographic observations support the following sequence of crystallization: zircon plus apatite; oxides, sulfides, and clinopyroxene(?); and allanite plus sphene. Hornblende, biotite, and plagioclase crystallized next, followed by quartz plus alkali feldspar (fig. 24).

SUMMARY OF THE BULK CHEMISTRY

The Passadumkeag River pluton is mineralogically and texturally zoned from rim to core facies, and this zoning is also shown in its bulk chemical composition (Ayuso and others, 1982a) (fig. 25). Some of the most important bulk chemical results are as follows: (1) The core facies is higher in CaO, MgO, Fe_2O_3, TiO_3, P_2O_5 and

structrual formulae of biotite from the Passadumkeag River pluton

C represent rim and core facies, respectively; nd, not determined]

17	18	19	20	21	22	23	24	25	26	27	28	29	30	31	32	33	34
29C	31C	34C	36C	73C	110C	112C	113C	2R	8R	10R	14R	27R	35R	74R	80R	88R	90R
Weight percent—continued																	
36.51	36.09	34.60	36.36	36.52	35.66	36.24	36.97	36.73	36.71	36.64	36.26	36.46	36.24	35.65	36.51	36.66	36.57
4.04	3.39	4.17	4.09	3.48	3.90	4.09	3.82	3.09	3.02	3.46	3.55	3.55	3.03	3.76	3.44	3.37	3.28
13.54	13.84	12.87	13.53	14.34	13.63	13.37	13.52	14.68	13.90	13.41	14.31	13.74	13.56	12.92	14.16	14.10	14.66
23.09	24.12	21.72	25.28	25.88	25.02	25.54	22.99	27.50	23.42	23.76	28.02	26.00	26.39	24.03	22.92	26.09	28.57
.34	.42	.48	.50	.44	.51	.47	.44	.85	.45	.43	.71	.40	.59	.49	.60	.55	1.06
9.09	8.32	7.13	7.37	7.20	7.44	7.31	8.83	5.39	8.86	8.17	4.37	7.87	6.43	8.39	8.38	7.55	4.03
.02	.00	.06	.07	.00	.07	.13	.23	.00	.08	.09	.00	.00	.07	.07	.05	.00	.00
.00	.00	.12	.08	.00	.15	.09	.08	.00	.12	.08	.00	.00	.05	.11	.06	.00	.00
9.44	9.45	9.00	9.60	10.03	9.29	9.17	9.55	9.62	9.79	9.70	9.44	9.34	9.26	9.85	8.87	9.57	8.85
.09	.08	.18	.19	.16	.21	.15	.18	.08	.18	.17	.10	.07	.09	.04	.03	.15	.06
.00	.00	.00	.00	.00	.00	.00	.00	.00	.00	.00	.00	.00	.01	.01	.01	.00	.01
.00	.00	.00	.00	.00	.00	.00	.00	.00	nd	nd	.00	.00	.00	.04	.05	.00	.00
.67	.55	.75	.44	.74	.57	.62	.81	.92	nd	.87	.85	.60	.40	.94	.98	.53	.91
.09	.06	.08	.13	.07	.13	.08	.08	.04	.11	.08	.07	.10	.05	.05	.07	.06	.10
96.92	96.32	91.16	97.64	98.86	96.58	97.26	97.50	98.90	96.64	96.86	97.68	98.13	96.17	96.35	96.13	98.63	98.10
Number of atoms—continued																	
2.80	2.80	2.83	2.81	2.79	2.78	2.81	2.82	2.82	2.84	2.83	2.83	2.80	2.85	2.78	2.81	2.80	2.83
.23	.20	.26	.24	.20	.23	.24	.22	.18	.18	.20	.21	.20	.18	.22	.20	.19	.19
1.22	1.27	1.24	1.23	1.29	1.25	1.22	1.22	1.33	1.27	1.22	1.31	1.24	1.26	1.19	1.30	1.29	1.34
1.48	1.57	1.48	1.63	1.65	1.63	1.65	1.47	1.76	1.51	1.53	1.83	1.67	1.74	1.57	1.48	1.67	1.85
.02	.03	.03	.03	.03	.03	.03	.03	.06	.03	.03	.05	.03	.04	.03	.04	.04	.07
1.04	.96	.87	.85	.82	.87	.84	1.00	.62	1.02	.94	.51	.90	.75	.98	.96	.86	.47
.00	.00	.01	.06	.00	.01	.01	.02	.00	.01	.01	.00	.01	.01	.00	.00	.00	.00
.00	.00	.02	.01	.00	.02	.01	.01	.00	.02	.01	.00	.01	.02	.01	.00	.00	.00
.92	.94	.94	.95	.98	.93	.91	.93	.94	.97	.96	.94	.91	.93	.98	.87	.93	.87
.00	.00	.01	.01	.01	.01	.01	.01	.00	.01	.01	.00	.00	.00	.00	.00	.00	.00
.00	.00	.00	.00	.00	.00	.00	.00	.00	.00	.00	.00	.00	.00	.00	.00	.00	.00
.00	.00	.00	.00	.00	.00	.00	.00	.00	.00	nd	nd	.00	.00	.00	.00	.00	.00
.16	.14	.19	.11	.18	.14	.15	.20	.22	nd	.21	.21	.15	.10	.23	.24	.13	.22
.01	.01	.01	.02	.01	.02	.01	.01	.01	.01	.01	.01	.01	.01	.01	.01	.01	.01
.59	.62	.63	.66	.67	.65	.66	.60	.74	.60	.62	.78	.65	.70	.62	.61	.66	.80

Al_2O_3; (2) silica increases in a regular gradient from 65 percent in the core to 77 percent in the rim; and (3) the total alkali element content shows no significant enrichment in the more felsic rocks (table 11; fig. 25).

Normative composition of this pluton shows that it is slightly corundum normative (less than 2 percent) and that it exhibits higher normative anorthite in the core facies. As in the Whitney Cove pluton, normative compositions are not directly correlated with the abundance of silica.

Preliminary analyses of the same suite of trace elements analyzed in the Whitney Cove pluton confirm the reverse zonation in the Passadumkeag River pluton. Higher zirconium, yttrium, and strontium abundances are characteristic of most of the interior rocks of the Passadumkeag River pluton; niobium shows little variation in abundance from rim to core. More mafic granitic rocks tend to have higher barium than the more felsic rocks. With increasing silica, the variation of rubidium in the core and rim facies of the Passadumkeag River pluton suggests that each facies follows a slightly different trend. The Passadumkeag River pluton has lower contents of strontium at a given silica value than the Whitney Cove pluton.

The compositional diversity and field relations determined from representative analyses of wall-rock xenoliths argue for a minimum degree of interaction with the granitic melt. Control of the mafic xenoliths on the evolution of the granitic melt is uncertain, however, partly because of the petrographic diversity evident even within single outcrops. This diversity is indicated in the spread of compositions of the mafic xenoliths, as they are only broadly correlated to the trend defined by the granites.

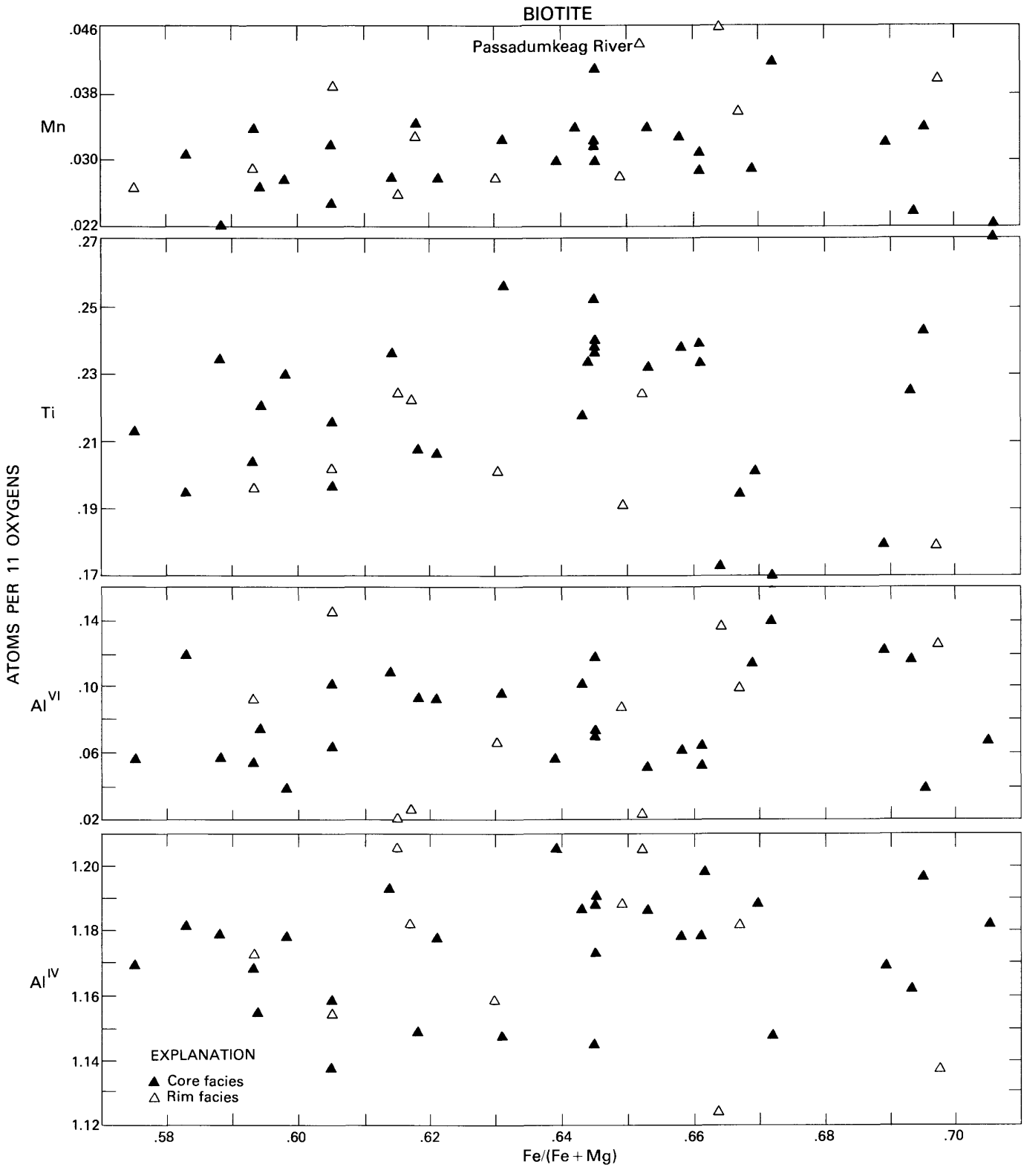

FIGURE 19.—Compositions of biotite in the Passadumkeag River pluton as a function of Fe/(Fe+Mg). Note that biotite from the core and rim facies has similar contents of titanium. Biotite from the rim facies has a wide range in Fe/(Fe+Mg) ratios. See table 9 for specific manganese, titanium, and Fe/(Fe+Mg) values.

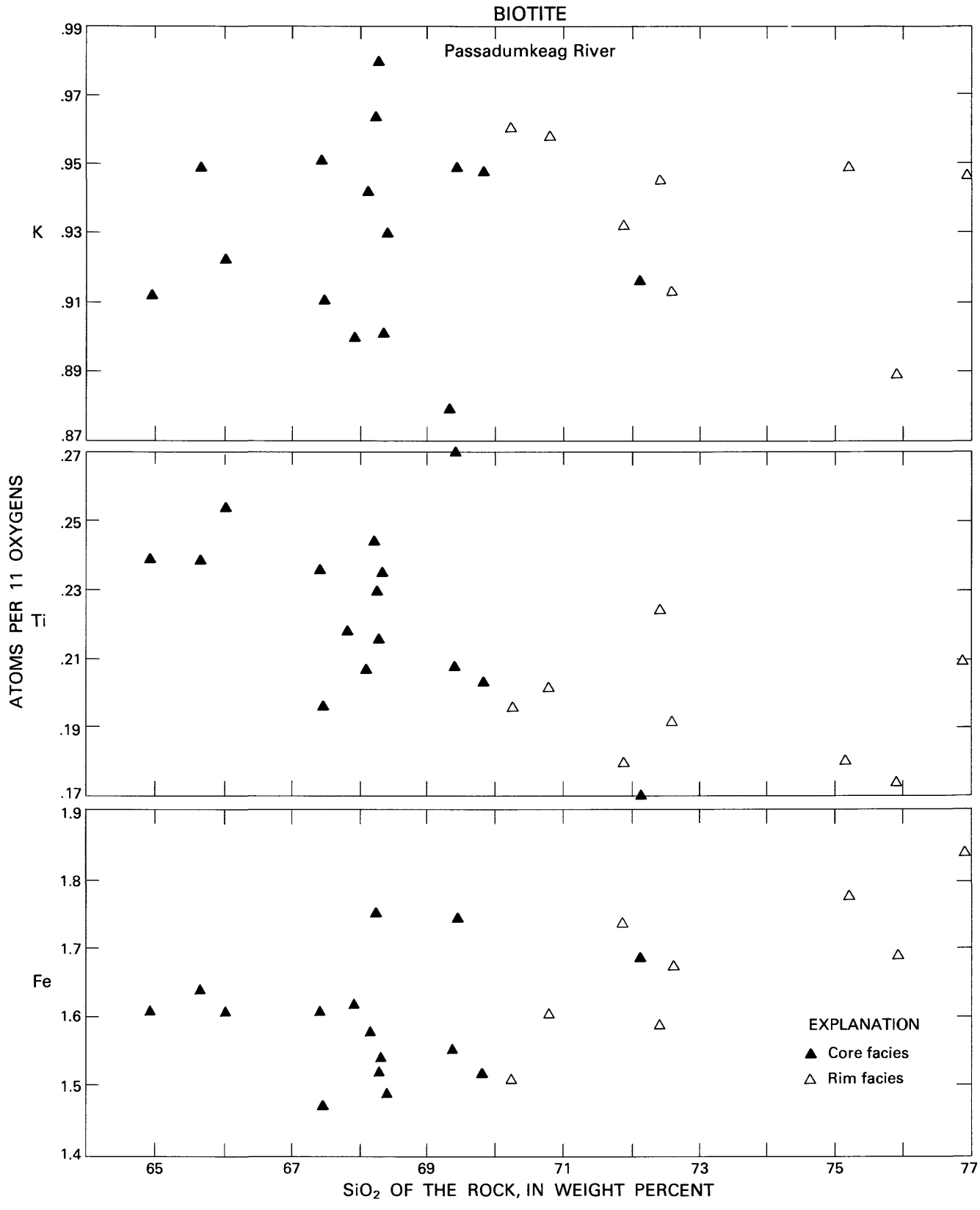

FIGURE 20.—Compositions of biotite composition as a function of the SiO_2 content of the rock in the Passadumkeag River pluton. Note the general correlation between titanium and the silica content of the rock in samples from the core and rim facies. Potassium and iron show no clear correlation with the silica content of the rock.

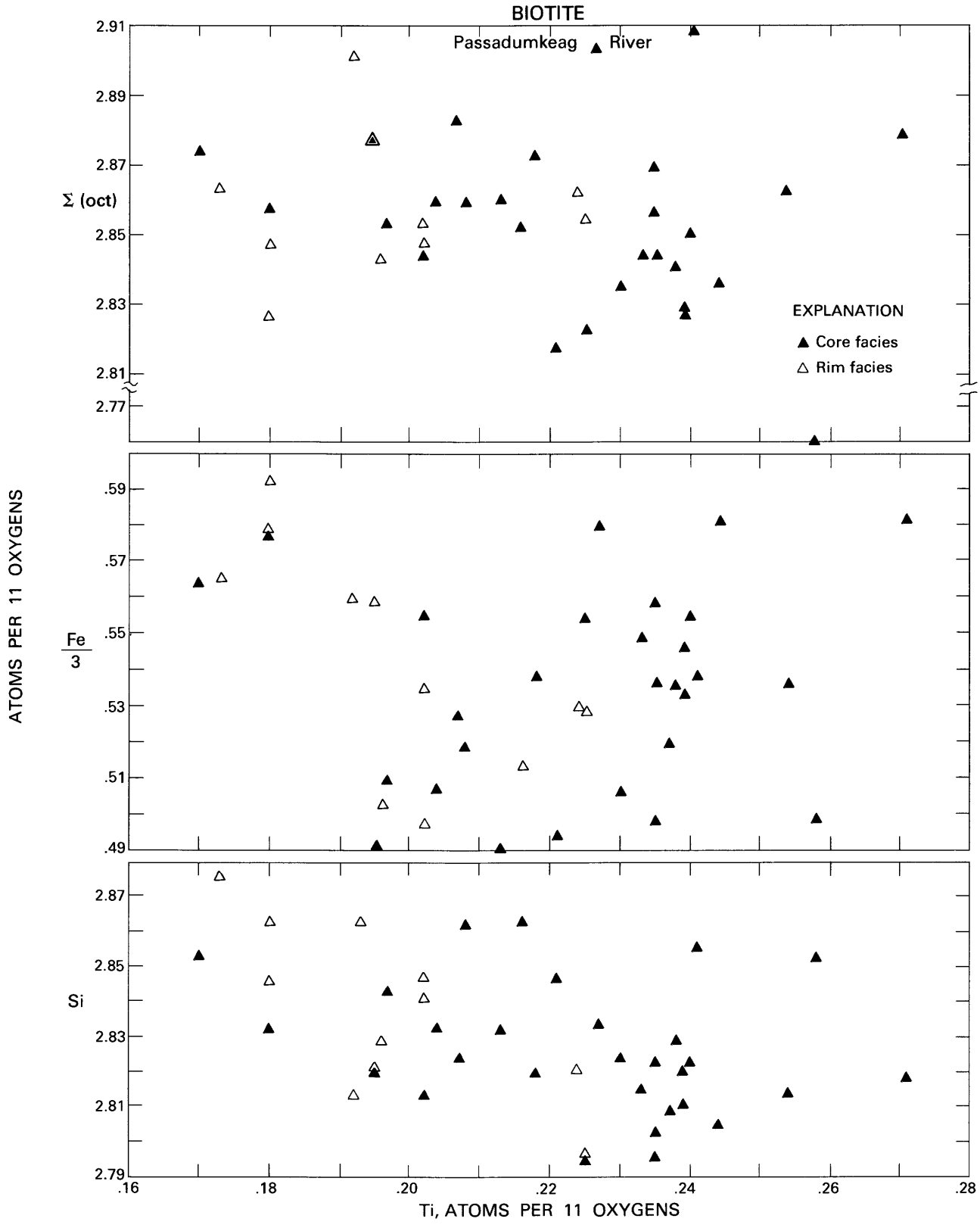

FIGURE 21.—Compositions of biotite in the Passadumkeag River pluton as a function of titanium content. Values are normalized to 11 oxygens. Note the lack of correlation between the total octahedral content, Fe/3, and silicon with the titanium content of biotite. See table 9 for specific titanium and silicon values.

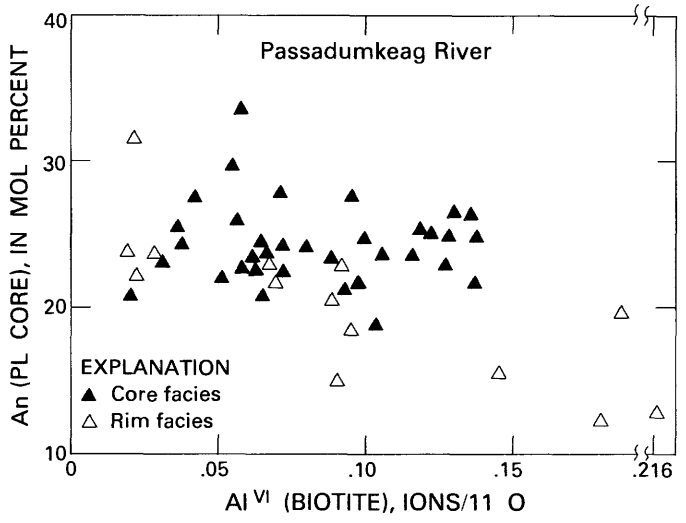

FIGURE 22.—The anorthite content (An) of plagioclase cores expressed as a function of the Al^{VI} content of biotite in the Passadumkeag River pluton. Higher anorthite in plagioclase generally occurs in the core rather than in the rim facies at a given value of Al^{VI} in biotite. No general trend is evident for the pluton as a whole. Lower An in plagioclase from the rim facies is broadly correlated with higher contents of Al^{VI} in biotite.

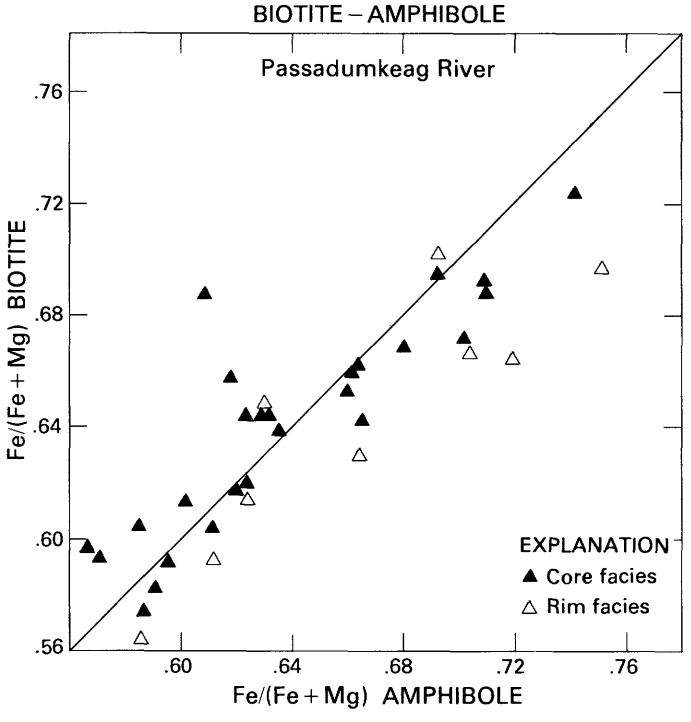

FIGURE 23.—Change in the Fe/(Fe+Mg) ratios of biotite coexisting with amphibole in the Passadumkeag River pluton. For comparison, the 1:1 line is also shown. Note that the compositions scatter about the 1:1 line and that both biotite and amphibole have similar ranges in Fe/(Fe+Mg).

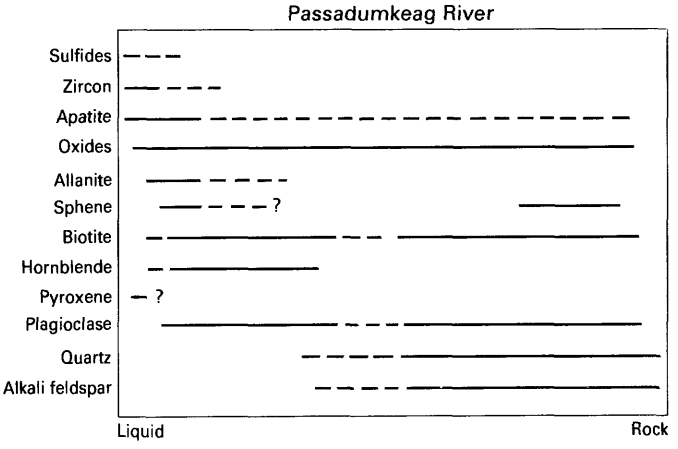

FIGURE 24.—The generalized order of crystallization in the Passadumkeag River pluton. Plagioclase, quartz, and alkali feldspar crystallized after biotite, hornblende, and the accessory suite.

Regular compositional variation in the Passadumkeag River pluton supports the contention that the core and rim facies are directly related. With the exception of the K_2O abundance, straight linear variations from the margins to the interiors are the norm. Overlap in bulk composition between the core and rim facies also supports a comagmatic origin for the entire pluton in the same manner evident in the Whitney Cove pluton.

Granitic rocks and their mafic xenolith hosts are strikingly different in bulk composition. Linear variations shown by the granite hosts contrast with the dispersed spread of the xenoliths and argue that although a certain degree of reaction must have taken place, the granite magma and xenoliths did not re-equilibrate fully. Lower silica and a more mafic bulk composition is characteristic of the mafic xenoliths, although they also exhibit irregular variations in Al_2O_3, MgO, CaO, K_2O, and P_2O_5 (fig. 25). The regression line obtained through the composition of the granitic rocks passes through the field defined by the mafic xenoliths. Given the dispersion of the bulk composition of the mafic xenoliths, it is difficult to relate them to the host rocks.

Crystallization of about 25 percent of the liquid with removal of 17 percent plagioclase, 8 percent biotite (and amphibole), and 0.5 percent apatite (and zircon) may account for the major and trace element variation from representative rocks from the core to rim facies. Results indicated, however, that the mafic xenoliths were not related to the host granites by any reasonable fractionation mechanism. Thus, they cannot represent autoliths, and more logically the xenoliths may be thought of as unrelated and accidental blocks obtained at depth by

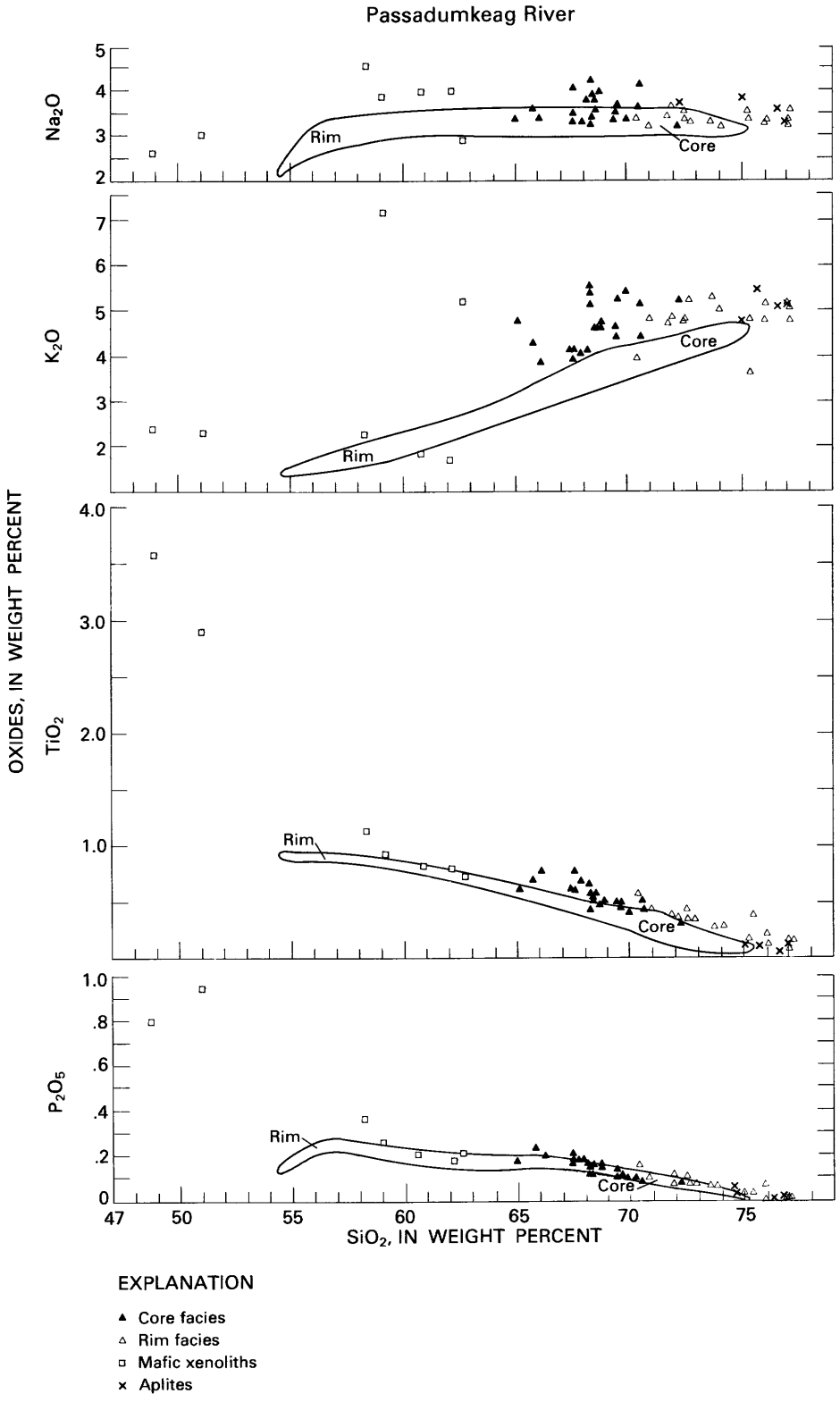

FIGURE 25.—Variation diagrams in the Passadumkeag River pluton showing the core and rim facies. The composition of the mafic xenoliths and aplites are also plotted. Most of the oxides are highly correlated with the silica content of the rock. Note the absence of major compositional gaps, and especially the more siliceous nature of the rim facies. Samples from the rim facies are lower in Al_2O_3, Fe_2O_3, MgO, TiO_2, P_2O_5 and CaO than the core facies. This compositional zoning of rocks from a single pluton is opposite to the arrangement occurring in concentric and normally zoned plutons. Note the large fields defined by the composition of the mafic xenoliths, extending toward less silicieous compositions than the host granites. The generalized compositional field for the Mount Givens granodiorite (Bateman and Nokleberg, 1978)

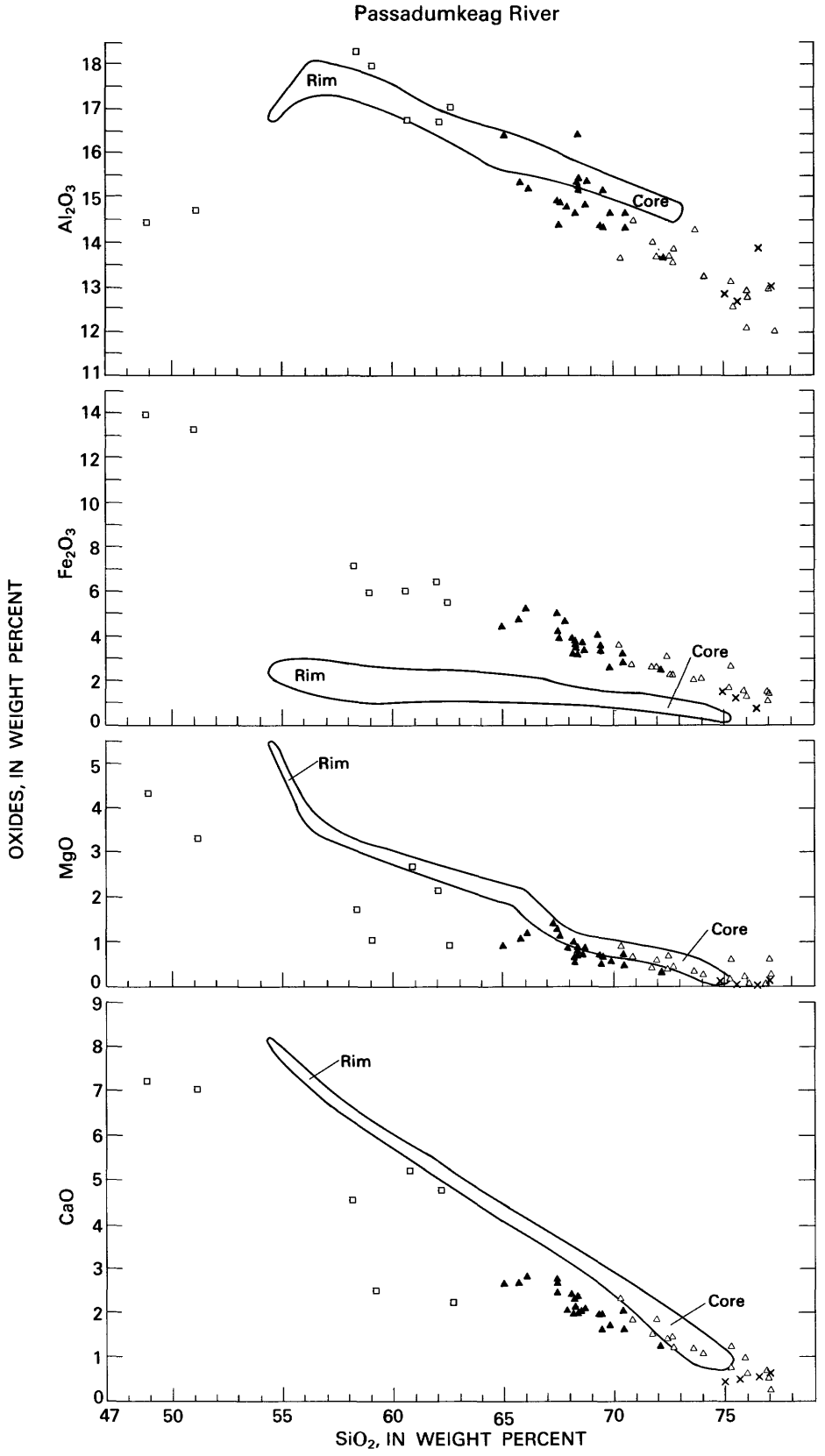

showing the core and rim portions of a typical normally zoned pluton is illustrated for contrast with the reversely zoned Passadumkeag River pluton.

TABLE 11.—*Representative major and trace element analyses and norm compositions of the Passadumkeag River pluton*

[R and C refer to rim and core facies, respectively; total iron as Fe_2O_3; LOI, loss on ignition]

Column	1	2	3	4	5	6	7	8	9	10	11	12
Sample number	2R	6R	8R	10R	14R	15R	27R	13C	16C	17C	20C	21C
Weight percent												
SiO_2	75.17	71.72	70.25	70.79	76.98	76.00	72.59	69.82	68.52	68.27	67.81	72.12
TiO_2	.19	.41	.58	.44	.16	.14	.36	.41	.52	.50	.67	.33
Al_2O_3	13.15	14.04	13.66	14.53	12.12	12.81	13.56	14.69	14.89	15.46	14.81	13.70
Fe_2O_3	1.72	2.81	3.59	2.78	1.50	1.39	2.32	2.65	3.61	3.21	4.66	2.57
MnO	.06	.05	.06	.03	.03	.03	.03	.05	.06	.06	.11	.05
MgO	.15	.46	.89	.67	.06	.11	.38	.62	.73	.70	.87	.36
CaO	.81	1.55	2.35	1.87	.54	.69	1.17	1.75	2.02	2.10	2.47	1.28
Na_2O	3.52	3.41	3.36	3.19	3.30	3.35	3.24	3.35	3.55	3.30	3.31	3.09
K_2O	4.80	4.73	3.98	4.77	5.13	5.18	5.22	5.40	4.76	5.53	4.03	5.27
P_2O_5	.04	.09	.16	.11	.02	.01	.08	.10	.14	.13	.18	.08
LOI	.41	.31	.47	.45	.44	.33	.33	.47	.56	.38	1.15	.27
Total	100.02	99.58	99.35	99.63	100.28	100.04	99.28	99.31	99.36	99.64	100.07	99.12
Norm												
Q	34.47	30.16	30.64	25.97	36.86	35.06	31.14	25.45	24.79	22.82	27.03	31.20
C	.79	.71	.13	.03	.20	.46	.65	.40	.56	.54	.94	.78
Or	28.36	28.07	23.81	28.26	30.23	30.60	31.07	32.13	28.61	32.80	23.80	31.42
Ab	29.78	28.98	27.76	31.98	27.85	28.34	27.62	28.54	30.23	28.03	27.99	26.38
An	3.76	7.13	10.75	8.58	2.54	3.36	5.32	8.08	9.17	9.60	11.07	5.88
En	.37	1.15	2.24	1.67	.15	.27	.92	1.56	1.83	1.75	2.17	.91
Hm	1.72	2.82	3.64	2.79	1.50	1.39	2.34	2.67	3.63	3.22	4.66	2.59
Il	.13	.11	.13	.06	.06	.06	.07	.11	.13	.13	.24	.11
Tn	.00	.00	.00	.00	.00	.00	.00	.00	.00	.00	.00	.00
Ru	.12	.36	.52	.41	.13	.11	.33	.36	.46	.43	.55	.28
Ap	.10	.21	.38	.26	.05	.02	.19	.24	.33	.31	.43	.19
Trace elements in ppm												
Rb	266	129	132	137	229	170	178	170	184	152	151	230
Sr	52	150	192	163	34	46	126	178	181	218	208	146
Y	26	36	34	33	32	20	24	33	44	31	44	35
Ba	160	426	541	509	62	90	524	594	497	897	477	309
Zr	159	264	296	231	157	126	182	248	300	277	313	196
Nb	27	19	22	17	18	19	13	18	24	18	23	17

the granite magmas. As in the case of the Whitney Cove pluton, fractional crystallization cannot fully explain the reverse zoning in the Passadumkeag River pluton. Furthermore, the wide range in petrographic features and the dispersal in modal and bulk chemical abundances are difficult to explain simply by fractionation.

XENOLITHS IN THE BOTTLE LAKE COMPLEX

The two plutons of the Bottle Lake Complex, the Whitney Cove and the Passadumkeag River plutons, are geographically closely associated, but each encloses different abundances and kinds of xenoliths (Ayuso, 1979). Two xenolith types are recognized in the Bottle Lake Complex: metasedimentary and mafic.

METASEDIMENTARY XENOLITHS

Metasedimentary inclusions are concentrated near the granite-country rock contact and are of limited importance in affecting the evolution of the Bottle Lake Complex. The size and abundance of these xenoliths decreases toward the interior of the granites. Also, they retain characteristic bedding styles, structural and petrographic features that match protoliths in the country rock.

MAFIC XENOLITHS

Mafic xenoliths exhibit significant petrographic diversity among themselves as evidenced by their variable grain size, maximum dimension, abundance of

feldspar megacrysts, and wide range of biotite-to-amphibole ratios (Ayuso and Wones, 1980). The most abundant mafic xenoliths are porphyritic quartz-diorite rocks, fine to medium grained with prominent feldspar megacrysts. They are randomly distributed throughout the core facies of both granites but are especially abundant in the Passadumkeag River pluton. Mineralogic and size variability characterizes the xenoliths, as they range from mafic- to felsic-rich and from a few centimeters to 1 m in length.

Preliminary studies of the mineral chemistry in the mafic xenoliths show that the compositions of the mafic minerals are distinguishable from those in the host granite. This distinction is especially evident in biotite and to a lesser degree in amphibole. In contrast, the composition of plagioclase in the mafic xenoliths exhibits similar ranges (An_{45} to An_{20}) as those documented in the Passadumkeag River pluton.

Biotite in the mafic xenoliths is generally higher in aluminum but lower in titanium and alkalies(?) compared to biotite in the host rocks. Both groups of biotite, however, show similar Fe/(Fe+Mg) ratios (0.50–0.70). Amphibole mimics the compositional change in biotite and shows progressively higher titanium, iron, and alkalies but lower magnesium in amphibole of the granite coexisting with the xenolith.

The compositions of mafic and country rock xenoliths are plotted on the granite variation diagrams (figs. 12 and 25) for comparative purposes. Although wall-rock xenoliths may exert control over the chemistry of a pluton, small-scale assimilation of such xenoliths by granitic liquids of the Bottle Lake Complex resulted primarily in dilution of the granitic components. This dilution is suggested by the broadly calc-alkaline nature of the Bottle Lake Complex compared to the strongly silicic and peraluminous compositions of most country rocks. Also, the variation from more mafic to felsic rocks in the plutons follows a well-defined trend despite the wide range of lithologies representative of the country rocks. Finally, country rocks are significantly higher in $\delta^{18}O$ (12.0–13.4 permil) compared to the granites (8.3–9.9 permil) and mafic xenoliths (6.8–9.0 percent) (A. Andrew, 1982, written commun.) arguing against major interaction between these rock types.

COMPARISON OF GRANITES IN THE BOTTLE LAKE COMPLEX

Because of the scatter in the abundance of the alkali elements, the calc-alkali indices for the Bottle Lake plutons are roughly constrained to between 53 and 57. The range is lower than expected for calc-alkaline suites (60–64). Plotted on an AFM ($A=Na_2O+K_2O$; $F=FeO$; $M=MgO$) diagram, the composition of the plutons defines a band trending away from the FeO–MgO sideline toward the alkalies (fig. 26). This trend suggests a broadly calc-alkaline trend. Wall-rock xenoliths are distinct from this trend, while mafic xenoliths are generally alined in agreement with the plutons and plot more closely to the FeO–MgO sideline.

The composite nature of the Bottle Lake Complex, the circular or elliptical shape of the plutons, the development of an aureole by contact metamorphism, the range in the lithological variety of granitic rocks, and the presence of mafic-rich inclusions in the Bottle Lake Complex are in agreement with the field relations outlined by Chappell and White (1974) characteristic of I-type granites. On the basis of petrographic observations, it is also reasonable to classify the plutons as belonging to the magnetite-series of Ishihara (1977).

FELSIC DIKES

Aplites are relatively uncommon in the Bottle Lake Complex. However, one of the differences between the two plutons is that the Whitney Cove pluton is comparatively richer in felsic dikes (aplites, pegmatites, granophyres) than the Passadumkeag River pluton. Additionally, a few small miarolitic cavities (1–3 mm) are concentrated in the Whitney Cove pluton, west of Pug Lake (V) in the Scraggly Lake quadrangle, but appear to be absent in the Passadumkeag River pluton (pl. 1). The aplite dikes consist of fine-grained leucocratic rocks ranging from a few centimeters to 0.8 m in thickness. They often show diffuse contacts with the host granites, extreme variation in attitude, and mineralogical banding from felsic borders to thin biotite zones which culminate in a pegmatitic core.

Muscovite is present in some of the aplites exposed within the plutons, especially in the core of the Whitney Cove pluton. Muscovite is best developed, however, in pegmatitic pods near granite-country rock contacts together with long blades (3–5 cm) of black tourmaline. These areas are exposed west of Almanac Mountain (A) and north of Bowers Mountain (S) in the Springfield and Scraggly Lake quadrangles (pl. 1).

Within the Bottle Lake Complex, felsic dikes are common east of Sysladobsis Lake (M) and along the shores of McLellan Cove (W), in Getchell Mountain (E) and south of Chamberlain Ridge (X). Felsic dikes are typically low in mafic minerals, accessories, and plagioclase. Compositonally, they represent the most felsic rocks of each pluton and characteristically contain less strontium but more rubidium than the associated granites.

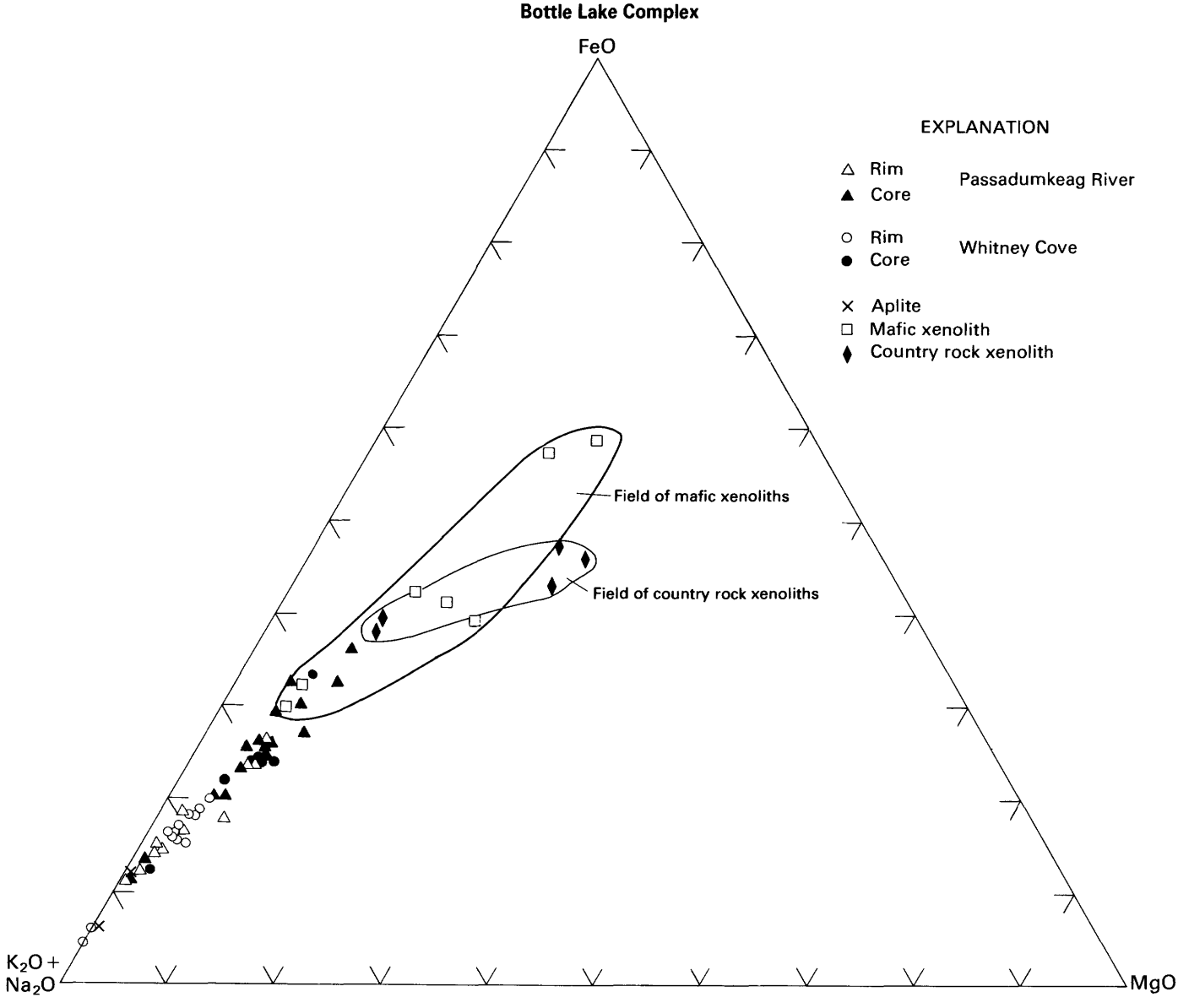

FIGURE 26.—AFM (A=Na_2O+K_2O; F=FeO; M=MgO) diagram showing the Bottle Lake Complex, the mafic xenoliths, and aplites. The composition of the plutons defines an array trending toward the alkalies and is broadly calc-alkaline. Mafic xenoliths of the Passadumkeag River pluton plot closest to the FeO–MgO sideline.

AMPHIBOLITE UNIT

An amphibolite unit crops out in the Scraggly Lake area, entirely confined within the cataclastic zone (pl. 1). This unit is best exposed in Hasty Cove (Y) and on islands near the southern shores of Mud Cove (DD). Most amphibolite outcrops are intensely sheared, jointed, and exhibit a strong northeast-trending foliation parallel to that of the granitic rocks. The predominant rock type is a fine-grained, greenish-black (5 GY 2/1) unit with sparse plagioclase phenocrysts. Contacts with the granitic rocks of the Whitney Cove pluton are characterized by a hybrid zone where porphyritic greenish-gray (5 G 6/1) rocks are abundant. Felsic dikes cut the hybrid zone and the amphibolite.

The mineralogy of the amphibolite consists of plagioclase, amphibole, and biotite with minor amounts of quartz and alkali feldspar. Apatite, allanite, sphene, ilmenite, magnetite, and zircon are also present. Apatite, however, is the most conspicuous accessory in this rock.

STRUCTURES

The generally massive fabric of the Bottle Lake Complex commonly persists outward to the granite-country rock contact. In foliated rocks, however, the feldspars are generally alined with (010) parallel to the contact. Extensive granite outcrops are developed on Lombard Mountain (R) and Getchell Mountain (E). Several areas within the granites also show foliated rocks consisting of the following: (1) zones within the core facies of the Passadumkeag River pluton; (2) foliated rocks of the rim facies of the Whitney Cove pluton developed in a cataclastic zone; and (3) rocks within the core facies of the Whitney Cove pluton.

Foliation within the core of the Passadumkeag River pluton is alined to the northeast but is not accompanied by the strong cataclastic deformation characteristic of most foliated areas in the Whitney Cove pluton. Foliated areas within the Whitney Cove pluton are commonly cut by bands of cataclastically deformed rocks. The two most important cataclastic areas are the northeast-trending fault zone of the Norumbega fault system and the fault zone which cuts the Whitney Cove pluton. Each of these zones is also characterized by foliated granitic rocks preferentially alined to the northeast in contrast with the apparent lack of regional alinement in the foliated rocks of the core facies in the Whitney Cove pluton.

At least three fault zones are exposed in the Bottle Lake Complex: the wide band of shearing that cuts the Whitney Cove pluton; the Norumbega fault system; and the fault that cuts the Topsfield facies which was mapped by Ludman (1978b). The northeast-trending (N40–50°E) cataclastic zone that cuts the Whitney Cove pluton terminates against the Passadumkeag River pluton. This zone extends from Orie Lake (Z) to Junior Lake (AA) in a well-exposed, 1.5–3.0-km-wide band in the Scraggly Lake quadrangle (pl. 1). Typical rocks are cataclastically deformed, sheared, and crisscrossed by quartz and epidote veins. Most outcrops in this zone show at least one set of mylonitic foliation to the northeast, although many show significant scatter in attitude. Spindle-shaped quartz grains are common in most exposures. Many outcrops also show evidence of right-lateral motion and up to 50 cm of displacement in east-trending fractures across individual mylonitic zones. Granitic rocks are pervasively and massively altered. Feldspars are crisscrossed by thin, epidote-rich veins and show extreme alteration, disintegration, shearing, and displacement, especially within plastic bands of recrystallized quartz and biotite.

The Norumbega fault zone is the major northeast-trending right-lateral system in the region and locally constitutes the southern contact of the Whitney Cove pluton (pl. 1). According to Wones (1979) the amount of displacement along the fault is unknown. Outcrops in Farm Cove (BB) of West Grand Lake in the Wabassus Lake quadrangle are good examples of intensely sheared, silicified and mylonitized granitic rocks.

A left-lateral fault mapped by Ludman (1978b) along the southern shores of East Musquash Lake (CC) near State Route 6 separates the Topsfield facies from the main mass of the Whitney Cove pluton (pl. 1). The fault is oriented east-west and is characterized by epidotized and intensely sheared red granitic rocks.

Mylonite veins are relatively common near the traces of the fault zones and also as randomly distributed and oriented features within the Whitney Cove pluton. Many of these veins are probably related to the identified faults in the region. However, the preponderance of mylonites showing a pronounced east-west trend is suggestive of a distinct and possibly later deformation unrelated to the identified faults.

Joints and fractures are common in most outcrops throughout the Bottle lake Complex. They often show large variation in attitude even within individual outcrops. On the basis of preliminary observations, no regional trend is displayed within the granitic rocks. Jointing is significantly increased with proximity to the areas of intense cataclastic deformation.

ESTIMATE OF INTENSIVE PARAMETERS DURING CRYSTALLIZATION

ESTIMATE OF PRESSURE

A combination of textural, chemical, and geologic observations may be used to place constraints on pressure, temperature, fugacity of water, and oxygen fugacity during crystallization of the Bottle Lake Complex. Total pressure is among the most difficult parameters to estimate. Plutons of the Bottle Lake Complex intruded country rock in the lower greenschist facies, almost certainly within the stability field of andalusite. Ludman (1978b) observed only andalusite in metamorphic rocks in the area to the northeast, and contiguous to the Bottle Lake Complex. Depending on the choice of equilibrium curves, maximum pressure estimates based on andalusite stability range from about 3.5 kbar (Holdaway, 1971) to about 5.5 kbar (Richardson and others, 1969). Rast and Lutes (1979) estimated a pressure range of 1.5 to 3 kbar at the contact of the Pokiok-Skiff Lake granite (immediately to the northeast of the Bottle Lake Complex) on the basis of presence of

coexisting garnet-cordierite-andalusite-biotite assemblages. Similarly, the existence of garnet-cordierite-biotite assemblages (Hess, 1969) in the country rock intruded by the Bottle Lake Complex suggests a pressure interval of 1.5 to 4.5 kbar.

Rast and Lutes (1979) cite the estimate by Garland (1953) of about 2 kbar for the maximum thickness of cover north of the Bottle Lake Complex. This estimate is also consistent with $P=2$ kbar for the emplacement of the Center Pond pluton (Scambos, 1980) which lies immediately west of the Passadumkeag River pluton.

Obvious signs of crystallization of the Bottle Lake Complex under water-saturated conditions are absent. It seems reasonable to suggest that because of the small number of aplites, pegmatites, and miarolitic cavities, only the most evolved rocks are equivalent to the synthetic Q–Ab–Or–H_2O system (Tuttle and Bowen, 1958; Luth, 1969; James and Hamilton, 1968). Each of these units yields an estimate of pressure during emplacement. On this basis, and assuming that $P_{H_2O}=P_{total}$, a range between 1.5 and 2.5 kbar probably existed during emplacement of the Bottle Lake Complex (fig. 27). Assuming that $P_{H_2O}=P_{total}=2$ kbar and that normative Ab/An=5.2 in the rock, a temperature of 685°C (±50°C) is estimated from the experimental data for granite minimum melts studied by von Platen (1965).

ESTIMATE OF WATER CONTENT

Water content in the original magmas of the Bottle Lake Complex was estimated by comparison of the order of crystallization with granodiorite experimental systems obtained by Naney (1978) and in conjunction with experimental systems documenting the paragenetic sequence of mafic phases in K_2O-rich magmas (Wones and Dodge, 1977). Early crystallization of euhedral hornblende together with euhedral biotite imposes minimum water contents on these granitic magmas. In the case of relatively high water activity, amphibole precedes phlogopite in the crystallization sequence. Such a sequence is present in the Passadumkeag River pluton, supporting the suggestion that water activity was relatively high during much of the crystallization of this granitic magma. Comparison of the mineralogy and order of crystallization observed in the Passadumkeag River pluton with pertinent systems studied by Naney (1978) suggests that water saturation occurred only in the latest stages of solidification. Water content probaby never exceeded 4 weight percent.

The established order of crystallization for the Whitney Cove pluton also limits the water content of the magma. Vapor saturation occurred relatively late but at an earlier stage than in the Passadumkeag River pluton. Melts in this pluton probably never exceeded a maximum water content of 5 weight percent. Prominent alkali feldspar megacrysts are present in the core facies of this pluton because they grew faster than plagioclase and quartz (Swanson, 1977; Fenn, 1973), although this growth occurred relatively late in the sequence when water conditions in the pluton were still undersaturated.

ESTIMATE OF t, f_{O_2}, f_{H_2O}

Although temperature of crystallization may be estimated from the equilibrium distribution of the albite molecule in coexisting plagioclase and alkali feldspar, the approach is not useful in the case of the Bottle Lake complex because of substantial feldspar reequilibration. Sanidization of alkali feldspar and use of powder diffraction techniques (Wright, 1968; Wright and Stewart, 1968) suggest that the bulk composition is in the range of Or_{85} to Or_{98}. Application of the feldspar geothermometer (Stormer, 1975) yields a large spread in temperature from 450 to 800°C with most estimates clustered at about 450 to 550°C. These temperatures are lower than expected for a minimum melt at about 2 kbar (about 685°C) and result from the high orthoclase content of the alkali feldspar, probably caused by secondary processes.

Examination of coexisting oxides provides a way of simultaneously estimating f_{O_2} and t (temperature in °C). Unfortunately, such estimates also yield unrealistically low temperatures (400–500°C) of equilibration of the Bottle Lake Complex. The composition of ilmenite is enriched in MnO probably making this phase untractable by the Buddington and Lindsley (1964) scheme (Czamanske and Mihalik, 1972). Despite the coexistence of magnetite and ilmenite, the use of the geothermometer yields temperatures probably reflecting secondary processes.

The modal abundance of magnetite and ilmenite displays significant variation in the Bottle Lake Complex. Either magnetite or ilmenite may be dominant in a sample. In at least one sample in the Whitney Cove pluton, inclusions within plagioclase were exclusively ilmenite, while magnetite predominated in the matrix. Within the core of the Passadumkeag River pluton, many samples were dominantly of ilmenite rather than magnetite, but nearby rocks had subequal amounts of both phases.

Coexistence of sphene and magnetite throughout the Bottle Lake Complex and essentially throughout the crystallization history marks the minimum f_{O_2} during crystallization. Wones (1966) suggested that this

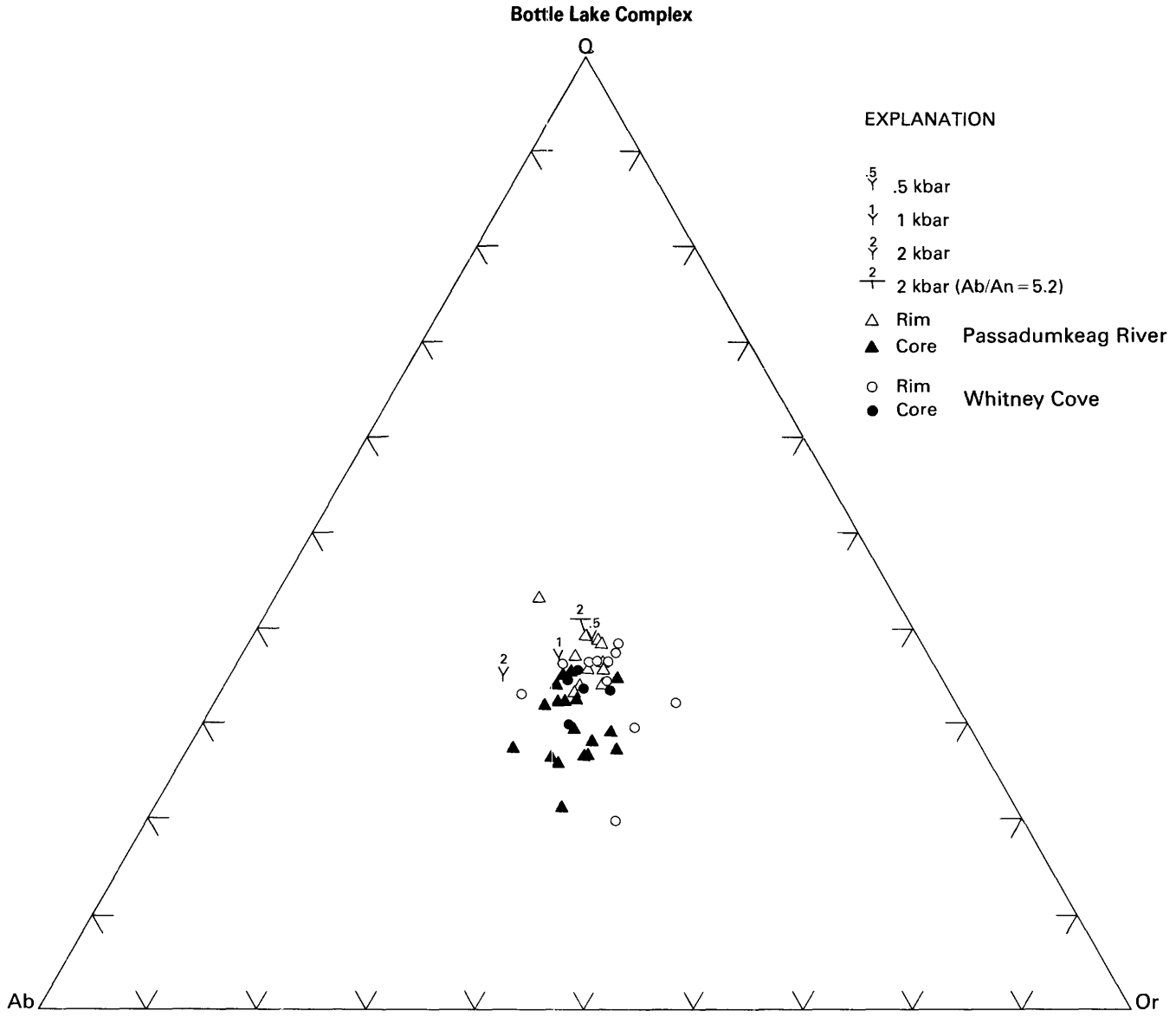

FIGURE 27.—Normative quartz-albite-orthoclase-water (Q-Ab-Or-H_2O) diagram for rocks of the Bottle Lake Complex. Experimentally derived minima are from Tuttle and Bowen (1958), Luth and others (1964), Luth (1969), and James and Hamilton (1968). Data for 2 kbar and Ab/An=5.2 are from von Platen (1965). Rocks from the rim facies of the Passadumkeag River pluton are more restricted in composition than the core facies and plot near the ternary minima ($P_{H_2O}=P_{total}$) for 0.5 kbar and 1 kbar; they are also close to the 2 kbar minimum for Ab/An=5.2. Rim facies rocks of the Whitney Cove pluton are widely scattered in comparison to the core facies.

equilibrium lies at slightly higher oxygen fugacities than the Ni-NiO buffer curve (Huebner and Sato, 1970). An estimate of the highest f_{O_2} during crystallization is represented by the Fe_3O_4-Fe_2O_3 buffer curve (Eugster and Wones, 1962; Chou, 1978) because primary hematite is absent.

Subsolidus or late changes in f_{O_2} are exemplified by the appearance of secondary sphene rims around granular ilmenite and by the growth of alined opaque minerals (magnetite and ilmenite) in biotite. Both phenomena are common in the Whitney Cove pluton, but they are also present in the Passadumkeag River pluton. Feathery intergrowths in biotite, ilmenite, and magnetite, and extremely fine-grained felsic phases also attest to the effect of secondary changes late in the crystallization history of the Bottle Lake Complex.

The oxidation-dehydration reaction

annite+oxygen=sanidine+magnetite+water

$$KFe_3AlSi_3O_{10}(OH)_2+1/2\ O_2=KAlSi_3O_8+Fe_3O_4+H_2O$$

can be used to estimate t, f_{H_2O}, and f_{O_2} (Wones and Eugster, 1965; Wones, 1972). The most recent description of the curve relating that assemblage is given by

$$\log f_{H_2O}= \frac{4819}{t}+6.69+3\log X_{ann}-\log a_s-\log a_m$$

$$+1/2\log f_{O_2}- \frac{0.011\ (P-1)}{T}\ ,$$

determined by D. A. Hewitt (oral commun., 1980), where X_{ann} is the mole fraction of iron in octahedral coordination in biotite; T is the temperature in °K, and P is pressure in kilobars. The activity of sanidine in the feldspar solid solution (a_s) is assumed to be about 0.6 (Waldbaum and Thompson, 1969), reflecting magmatic compositions prior to the onset of secondary processes resulting in feldspar reequilibration. The activity of magnetite (a_m) is unity because this phase is nearly pure. Values of f_{H_2O} were taken from Burnham and others (1969).

Although biotites in the Bottle Lake Complex evolved under relatively high f_{O_2} conditions, they did not coexist with primary hematite. Nevertheless, the amount of Fe^{+3} in these biotites is unknown and this could considerably extend their calculated stabilites (Wones, 1972). In the same manner, Czamanske and Wones (1973) suggested that substitution of F^- or O^{2-} for OH^- lowers the activity of annite and increases the stability of biotite. Similar results may arise from the effects of titanium (Robert, 1976) and aluminum (Rutherford, 1972).

Curves relating oxygen fugacity to temperature were generated by determining the composition of coexisting phases and by assuming constant fugacities of H_2O. These curves constrain f_{O_2} and t when plotted against estimates of f_{O_2} derived from examination of coexisting assemblages (sphene+magnetite+quartz) and estimates of the stability curves of coexisting oxides (Buddington and Lindsley, 1964). In this way, the intersection of the average biotite stability curve for each facies and appropriate oxide or buffer curve limits the maximum t and f_{O_2} for that granite facies at the chosen f_{H_2O}.

Biotite stability curves in figure 28 show the range of $f_{O_2}-t$ variation found in the Bottle Lake Complex. The intersection with the Ni-NiO buffer curve provides for upper temperature limits as the Fe^{+3} content of the biotite is unknown. Temperatures from 720 to 780°C are indicated, although the range may be lower for oxygen fugacities higher than the Ni-NiO curve and more representative of the assemblage for magnetite and sphene.

Typical biotite samples from the core and rim facies of the Whitney Cove pluton are separated by almost one log unit f_{O_2}. Higher temperature and f_{O_2} conditions apparently describe the core facies of this pluton in comparison to the rim. The two representative samples of the Passadumkeag River pluton show that the core and rim facies have a similar $f_{O_2}-t$ interval of crystallization. However, the values of f_{O_2} in core samples of the Passadumkeag River pluton indicate that oxidation differences in the assemblages of continuous outcrops are probably still evident.

The variation in magnetite/ilmenite ratios in outcrops and of f_{O_2} in the Bottle Lake Complex suggests that intrinsic oxidation variations may still be present, probably as a reflection of the source materials. Although the Whitney Cove pluton has a larger range in f_{O_2} than

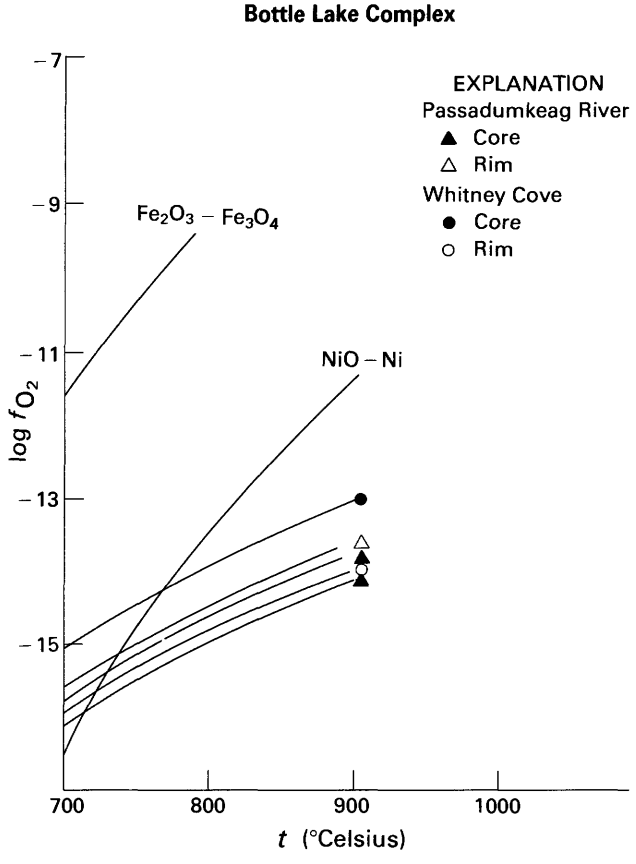

FIGURE 28.—Stability curves of biotite from the Bottle Lake Complex on a log $f_{O_2}-t$ graph. Curves for the assemblages $Fe_2O_3-Fe_3O_4$ and NiO-Ni are shown for comparison. For the Whitney Cove pluton, biotite from the core facies shows higher f_{O_2} and temperature of equilibration than biotite from the rim facies. In the Passadumkeag River pluton, biotite from the core and rim facies shows similar values for temperature and f_{O_2}.

the Passadumkeag River pluton, the two plutons show a large degree of overlap.

Core samples of the Whitney Cove pluton indicated the highest temperature (780°C) while the rim facies showed the lowest (725°C). Core facies samples of the Passadumkeag River pluton show an interval of maximum temperature from 720 to 740°C, whereas biotite from the rim facies shows a slightly higher temperature (745°C). However, because of the range and variation in Fe/(Fe+Mg) ratios of biotite within each facies and the assumptions inherent in the calculation of the biotite stabilities, this discrepancy is probably not significant.

Estimate of the $f_{H_2O}-t$ relations may also be made through the use of the biotite stability curves and the granite minimum melting curve (Tuttle and Bowen, 1958). An approximate range in f_{H_2O} from 760 to 1,250 bars, and in t from 715 to 750°C is estimated from figure 29. This fugacity corresponds to a pressure ranging from 1 to 1.8 kbar (Burnham and others, 1969). The lowest f_{H_2O} and highest temperature is present in the core sample of the Whitney Cove pluton, while the highest f_{H_2O} and lowest temperature was obtained from the rim of the Passadumkeag River pluton.

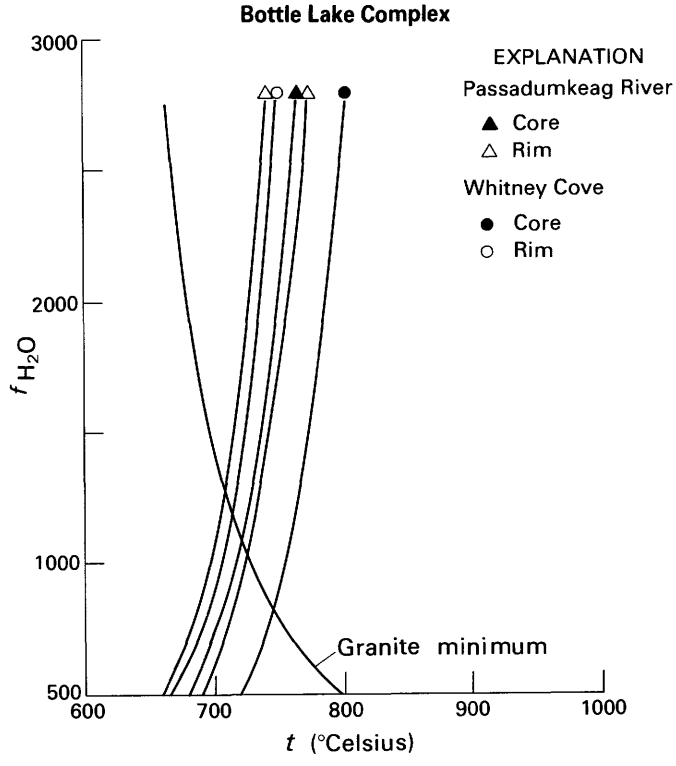

FIGURE 29.—Calculated stability curves of biotite from the Bottle Lake Complex and the minimum melting curve in the system Q—=Ab-Or (Tuttle and Bowen, 1958) plotted on a graph of f_{H_2O} and temperature. The core facies of the Whitney Cove pluton indicate lower f_{H_2O} values and higher temperature than the rim facies. Biotites from the rim facies of the Passadumkeag River pluton show a wide range in minimum temperature and water pressure values necessary for crystallization in a granitic melt.

GENERAL CHARACTERISTICS OF THE GRANITE SOURCE REGION

Petrologic similarities within the Bottle Lake Complex suggest that the two plutons were derived generally from geochemically equivalent but different source materials. Both plutons are basically alike in their essential mineralogy and key index accessory phases (primary sphene, allanite, zircon, apatite). The Passadumkeag and Whitney Cove plutons also show similar major element variations and abundances characterized by overlap in composition and trend.

The absence of relict aluminous phases (garnet, aluminosilicates, cordierite, or muscovite) and the presence of sphene and hornblende argue against a peraluminous source. Instead, source rocks of the Bottle Lake Complex must be dominated by a protolith of igneous character as suggested by field relations, accessory mineralogy, major and trace element composition, and relatively low initial ratios for lead and strontium.

A volcaniclastic source is consistent with the range in lead and strontium isotopic compositions in the Bottle Lake Complex (Ayuso and others, 1982b). Progressive melting of the granite sources implies that a compositional gradient be established, and this gradient is reflected in the isotopic makeup of the plutons. Although the Whitney Cove and Passadumkeag River plutons have distinctive lead and strontium isotopic compositions, a gradual trend exists from the least radiogenic values in the Passadumkeag River pluton to more radiogenic values in the Whitney Cove pluton. No isotopic distinction can be made between the marginal and interior facies. The isotopic composition of lead in whole rock and alkali feldspars (Ayuso, 1982) shows a trend in initial ratios from the Passadumkeag River pluton ($^{206}Pb/^{204}Pb$: 18.27–18.43; $^{207}Pb/^{204}Pb$: 15.62–15.68; $^{208}Pb/^{204}Pb$: 37.55–38.42) to the mafic xenoliths ($^{206}Pb/^{204}Pb$: 18.29–18.52; $^{207}Pb/^{204}Pb$: 15.64–15.67; $^{208}Pb/^{204}Pb$: 37.85–38.36) and the Whitney Cove pluton ($^{206}Pb/^{204}Pb$: 18.34–18.66; $^{207}Pb/^{204}Pb$: 15.66–15.71; $^{208}Pb/^{204}Pb$: 37.92–38.28). The initial Pb isotopic ratios in the metasediments ($^{206}Pb/^{204}Pb$: 18.37–25.79; $^{207}Pb/^{204}Pb$: 15.66–16.25; $^{208}Pb/^{204}Pb$: 38.42–45.71) are significantly more radiogenic than the plutons, implying that no major interaction occurred between the granites and the metasediments. The finding is in agreement with the δO^{18} values in the Bottle Lake Complex (8.3–9.9 permil) compared with the composition of the metasediments (13.0–13.4 permil) (A. Andrew, written commun., 1980).

The lead isotopic composition in the Bottle lake Complex suggests a gradual change in the source of the granites toward a volcaniclastic (graywacke) source with increasing input from continental debris. Lead isotopic compositions argue against an origin directly from mantle sources, from granulite rocks in the lower continental crust, or from the upper continental crust as represented by sediments exposed near the Bottle Lake Complex.

Whole-rock Rb–Sr determinations in the Bottle Lake Complex yield $^{87}Sr/^{86}Sr$ initial ratios of 0.7043±0.0001 for the Passadumkeag River pluton, and 0.7055± 0.0001 for the Whitney Cove pluton (Ayuso and Arth, 1983). The higher initial strontium isotopic ratios in the Whitney Cove pluton are in agreement with the trend toward more radiogenic initial lead isotopic compositions. Initial ratios for strontium in the range found in the Bottle Lake Complex are compatible with a volcaniclastic pile generally consisting of an oxidized, calcic source.

GEOLOGIC INTERPRETATION

Field studies indicate that the plutons of the Bottle Lake Complex are lithologically zoned (Ayuso and others, 1982a). In contrast to the more common normal zonation, the plutons are mineralogically and chemically reversely zoned. This reversal is suggested by a mappable interior facies richer in mafic minerals than normally forms during precipitation at higher temperatures (Bateman and Chappell, 1979). More felsic rocks are concentrated in the outer envelope and contradict the commonly accepted model of progressive crystallization toward the interior (see, for example Vance, 1961.) This arrangement of rock types in the Bottle Lake Complex is in marked contrast to that found in normally zoned plutons (Compton, 1955; Reesor, 1956; Bateman and others, 1965; Cobbing and Pitcher, 1972; Halliday and others, 1980). Bateman and Nokleberg (1978) demonstrated that in the Mount Givens granodiorite, an example of normal zonation, felsic minerals increase and mafic minerals decrease coreward. Also, the composition of plagioclase becomes more anorthite-poor in the Mount Givens granodiorite toward the interior of the pluton. All of these changes are reflected in the bulk composition of the rocks so that the most siliceous rocks are near the core of the intrusion (figs. 12, 25). The Bottle Lake Complex, as indicated in the previous sections, shows gradients in mineralogy and bulk compositon that are opposite of those found in typical normally zoned plutons. A summary of petrographic and geochemical features distinguishing the reversely zoned plutons in the Bottle Lake Complex from normally zoned granites is given in table 12.

The preservation of reverse zoning in plutonic rocks, in contrast to the more common normal zoning, implies that the stages of plutonic evolution are far more complex than usually envisioned. Thus, although the processes leading to zonation in plutonic rocks (for example, multiple injection, fractional crystallization, and so on) may be theoretically identifiable, it is the timing and interaction of these processes together with the level of erosion and depth of emplacement that may be more critical in preservation of reverse zoning compared to normal zoning.

PROCESSES LEADING TO REVERSE ZONING

Several mechanisms that might explain the reverse zoning in the Bottle Lake Complex include contamination; flow differentiation; intrusion of nonconsanguineous magmas; late-stage crystallization fluxed by hydrous fluids; progressive melting and sequential emplacement; chemical stratification in magma chambers and remobilization (resurgence); and fractional crystallization.

CONTAMINATION

Detailed studies of the West Farrington pluton (Ragland and Butler, 1972) and the White Creek batholith (Reesor, 1956) suggest a contamination mechanism to explain lithological zoning. In the Bottle Lake Complex, contamination cannot be the dominant process because country rock xenoliths are locally concentrated and only become abundant immediately adjacent to the granite-country rock contact. In addition, country rocks are notably heterogeneous in lithology and composition so that contamination of granitic magmas would have disrupted the generally regular geochemical variations observed in both plutons of the Bottle Lake Complex. Contamination with country rock of widely different bulk chemistry might be expected to destroy the internal gradients in the plutons and to establish local compositional control according to the composition of the immediate country rock. Such geochemical disruption is not supported by the trace element composition, the Rb–Sr isotopic results suggesting that each pluton started its evolution with the same initial $^{87}Sr/^{86}Sr$ ratio (Ayuso and Arth, 1983), or by the large isotopic difference in oxygen (A. Andrew, written commun., 1980) and in lead (Ayuso, 1982).

TABLE 12.—*Generalized features of normally zoned plutons compared to the reversely zoned plutons of the Bottle Lake Complex*

	Normal zoning		Reverse zoning	
	Rim facies	Core facies	Rim facies	Core facies
Rock types	Most mafic (diorite, grandiorite, etc.)	Least mafic (leucogranite)	Least mafic (granite)	Most mafic (grandiorite, quartz monzonite)
Abundance of minerals and xenoliths				
Plagioclase	High	Low	Low	High
Alkali feldspar	Low	High	High	Low
Quartz	Low	High	High	Low
Biotite	High	Low	Low	High
Amphibole	High	Low	Low	High
Muscovite	Low	High	Not found	Not found
Accessories	High	Low	Low	High
Opaques	?	?	Unknown	Unknown
Mafic xenoliths	High(?)	Low	Low	High
Country rock xenoliths	High	Low	High	Low
Mineral chemistry				
Feldspar	High An in plagioclase	Lower An in plagioclase	Low An in plagioclase	Higher An in plagioclase
Mafic minerals	Low Fe/(Fe+Mg) in mafic minerals	Higher Fe/(Fe+Mg) in mafic minerals	High Fe/(Fe+Mg) in mafic minerals	Lower Fe/(Fe+Mg) in mafic minerals
Bulk composition				
Major elements -	High CaO, FeO, MgO, TiO_2, low K_2O, SiO_2;	Low CaO, FeO, MgO, TiO_2, high K_2O, SiO_2;	Low CaO, FeO, MgO, TiO_2, high K_2O, SiO_2;	High CaO, FeO, MgO, TiO_2, low K_2O, SiO_2;
Trace elements --	High Sr ----------	Low Sr ----------	Lower Sr, Y, BA, Zr, Nb --	Higher Sr, Y, Ba, Zr, Nb
Presence of vapor phase	No	Yes	Yes(?)	No
Process	Fractional crystallization (lateral accretion, gravitational settling)		Autointrusion by remobilization and resurgence	
Examples	Tuoluomne Series (Bateman and Chappel, 1979) Mount Givens Granodiorite (Bateman and Nokleberg, 1978)		Whitney Cove and Passadumkeag River plutons in the Bottle Lake Complex	

FLOW DIFFERENTIATION

Flow differentiation (Bhattacharji and Smith, 1964) could explain the concentration of phenocrysts and mafic xenoliths toward the interior of the plutons. Experimental studies by Bhattacharji (1967) and Komar (1972) demonstrated the important control that flowage imposes on the distribution of rock types and geochemical fractionation. Flow differentiation in mafic systems (feeder dikes of the Muskox intrusion) show progressive segregation of crystals toward the central axis conduit, and thus this mechanism may be expected to result in reverse zoning. According to Barriere (1976) the diameter of the intrusion undergoing flow differentiation must be less than 100 m.

The Perth Road pluton (Ermanovics, 1970) and the Loon Lake pluton (Dostal, 1975) in the province of Ontario (Canada) are zoned bodies resulting from flow differentiation. Ermanovics (1970) described the zonation of the Perth Road pluton from gabbro at the center to granite at the margins. He interpreted the zonation as a result of flow differentiation in a chamber undergoing folding. In a similar manner, Dostal (1975) explained the reversely zoned Loon Lake pluton on the basis of flow differentiation. To explain reverse zoning in that case, however, the variation in bulk composition (Dostal, 1975; Shieh and others, 1976; Heaman and others, 1982) also mandated the effects of multiple intrusions of magma, fractional crystallization, major contamination with the country rocks, and flowage differentiation.

Flow differentiation is clearly significant in development of the small (less than 5 km) Perth Road pluton, but the relative importance of flow differentiation in the Loon Lake pluton is more difficult to ascertain as a result of the effects of the other major igneous processes. In the Bottle Lake Complex, although the phenocrysts and mafic xenoliths are concentrated in the interiors, a progressive and gradual segregation of mafic xenoliths and phenocrysts is not well developed.

Igneous systems showing flow differentiation tend to be less felsic than the Bottle Lake Complex, as in the Muskox intrusion (Bhattacharji and Smith, 1964), and are not directly compatible with the felsic magmas of the Bottle Lake complex. Barriere (1976), for example, studied the relation between felsic magmas and flow differentiation and suggested that flow differentiation could not be involved to explain the zoning of the granitic Ploumanac'h complex (France). In the case of the Bottle Lake Complex, the felsic magmas are strikingly different in composition from the ultramafic and mafic sills showing flow differentiation. In addition, component plutons of the Bottle Lake Complex have diameters in the order of kilometers, significantly larger than the maximum of 100 m necessary to sustain the flow differentiation process.

INTRUSION OF NONCONSANGUINEOUS PLUTONS

Individual plutons in the Botle Lake Complex might represent nonconsanguineous portions derived from distinct sources. As previously noted, however, the plutons show regular variations in bulk composition from the margins to the interior and suggest instead magma consanguineity across each pluton. The initial $^{87}Sr/^{86}Sr$ isotope composition obtained on samples from both the core and rim facies (Whitney Cove pluton) also support magma consanguineity and strongly suggest that this granite represents one crystallizing system.

This finding is in contrast to the conclusion reached by Ragland and others (1968) in their study of the concentrically but reversely zoned Enchanted Rock batholith. They suggested that the core facies constituted a separate, younger intrusive. Furthermore, in addition to multiple injection of unrelated magmas, they appealed to either selective transport of mobile elements (Li, Rb, U) by a vapor phase pervading the marginal portions of the batholith or to mobilization by late-stage hydrothermal solutions.

LATE-STAGE RECRYSTALLIZATION

Late-stage recrystallization fluxed by hydrous fluids was suggested by Karner (1968) to account for the zoning in the alkaline Tunk Lake pluton (Maine). In contrast to the Bottle Lake Complex, SiO_2 increases toward the core of the Tunk Lake pluton while Al_2O_3, the sum of the alkalies, and total iron decrease. In addition, the Tunk Lake pluton does not exhibit the reversal of bulk composition gradient found in the Bottle Lake Complex, and its total mafic mineral content decreases toward the interior. Also, while granophyric textures and miarolitic cavities are common in the core of the Tunk Lake pluton, they are rare in the Bottle Lake Complex. Field observations also demonstrate the paucity of aplites and pegmatites in the Bottle Lake Complex. Together with a narrowly constrained contact metamorphic zone, both observations suggest a fluid-poor nature for the magmas in the Bottle Lake Complex. Large scale recrystallization in the interior facies of the Whitney Cove and Passadumkeag River plutons was negligible and cannot account for the reverse zoning.

PROGRESSIVE MELTING AND SEQUENTIAL EMPLACEMENT

Reversely zoned granites might result from progressive and incremental melting of the source followed by sequential emplacement of the magmas. Hutchinson (1960) and Hall (1966) appeal to a process of incremental anatexis of the source resulting in magmas of varying composition from felsic (initial stages of melting) to more mafic (later stages of melting) that are sequentially emplaced. It is conceivable that if the more mafic granitic magmas are emplaced in the more interior zones of the felsic portions, the resulting geometric arrangement will be a reversely zoned pluton with respect to bulk composition and lithology.

Multiple injection in the Bottle Lake Complex is suggested by the occurrence of two distinct plutons as well as by their respective interior subdivisions. Thus, it is possible that the reversely zoned character of each pluton reflects progressive melting of the source and sequential emplacement of the granitic liquids produced. Within each pluton, the core facies might represent higher degrees of melting of the source (more mafic magma) intruded after the early stages of magma generation and emplacement.

CHEMICAL STRATIFICATION IN MAGMA CHAMBERS

The reversely zoned character of the Bottle Lake Complex may be adequately explained by a combination of processes occurring in felsic magma chambers. Among the most important studies dealing with the evolution of felsic magma chambers are the descriptions of the evolution of resurgent cauldrons by Smith and

Bailey (1968) and Smith (1979). The critical concepts illustrated in these studies provide a powerful conceptual framework for understanding the initial stages in the evolutionary path leading to normally or reversely zoned plutons. In a previous study, Smith and Bailey (1966) suggested the presence of chemical and physical gradients leading to mineralogical and bulk chemical zonation in felsic magma chambers. This suggestion is now supported by many other case studies (Hildreth, 1979; Mahood, 1981; Smith, 1979) so that the concept of compositional stratigraphy in a magma chamber seems well established.

Among the most important mechanisms suggested to account for this chemical stratigraphy are crystal fractionation and thermogravitational diffusion. In most cases, however, crystal fractionation is inadequate to account for the zonation (Lipman and others, 1966; Hildreth, 1979). The most exciting new suggestion to explain the inferred bulk compositional differences existing in the magma chamber is thermogravitational diffusion. This process of convection-aided Soret differentiation brings about diffusion of chemical species in the liquid state in response to a temperature gradient in felsic magma chambers (Shaw and others, 1976; Hildreth, 1977). In this manner, chemical stratification possibly leading to zoned plutons may be obtained.

Hildreth (1981) suggested that concentrically zoned (normal) plutons forming by inward solidification probably represent the waning stages in the evolution of a crystallizing chamber. In contrast, thermal inputs during the waxing stages promote the outward enrichment of volatiles and volatile-complexed components (diffusive differentiation) resulting in reversely zoned plutonic equivalents of the pre-eruptive zoning of silicic magma chambers (Mahood and Fridrich, 1982). The volatile-poor nature of the Bottle Lake Complex plutons suggests that if diffusive differentiation occurred, it operated during a limited time span before another process (for example, fractionation) was superimposed.

It seems reasonable, however, to emphasize that the plutons in the Bottle Lake Complex probably passed through a stage characterized by chemical stratification. As previously mentioned, the interior of the plutons is characteristically lower in SiO_2 and K_2O but higher in MgO, Al_2O_3, CaO, TiO_2, Fe_2O_3, MnO, and P_2O_5; Na_2O shows little difference between the two facies. Trace element abundances exhibit a range of values within individual facies, although strontium, niobium, yttrium, and zinc are generally higher coreward in the plutons. Relative enrichments, however, are difficult to determine because of the wide range in composition of each facies. Enrichment factors for the trace element abundances of core and rim facies rocks are a direct function of the particular sample selected as the reference. In the high-silica rhyolites represented by the Bishop Tuff, Hildreth (1979) demonstrated roofward enrichment in SiO_2, Na_2O, and MnO among the major oxides and in rubidium, yttrium, and niobium among the trace elements. Given the compositional heterogeneity, less siliceous nature, and protracted evolution of the Bottle Lake Complex plutons compared to the high-silica rhyolites, it is not surprising that the plutons and rhyolites are dissimilar in their pattern of enrichment. Nevertheless, it seems reasonable to suggest that major compositional differences inherently existed between the core and rim facies of the plutons.

From this conceptual framework, the evolution of the Bottle Lake Complex may be considered as a variant of the more commonly accepted plutonic evolutionary path of normally zoned plutons. In a compositionally layered chamber, the hotter and more mafic magmas are at the base, becoming progressively more felsic and volatile enriched toward the top (Smith and Bailey, 1966; Lipman, 1967; Hildreth, 1977; Lipman and others, 1966). Reversely zoned plutons in the Bottle Lake Complex represent this arrested stage in the magma chamber before fractionation, mixing, and convective transport destroyed the vestiges of the chemical stratification. Reverse zoning resulted from remobilization (resurgence) of the hotter, more mafic layers into the upper parts of the chamber; this process is discussed at length below.

Shaw (1965) demonstrated different types of natural convection depending on the flow conditions in the magma chamber, and Bartlett (1969) suggested that convection increased as a function of the size of the chamber. Plutons in the Bottle Lake Complex are large (>20 km in diameter) and probably sustained vigorous convection. Shaw (1974) suggested that convection of granitic magma resulted in efficient and systematic elemental gradients. This suggestion is in agreement with the results of Spera and Crisp (1981), who showed that chemical convection produces vertical composition gradients in magma chambers. Field and petrologic studies have suggested, for example, that in the Criffell-Dalbeattie pluton (Phillips and others, 1981) convection circulation was asymmetrical and occurred toward the end of the emplacement process.

In the Bottle Lake Complex, both plutons probably established convective paths conducive to maintaining regular but vertically stratified bulk compositional gradients. However, mobilization of hotter, deeper granitic magma (thermal inputs), probably best characterized as a crystal mush, and upwelling into the higher convecting and fractionating systems, resulted in disruption of local equilibrium between liquid and crystals. Thus, significant mineral redistribution and mixing of liquids also occurred. Smith (1979) speculated on some of the

compositional and mechanical effects of thermal inputs (surges of new magma) into a crystallizing chamber and suggested that remelting and mixing of partially solidified magma might be expected.

Volcanic equivalents of the Bottle Lake Complex plutons are unknown. Thus, it is difficult to document the interplay between volcanism, with its attendant evisceration of the magma chamber, and resurgence as suggested by Bailey (1976) to explain the mechanism of resurgent doming. On the basis of available data, it cannot be demonstrated that remobilization of the core facies in the Bottle Lake Complex plutons was accompanied by structural resurgence or by venting of the magma chamber. Nevertheless, it is interesting to note that the diameters (about 20 km), general shape, and arrangement of the plutons in the Bottle Lake complex are similar to those of the Toledo and Valles calderas in the Jemez Mountains of New Mexico. These calderas were described in the classic study of resurgence by Smith and Bailey (1968). According to their scheme, resurgent cauldrons pass through a number of stages beginning with a chemically stratified magma chamber. The intervening stages, which consist of volcanic events (ash-flow eruptions, caldera collapse, pyroclastic eruptions, and so on) leading to resurgence, may be speculated to have preceded the emplacement of the core facies of the plutons in the Bottle Lake Complex. Here again, however, the volcanic record of these processes has not been recognized. The relative timing of events in the Bottle Lake Complex is not well constrained. Although the core facies are in each case relatively younger than the rim, it is not possible to distinguish which pluton is younger by the Rb–Sr method.

On the basis of field observations, however, the Whitney Cove pluton was suggested to predate the Passadumkeag River pluton. In comparison to the time necessary to complete the evolution of resurgent cauldrons in multiple calderas (for example, the Valles caldera), the evolution of the Bottle Lake Complex plutons may have taken at least as long as possibly longer to develop. For example, amphibole from the core and rim faces of the Passadumkeag River pluton differs by a minimum of about 2 m.y. in age as suggested by preliminary argon release studies (J. F. Sutter, 1983, oral commun.)

FRACTIONAL CRYSTALLIZATION

Fractionation of the phenocryst assemblage in the plutons of the Bottle Lake Complex is not the critical mechanism accounting for the reverse zonation but was superimposed on the original chemical zonation of the convecting magma chamber. Fractional crystallization may be accomplished by lateral accretion of crystals (Bateman and Chappell, 1979) with inward displacement of the melt and by gravitational settling. Rice (1981) considers gravitational settling unimportant in producing fractionation in felsic magmas because of the high-viscosity barriers. Shaw (1965), however, suggested that gravitational settling of mafic minerals and plagioclase was an adequate mechanism operating in granitic magmas. Emmeleus (1963) had previously appealed to this mechanism to explain layering in granites from Greenland. More recently Robinson (1977) suggested that crystal settling resulted in the lithological zoning of the Tuolumne Intrusive Suite of the Sierra Nevada. For the Bottle Lake Complex, the relative importance of crystal settling compared to lateral accretion cannot be adequately judged with existing data, and it is likely that both were in operation. Nevertheless, it seems evident that in the Bottle Lake Complex, the assemblage consisting of plagioclase, biotite, amphibole, apatite, zircon, and magnetite-ilmenite partly controlled the change from some of the last fractionated to the most fractionated rocks (Ayuso, 1982). The core facies of both plutons represents a mixture of material from the lower parts of the chamber, new additions to the crystallizing chamber in the form of the crystal mush obtained from the new influxes of more mafic granitic magma, and of the accumulated fractionated assemblage. It should be emphasized, however, that although fractionation occurred during the evolution of the Bottle Lake Complex, this process by itself cannot account for the reverse zoning of the plutons.

The Whitney Cove pluton shows a better defined gradient in its mineral abundances and mineral compositions coreward compared to the Passadumkeag River pluton. One dramatic result of mobilization and input of hotter granitic liquid into the chamber may be the more widely dispersed compositional variation of the minerals, the lack of systematic mineral gradients, and abundance of mafic clots in the Passadumkeag River pluton. Such influx of more mafic granitic liquid, coupled with vigorous stirring in a convective system, may have mixed phases that originally crystallized and settled at the bottom or were eroded off the walls of the chamber with phases in equilibrium with liquids at different stages of fractionation, especially from new surges of magma. Thus, textural and chemical heterogeneity probably reflect processes related to the intrusion and mechanical mixing of different parts of the same crystallizing system and are not a direct result of fractionation. Especially in the case of the Passadumkeag River pluton, the abundance of mafic and felsic mineral clusters, the relict textures and compositional diversity of liquidus phases (biotite, plagioclase, and hornblende),

and the abundance of a complex refractory suite suggest that the granite may have inherited some of its heterogeneity at the source. This suggestion is in agreement with observations by Marsh (1982), who indicated that diapiric movement probably involves motion of liquids and remains from the source region.

The presence of mafic xenoliths and mafic mineral clots in the Passadumkeag River pluton also suggests that some of the petrographic variation resulted from differential reaction between granitic magma and xenoliths. Mafic xenoliths were probably obtained at depth from the country rock. In contrast, mafic clots might represent aggregates of the fractionated assemblage during earlier stages of crystallization. Also, it might be speculated that surges of hot, less differentiated or more mafic granitic magma into the crystallizing chamber triggered the process of remobilization and autointrusion of the lower layers and of portions of the magma rich in mafic xenoliths, mafic clots, and mixtures of the fractionating assemblages into the upper part of the chamber.

SUMMARY OF MECHANISMS LEADING TO REVERSELY ZONED PLUTONS IN THE BOTTLE LAKE COMPLEX

Reverse zoning in the Bottle Lake Complex is a result of remobilization (resurgence) of the deeper (hotter) parts of the system. The Bottle Lake Complex represents a composite batholith derived from sequential melting, but each pluton evolved as an independent geochemical system. The initial state of the evolutionary path after the individual magma chambers were established was the development of chemical stratification, with hotter, more mafic magma at the base of the chamber (fig. 30). Convection in the magma chamber promoted the chemical gradients, which were aided by periodic influxes of more mafic granitic magma.

Crystal-liquid equilibria were of secondary importance to explain the reverse zoning and were superimposed on the original chemical zonation of the magma chamber (fig. 30). The stratification and division of the chamber into domains assured that the fractionating assemblage precipitated in these individual domains maintained equilibrium with only part of the chamber. Fractional crystallization by accretion and settling may have resulted, for example, in some accumulation of the most calcic plagioclase and the most magnesian mafic minerals. Periodic influxes of more mafic granitic magma at the base of the chamber would probably result in disruption of the convective cells, mixing of magmas at different stages of differentiation, and mixing of minerals of different compositions depending on their position in the magma chamber.

Surges of hotter granitic magma into the base of the chamber resulted in resurgence or remobilization of the lower, more mafic crystal mush into the upper, more felsic layers. Alternatively, Bailey (1976) suggested that resurgent doming might occur from partially removing the top of the chamber as a result of volcanism. He suggested that isostatic equilibrium is restored by inward flow in the magma root zone leading to a rise in the subcauldron crustal column and magma chamber. In either case, field observations suggest that for both the Whitney Cove and Passadumkeag River plutons, the core facies were emplaced at this level of exposure subsequent to the rim facies (fig. 30).

The plutons were intruded high in the crust, and this placement may explain the preservation of their reversely zoned features. This shallow level of emplacement together with decreased replenishment of hotter granitic magma at the base of the chamber might have resulted in a faster rate of cooling, less efficient convection, and an increase in viscosity. As elemental diffusion became more sluggish and less systematic, the solidus temperature was reached. The granites consolidated and froze the reversely zoned features that are typically destroyed in plutons that have longer evolutionary paths.

CONCLUSIONS

The plutons in the Bottle Lake Complex constitute outstanding examples of reversely zoned granites. Mineral abundances as well as bulk compositions of each granite indicate that the interiors are enriched in mafic minerals and that they show higher contents of oxides typically expected to be concentrated along the margins.

Remobilization (resurgence) and autointrusion of deeper parts of the system into the more felsic rocks of the margins explains the reverse zonation (fig. 30). Fractional crystallization was of secondary importance and probably accounts for the selective removal of the cumulative phases and mafic xenoliths. Convective transport resulted in redistribution and dispersal of the crystallizing assemblage in a chemically stratified system.

Calculated biotite stabilities indicate a temperature range from 720–780°C and a total pressure from 1 to 1.8 kbar during the emplacement of the Bottle Lake Complex. The f_{O_2} conditions are characteristically higher than the Ni–NiO equilibrium curve as suggested by the assemblage of magnetite and sphene.

The highly regular major oxide variations within each pluton, together with the Rb–Sr isotopic compositions resulting in linear isochrons, support the argument that

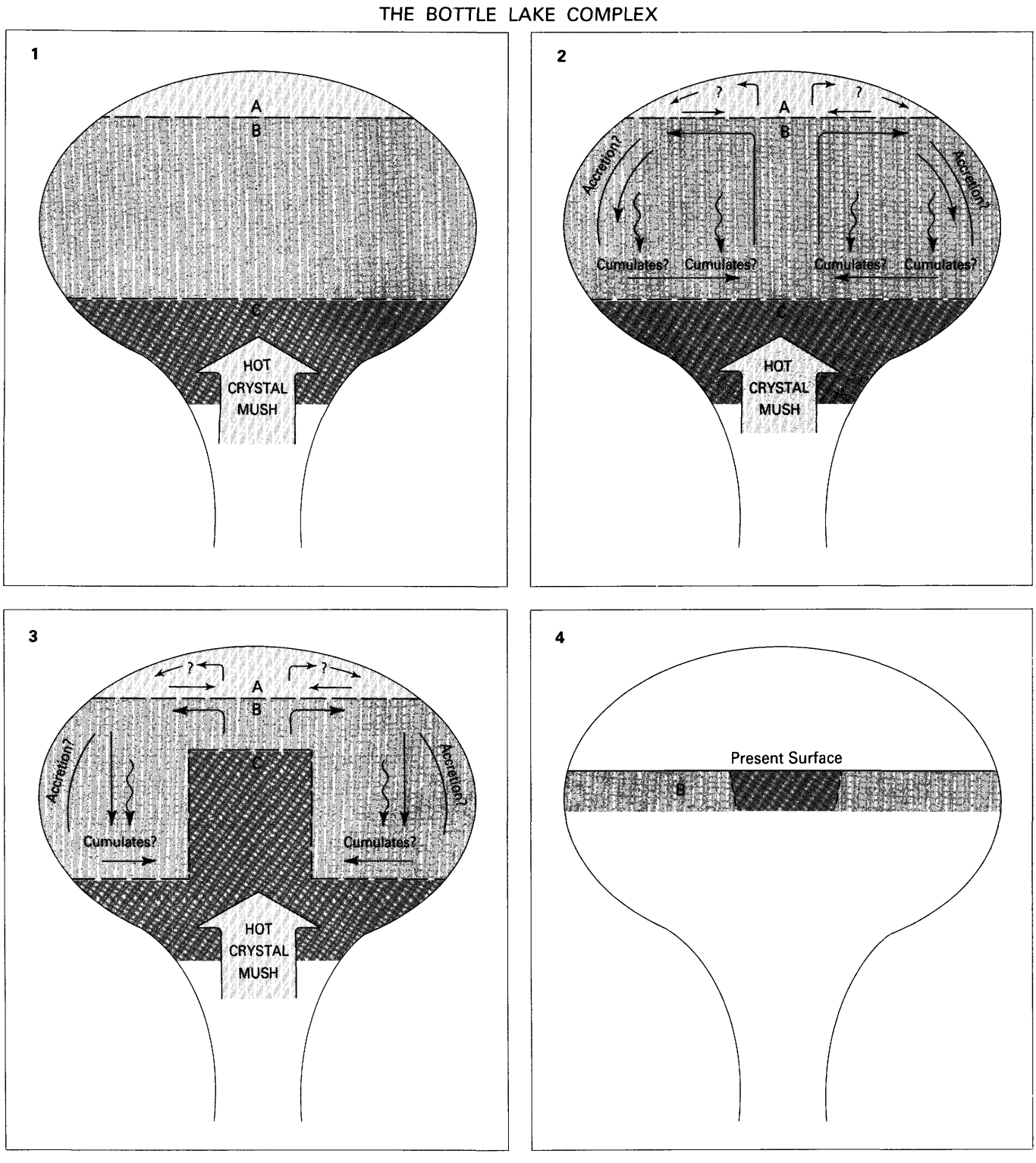

FIGURE 30.—Generalized diagram showing a model for the reversely zoned plutons of the Bottle Lake Complex. The Whitney Cove and Passadumkeag River plutons evolved as independent systems.

1.—The initial stage of evolution was characterized by a chemically stratified system with more mafic granitic magma at the base (layer C) to more felsic granitic magma toward the top (layer A).

2. —The system passed through a stage of vigorous convection that promoted the chemical gradients. Fractionation by accumulation and lateral accretion may have been initiated at this stage.

each pluton behaved as an individual geochemical system. Oxygen isotopic compositions of the granites and country rocks are in agreement with the bulk compositions gradients, suggesting that no significant interaction with country rocks occurred.

The source of the plutons in the Bottle Lake Complex progressively changed to include more continentally derived debris. In the Passadumkeag River pluton, initial strontium, lead, and oxygen isotopic compositions are lower than in the Whitney Cove pluton indicating a less continental character of the source. Lead isotopic studies rule out a source similar to the upper oceanic mantle, lower continental crust, or upper continental crust as exemplified by metasediments intruded by the Bottle Lake Complex.

The Bottle Lake Complex constitutes an example of reversely zoned plutons related by remobilization of more mafic but consanguineous magmas. Zoned granitic plutons elsewhere have been explained by assimilation, late-stage reaction, multiple injection, or by fractional crystallization without remobilization and resurgence. Vigorous stirring with convective transport and large-scale upwelling occurred in the Whitney Cove and Passadumkeag River plutons leading to the present arrangement of rock types. Reversely zoned granitic plutons are unknown in east-central Maine apart from the Bottle Lake Complex. In general, plutons intruded near the core of the Merrimack synclinorium and exemplified by the Bottle Lake Complex are rich in mafic minerals and show a distinct geochemical composition (Loiselle and Ayuso, 1980) characteristic of plutons intruded to the north of the Norumbega fault system. Reversely zoned plutons, in general, may be more numerous than recognized. It is conceivable that remnants of the reverse zoning become more difficult to discern as the plutonic rocks reach the latest stages of their evolution. In this case, the Bottle Lake Complex represents an earlier stage in the evolution of a felsic system that is usually represented by the final stages in normally zoned plutons.

REFERENCES

Ayuso, R. A., 1979, The late Paleozoic Bottle Lake Complex, Maine (abs.): Northeastern Section Geological Society of America, Abstracts with Programs, v. 11, no. 1, p. 2.

_____1982, Geology of the Bottle Lake Complex, Maine: Ph.D. unpublished dissertation, Virginia Polytechnic Institute and State University, Blacksburg, Va.

Ayuso, R. A., and Arth, J. G., 1983, Comparison of U-Pb zircons, Rb-Sr whole-rock, and K-Ar ages in Devonian plutons of the Bottle Lake Complex, Maine (abs.): Geological Society of America Abstracts with Programs, v. 15, no. 3, p. 146.

Ayuso, R. A., Loiselle, M., Scambos, T., and Wones, D. R., 1980, Comparison of field relations of granitoids across the Merrimack synclinorium, eastern Maine (abs.), *in* Wones, D. R., ed., Proceedings of "The Caledonides of the U.S.A.": Blacksburg, Virginia Polytechnic Institute, Department of Geological Sciences memoir no. 2, IGCP Project no. 27, p. A-17.

Ayuso, R. A., Wones, D. R., and Sinha, A. K., 1982a, Genesis of reversely zoned granites: Bottle Lake Complex, Maine (abs.): Geological Society of America Abstracts with Programs, v. 14, no. 1-2, p. 3.

Ayuso, R. A., Sinha, A. K., Arth, J. G., and Wones, D. R., 1982b, Pb and Sr isotopic variations and constraints on granitic sources in the Merrimack Synclinorium: Bottle Lake Complex, Maine (abs.): Geological Society of America Abstracts with Programs, v. 14, no. 7, p. 436.

Ayuso, R. A., and Wones, D. R., 1980, Geology of the Bottle Lake Complex, Maine, *in* Roy, D. C., and Naylor, R. S., eds., A guidebook to the geology of Northeastern Maine and neighboring New Brunswick: 72d Annual Meeting of the New England Intercollegiate Geological Conference, p. 32-64.

Bailey, R. A., 1976, On the mechanisms of post subsidence central doming and volcanism in resurgent cauldrons (abs.): Geological Society of America Abstracts with Programs, v. 8, no. 5, p. 567.

Barriere, M., 1976, Flowage differentiation: Limitation of the "Bagnold Effect" to the narrow intrusions: Contributions to Mineralogy and Petrology, v. 55, p. 139-145.

Bartlett, R. W., 1969, Magma convection, temperature distribution, and differentiation: American Journal of Science, v. 267, no. 9, p. 1067-1082.

Bateman, P. C., and Chappell, B. W., 1979, Crystallization, fractionation, and solidification of the Tuolumne Intrusive Series, Yosemite National Park, California: Geological Society of America Bulletin, v. 90, no. 5, p. 465-482.

Bateman, P. C., and Nokleberg, W. J., 1978, Solidification of the Mount Givens granodiorite, Sierra Nevada, California: Journal of Geology, v. 86, no. 5, p. 563-579.

Bateman, P. C., Pakiser, L. C., and Kane, M. F., 1965, Geology and tungsten mineralization of the Bishop district, California: U.S. Geological Survey Professional Paper 470, 208 p.

Bence, A. E., and Albee, A. L., 1968, Empirical correction factors for the electron microanalysis of silicates and oxides: Journal of Geology, v. 76, no. 2, p. 382-403.

3. —Periodic disruptions of the convecting system resulted from thermal and material influxes (crystal mush). Liquid mixing and mechanical mixing of crystals from different domains in the magma chamber are expected. A mixture of layers C (mafic granitic magma) and B (a more felsic granitic magma) and their fractionated products was remobilized from deeper parts in the chamber into the upper parts (for example, into layer B). Remobilization or resurgence of the deeper more mafic layer was probably triggered by an influx of hotter material at the base of the magma chamber.

4. —The final stage of the system retains the reversely zoned character obtained by remobilization or resurgence of deeper layers (for example, layer C) into the upper part of the system (layer B). Placement of the present surface of exposure is diagramatic and merely indicates the possible arrangement of layers B and C.

Bhattacharji, Somder, 1967, Mechanics of flow differentiation in ultramafic and mafic sills: Journal of Geology, v. 75, no. 1, p. 101-112.

Bhattacharji, Somder, and Smith, C. H., 1964, Flowage differentiation: Science, v. 145, no. 3628, p. 150-153.

Boone, G. M., and Wheeler, E. P., 1968, Staining for cordierite and feldspars in thin section: American Mineralogist, v. 53, no. 1-2, p. 327-331.

Boucot, A. J., Griscom, Andrew, and Allingham, J. W., 1964, Geologic and aeromagnetic map of northern Maine: U.S. Geological Survey Geophysical Investigations Map GP-312, scale 1:250,000, with profile, separate text.

Buddington, A. F., and Lindsley, D. H., 1964, Iron-titanium oxide minerals and synthetic equivalents: Journal of Petrology, v. 5, no. 2, p. 310-357.

Burnham, C. W., Holloway, J. F., and Davis, N. F., 1969, Thermodynamic properties of water to 1,000°C and 10,000 bars: Geological Society of America Special Paper 132, 96 p.

Chappell, B. W., and White, A. J. R., 1974, Two contrasting granite types: Pacific Geology, v. 8, p. 173-174.

Chou, I. M., 1978, Calibration of oxygen buffers at elevated *P* and *T* using the hydrogen fugacity sensor: American Mineralogist, v. 63, p. 690-703.

Cobbing, E. J., and Pitcher, W. S., 1972, The Coastal batholith of central Peru: Journal of Geological Society of London, v. 128, p. 421-460.

Cole, J. M., 1961, Study of part of the Lucerne granite contact aureole in eastern Penobscot county, Maine: M. S. unpublished thesis, University of Virginia, 76 p.

Compton, R. R., 1955, Trondhjemite batholith near Bidwell Bar, California: Geological Society of America Bulletin, v. 66, no. 1, p. 9-44.

Czamanske, G. K., Isihard, Shunso, and Atkin, S. A., 1981, Chemistry of rock-forming minerals of the Cretaceous-Paleocene Batholith in Southwestern Japan and implications for magma genesis: Journal of Geophysical Research, v. 86, no. B11, p. 10431-10469.

Czamanske, G. K., and Mihalik, Peter, 1972, Oxidation during magmatic differentiation, Finnmarka Complex, Oslo area, Norway. Part I, the opaque oxides: Journal of Petrology, v. 13, no. 3, p. 493-509.

Czamanske, G. K., and Wones, D. R., 1973, Oxidation during magmatic differentiation, Finnmarka Complex, Oslo Area, Norway; Part 2, the mafic silicates: Journal of Petrology, v. 14, no. 3, p. 349-380.

Czamanske, G. K., Wones, D. R., and Eichelberger, J. C., 1977, Mineralogy and petrology of the intrusive complex of the Pliny Range, New Hampshire: American Journal of Science, v. 277, no. 9, p. 1073-1123.

Dodge, F. C. W., Papike, J. J., and Mays, R. E., 1968, Hornblendes from granitic rocks of the Central Sierra Nevada batholith, California, Journal of Petrology, v. 9, no. 3, p. 378-410.

Dostal, J., 1975, Geochemistry and petrology of the Loon Lake pluton, Ontario: Canadian Journal of Earth Sciences, v. 12, no. 8, p. 1331-1345.

Doyle, R. G., Young, R. S., and Wing, L. A., 1961, A detailed economic investigation of aeromagnetic anomalies in eastern Penobscot County, Maine: Maine Geological Survey Special Economic Studies Series, no. 1, 69 p.

Emeleus, C. H., 1963, Structural and petrographic observations on layered granites from southern Greenland, *in* Symposium on layered intrusion—International Mineralogical Association, 3d General Meeting, Washington, D.C., 1962: Mineralogical Society of America Special Paper 1, p. 22-29.

Ermanovics, I. F., 1970, Zonal structure of the Perth Road monzonite, Grenville Province, Ontario: Canadian Journal of Earth Sciences, v. 7, no. 2, p. 414-434.

Eugster, H. P., and Wones, D. R., 1962, Stability relations of the ferruginous biotite, annite: Journal of Petrology, v. 3, no. 1, p. 82-125.

Faul, H. T., Stern, T. W., Thomas, H. H., and Elmore, P. L. D., 1963, Ages of intrusion and metamorphism in the northern Appalachians: American Journal of Science, v. 261, no. 1, p. 1-19.

Fenn, P. M., 1973, Nucleation and growth of alkali feldspars from melts in the system $NaAlSi_3O_8$-$KAlSi_3O_8$-H_2O: Ph.D. thesis, Stanford University, Stanford, Calif.

Garland, G. D., 1953, Gravity measurements in the Maritime Provinces: Canada Dominion Observatory Publication, v. 16, no. 7, p. 185-275.

Goddard, E. N., chm., and others, 1948, Rock-color chart: Washington, D.C., National Research Council; reprinted by Geological Society of America, 1951.

Greenland, L. P., Gottfried, D., and Tilling, R. I., 1968, Distribution of manganese between coexisting biotite and hornblende in plutonic rocks: Geochimica et Cosmochimica Acta, v. 32, no. 11, p. 1149-1163.

Hall, A., 1966, A petrogenetic study of the Rosses granite Complex, Donegal: Journal of Petrology, v. 7, no. 2, p. 202-220.

Halliday, A. N., Stephens, W. E., and Harmon, R. S., 1980, Rb-Sr and O isotopic relationships in 3 zoned Caledonian granitic plutons, Southern Uplands, Scotland: evidence for varied sources and hybridization of magmas: Journal of Geological Society of London, v. 137, p. 329-348.

Heaman, L. M., Shieh, Y.-N., McNutt, R. H., and Shaw, D. M., 1982, Isotopic and trace element study of the Loon Lake pluton, Grenville Province, Ontario: Canadian Journal of Earth Sciences, v. 19, no. 5, p. 1045-1054.

Hess, P. C., 1969, The metamorphic paragenesis of cordierite in pelitic rocks: Contributions to Mineralogy and Petrology, v. 24, no. 3, p. 191-207.

Hildreth, W., 1977, The magma chamber of the Bishop Tuff: Gradients in temperature, pressure, and composition: Ph.D. thesis, University of California, Berkeley, 328 p.

———1979, The Bishop Tuff: Evidence for the origin of compositional zonation in silicic magma chambers: Geological Society of America Special Paper 180, p. 43-75.

———1981, Gradients in silicic magma chambers: Implications for lithospheric magmatism: Journal of Geophysical Research, v. 86, no. B11, p. 10153-10192.

Holdaway, M. J., 1971, Stability of andalusite and the aluminum silicate phase diagram: American Journal of Science, v. 271, no. 2, p. 97-131.

Huebner, J. S., and Sato, Motoaki, 1970, The oxygen fugacity-temperature relationships of manganese oxide and nickel oxide buffers: American Mineralogist, v. 55, no. 5-6, p. 934-952.

Hutchinson, R. M., 1960, Petrotectonics and petrochemistry of late Precambrian batholiths of central Texas and the north end of Pikes Peak batholith, Colorado: International Geological Congress, 21st, Copenhagen, 1960, pt. 14, p. 95-107.

Ishihara, Shunso, 1977, The magnetite-series and ilmenite-series granitic rocks: Mining Geology, v. 27, p. 293-305.

James, R. S., and Hamilton, D. H., 1968, Phase relations in the system $NaAlSi_3O_8$-$KAlSi_3O_8$-$CaAl_2Si_2O_8$-SiO_2 at 1 kilobar water vapour pressure: Contributions to Mineralogy and Petrology, v. 21, p. 111-141.

Karner, F. R., 1968, Compositional variation in the Tunk Lake granite pluton, southeastern Maine: Geological Society of America Bulletin, v. 79, no. 2, p. 193-221.

Kleinkopf, M. D., 1960, Spectrographic determination of trace elements in lake waters of northern Maine: Geological society of America Bulletin, v. 71, no. 8, p. 1231-1241.

Komar, P. D., 1972, Flow differentiation in igneous dikes and sills—Profiles of velocity and phenocryst concentration: Geological Society of America Bulletin, v. 83, no. 11, p. 3443-3447.

Larrabee, D. M., Spencer, C. W., and Swift, D. J. P., 1965, Bedrock geology of the Grand Lake area, Aroostook, Hancock, Penobscot, and Washington Counties, Maine: U.S. Geological Survey Bulletin 1201-E, 38 p.

Leake, B. E., 1978, Nomenclature of amphiboles: American Mineralogist, v. 63, nos. 11-12, p. 1023-1052.

Lipman, P. W., 1966, Water pressures during differentiation and crystallization of some ash-flow magmas from southern Nevada: American Journal of Science, v. 264, no. 10, p. 810-826.

———1967, Mineral and chemical variations within an ash-flow sheet from Aso caldera, southwestern Japan: Contributions to Mineralogy and Petrology, v. 16, no. 4, p. 300-327.

Lipman, P. W., Christiansen, R. L., and O'Connor, J. T., 1966, A compositionally zoned ash-flow sheet in southern Nevada: U.S. Geological Survey Professional Paper 524-F, 47 p.

Loiselle, M. C., and Ayuso, R. A., 1980, Geochemical characteristics of granitoids across the Merrimack Synclinorium, eastern and central Maine, *in* Wones, D. R., ed., Proceedings of "The Caledonides of the USA": Blacksburg, Virginia Polytechnic Institute, Department of Geological Sciences memoir no. 2, IGCP Project no. 27, p. 117-121.

Ludman, Allan, 1978a, Preliminary bedrock and brittle fracture map of the Fredericton 2° quadrangle: Maine Geological Survey, Regional Map Series, Open-File Map 78-2, scale 1:250,000.

_____1978b, Stratigraphy and structure of Silurian and pre-Silurian rocks in the Brookton-Princeton area, eastern Maine, *in* Guidebook for fieldtrips in southeastern Maine and southwestern New Brunswick, N.E.I.G.C. Guidebook, 70th Annual Meeting, p. 145-161.

_____1981, Significance of transcurrent faulting in eastern Maine and location of the suture between Avalonia and North America: American Journal of Science, v. 281, no. 4, p. 463-483.

Ludman, A., and Westerman, D. S., 1977, The geology of the inland rocks of the Calais-Wesley area, Maine: Maine Geological Society Guidebook, Field Trips 1 and 2.

Luth, W. C., 1969, The systems $NaAlSi_3O_8$-SiO_2 and $KalSi_3O_8$-SiO_2 to 20 kb and the relationships between H_2O content, P_{water} and P_{total} in granitic magma: American Journal of Science, v. 267-A, p. 325-341.

Luth, W. C., Jahns, R. H., and Tuttle, O. F., 1964, The granite system at pressures of 4 to 10 kilobars: Journal of Geophysical Research, v. 69, no. 4, p. 759-773.

Mahood, G. A., 1981, Chemical evolution of a Pleistocene rhyolitic center: Sierra La Primavera, Jalisco, Mexico: Contributions to Mineralogy and Petrology, v. 77 p. 129-149.

Mahood, G., and Fridrich, C., 1982, Differentiation in waxing and waning magma chambers (abs.): Geological Society of America Abstracts with Programs, v. 14, no. 7, p. 553-554.

Marsh, B. D., 1982, On the mechanics of igneous diapirism, stoping, and zone melting: American Journal of Science, v. 282, no. 6, p. 808-855.

Naney, M. T., 1978, Stability and crystallization of ferromagnesian silicates in water-vapour undersaturated melts at 2 and 8 kb pressure: Ph.D. unpublished thesis, Stanford University, Stanford, Calif.

Nockolds, S. R., 1947, The relation between chemical composition and paragenesis in the biotite micas of igneous rocks: American Journal of Science, v. 245, no. 7, p. 401-420.

Norrish, K., and Hutton, J. T., 1969, An accurate X-ray spectrographic method for the analysis of a wide range of geologic samples: Geochimica et Cosmochimica Acta, v. 33, no. 4, p. 431-453.

Nowlan, G. A., and Hessin, T. D., 1972, Molybdenum, arsenic, and other elements in stream sediments, Tomah Mountain, Topsfield, Maine: U.S. Geological Survey Open-File Report 1766, 18 p.

Noyes, H., 1978, Comparative petrochemistry of the Red Lake and Eagle Peak plutons, Sierra Nevada Batholith: Ph.D. dissertation, Massachusetts Institute of Technology, Cambridge, Mass.

Olson, R. K., 1972, Bedrock geology of the southeast one-sixth of the Saponac quadrangle, Penobscot and Hancock counties, Maine: M.S. unpublished thesis, University of Maine at Orono, 60 p.

Osberg, P. H., 1968, Stratigraphy, structural geology and metamorphism of the Waterville-Vassalboro area, Maine: Maine Geological Survey Bulletin no. 20, 64 p.

_____1980, Stratigraphic and structural relations in the turbidite sequence of south-central Maine, *in* Roy, D. C., and Naylor, R. S., eds., A guidebook to the geology of northeastern Maine and neighboring New Brunswick: 72d Annual meeting of the New England Intercollegiate Geological Conference, p. 278-296.

Otton, J. K., Nowland, G. A., and Ficklin, W. H., 1980, Anomalous uranium and thorium associated with a granitic facies at the Bottle Lake Quartz Monzonite, Tomah Mountain area, eastern Maine: U.S. Geological Survey, Open-File Report 80-991, 18 p.

Phillips, W. J., Fuge, R., and Phillips, N., 1981, Convection and crystallization in the Criffell-Dalbeattie pluton: Journal of Geological Society of London, v. 138, pt. 3, p. 351-366.

Pitcher, W. S., 1979a, The nature, ascent and emplacement of granitic magmas: Journal of the Geological Society of London, v. 136, p. 627-662.

Pitcher, W. S., 1979b, Comments on the geological environments of granites, *in* Atherton, M. P., and Tarney, J., eds., Origin of granite batholiths—geochemical evidence: Kent, United Kingdom, Shiva Publishers, p. 1-8.

Post, E. V., Lehmbeck, W. L., Dennen, W. H., and Nowlan, G. A., 1967, Map of southeastern Maine showing heavy metals in stream sediments: U.S. Geological Survey, Mineral Investigations Field Studies Map MF-301, scale 1:250,000, text.

Ragland, P. C., Billings, G. K., and Adams, J. A. S., 1968, Magmatic differentiation and autometasomatism in a zoned granitic batholith from Central Texas, U.S.A., *in* Ahrens, L. H., ed., Origin and distributon of the elements: Oxford, England, and New York, Pergamon Press, p. 795-823.

Ragland, P. C., and Butler, J. R., 1972, Crystallization of West Farrington pluton, North Carolina, U.S.A.: Journal of Petrology, v. 13, no. 3, p. 381-404.

Rast, N., and Lutes, G. G., 1979, The metamorphic aureole of the Pokiok-Skiff Lake granite, southern New Brunswick: Current Research, Pt. A, Geological Survey of Canada, Paper 79-1A, p. 267-271.

Reesor, J. E., 1956, Dewar Creek map-area with special emphasis on the White Creek Batholith, British Columbia: Canada Geological Survey memoir 292, 78 p., illustrations including geologic map.

Rice, Alan, 1981, convective fractionation: A mechanism to provide cryptic zoning (macrosegregation), layering, crescumulates, banded tuffs and explosive volcanism in igneous processes: Journal of Geophysical Research, v. 86, no. 1, p. 405-417.

Richardson, S. W., Gilbert, M. C., and Bell, P. M., 1969, Experimental determination of kyanite-andalusite and andalusite-sillimanite equilibria; the aluminum silicate triple point: American Journal of Science, v. 267, no. 3, p. 259-272.

Robert, J. L., 1976, Titanium solubility in synthetic phlogopite solid solutions: Chemical Geology, v. 17, no. 3, p. 213-227.

Robinson, C. A., 1977, Differentiaton of the Tuolumne Intrusive Series, Yosemite National Park, California (abs.): Geological Society of America Abstracts with Programs (Cordilleran Section), v. 9, no. 4, p. 487-488.

Robinson, Peter, Ross, Malcolm, and Jaffe, H. W., 1971, Composition of the anthophyllite-gedrite series, comparison of gedrite and hornblende, and the anthophyllite-gedrite solvus: American Mineralogist, v. 56, p. 1005-1041.

Ruitenberg, A. A., 1967, Stratigraphy, structure, and metallization, Piskahegan-Rolling Dam area (Northern Appalachians, New Brunswick, Canada): Leidse Geologische Medelinger, v. 40, p. 79-120.

Ruitenberg, A. A., and Ludman, A., 1978, Stratigraphy and tectonic setting of early Paleozoic sedimentary rocks of the Wirral-Big Lake area, southwestern New Brunswick and southeastern Maine: Canadian Journal of Earth Sciences, v. 15, no. 1, p. 22-32.

Rutherford, M. J., 1972, The phase relations of aluminous iron biotites in the system $KAlSi_3O_8$-$KAlSiO_4$-Al_2O_3-Fe-O-H: Journal of Petrology, v. 14, no. 1, p. 159-180.

Scambos, T. A., 1980, The petrology and geochemistry of the Center Pond pluton, Lincoln, Maine: M.S. unpublished thesis, Virginia Polytechnic Institute and State University, Blacksburg, Va., 40 p.

Shaw, H. R., 1963, Obsidian-H_2O viscosities at 1000 and 2000 bars in the temperature range 700° to 900°C: Journal of Geophysical Research, v. 68, no. 23, p. 6337-6343.

_____1965, Comments no viscosity, crystal settling, and convection in granitic magmas: American Journal of Science, v. 263, no. 2, p. 120-152.

_____1974, Diffusion of H_2O in granitic liquids: Part I. Experimental data; Part II. Mass transfer in magma chambers, *in* Hoffman, A. W., Giletti, B. J., Yoder, H. S., and Yund, R. A., eds., Geochemical transport and kinetics: Carnegie Institute of Washington, Pub. 634, p. 139-170.

Shaw, H. R., Smith, R. L., and Hildreth, Wes, 1976, Thermogravitational mechanisms for chemical variations in zoned magma chambers (abs.): Geological Society of America Abstracts with Programs, v. 8, no. 6, p. 1102.

Shieh, Y., Schwarcz, H. P., and Shaw, D. M., 1976, An oxygen isotope study of the Loon Lake pluton and the Apsley Gneiss, Ontario: Contributions to Mineralogy and Petrology, v. 54, p. 1–16.

Smith, R. L., 1979, Ash-flow magmatism: Geological Society of America Special Paper 180, p. 5–27.

Smith, R. L., and Bailey, R. A., 1966, The Bandelier Tuff—A study of ash-flow eruption cycles from zoned magma chambers: Bulletin Volcanologique, v. 29, p. 83–104.

_____1968, Resurgent cauldrons, *in* Coats, R. R., Hay, R. L., and Anderson, C. A., eds., Studies in volcanology—A memoir in honor of Howel Williams: Geological Society of America Memoir 116, p. 613–662.

Spera, F. J., and Crisp, J. S., 1981, Eruption volume, periodicity, and caldera area: Relationships and inferences on development of compositional zonation in silicic magma chambers: Journal of Volcanology and Geothermal Research, v. 11, no. 2–4, p. 169–187.

Steiger, R. H., and Jager, E., 1977, Subcommission on geochronology: Convention on the use of decay constants in geo- and cosmochronology: Earth and Planetary Sciences Letters, v. 36, p. 359–362.

Stormer, J. C., 1975, A practical two-feldspar geothermometer: American Mineralogist, v. 60, no. 7–8, p. 667–674.

Streickeisen, A. L., 1973, Plutonic rocks—classificaton and nomenclature recommended by the IUGS Subcommission of the Systematics of Igneous Rocks: Geotimes, v. 18, no. 10, p. 26–30.

Swanson, S. E., 1977, Relation of nucleation and crystal-growth rate to the development of granitic textures: American Mineralogist, v. 62, no. 9–10, p. 966–978.

Tuttle, O. F., and Bowen, N. L., 1958, Origin of granite in the light of experimental studies in the system $NaAlSi_3O_2$-$KAlSi_3O_8$-SiO_2-H_2O: Geological Society of America Memoir 74, 153 p.

Van der Plas, L., and Tobi, A. C., 1965, A chart for judging the reliability of point counting results: American Journal of Science, v. 263, no. 1, p. 87–90.

Vance, J. A., 1961, Zoned granitic intrusons—An alternative hypothesis of origin: Geological Society of America Bulletin, v. 72, no. 11, p. 1723–1727.

von Platen, Hilmar, 1965, Kristallisation granitischer Schmelzen: Contributions to Mineralogy and Petrology, v. 11, p. 334–381.

Waldbaum, D. R., and Thompson, J. B., 1969, Mixing properties of sanidine crystalline solutions, IV. Phase diagrams from equations of state: American Mineralogist, v. 54, no. 9–10, p. 1274–1298.

White, A. J. R., and Chappell, B. W., 1977, Ultrametamorphism and granitoid genesis: Tectonophysics, v. 43, p. 7–22.

Wing, L. A., 1959, An aeromagnetic and geologic reconnaissance survey of portions of Penobscot, Piscataquis, and Aroostock Counties, Maine: Maine Geological Survey GP [Geophysical] and G [Geological] Survey no. 4, 7 p., illustrations including geologic map.

Wones, D. R., 1966, Mineralogical indicators of relative oxidation states of magmatic systems (abs.): Transactions of American Geophysical Union, v. 47, no. 1, p. 216.

_____1972, Stability of biotite: A reply: American Mineralogist, v. 57, p. 316–317.

_____1979, Norumbega fault zone, Maine, *in* Turner, M. L., compiler, Summaries of technical reports, volume IX, National Earthquake Hazards Reduction Program: U.S. Geological Survey Open-File Report 80–6, p. 90.

Wones, D. R., and Dodge, F. C. W., 1977, The stability of phlogopite in the presence of quartz and dipside, *in* Fraser, D. G., ed., Thermodynamics and geology: Reidel Dortrecht, p. 229–247.

Wones, D. R., and Eugster, H. P., 1965, Stability of biotite: Experiment, theory, and application: American Mineralogist, v. 50, no. 9, p. 1228–1272.

Wones, D. R., and Stewart, D. B., 1976, Middle Paleozoic regional right-lateral strike-slip faults in central coastal Maine (abs.): Geological Society of America, Abstracts with Programs, v. 8, no. 2, p. 304.

Wright, T. L., 1968, X-ray and optical study of alkali feldspar, II. An X-ray method for determining the composition and structural state from measurement of 2θ values for three reflections: American Mineralogist, v. 53, no. 1–2, p. 88–104.

Wright, T. L., and Doherty, P. C., 1970, A linear programming and least squares computer method for solving petrologic mixing problems: Geological Society of America Bulletin, v. 81, no. 7, p. 1995–2007.

Wright, T. L., and Stewart, D. B., 1968, X-ray and optical study of alkali feldspar, I. Determination of composition and structural state from refined unit-cell parameters and *2V*: American Mineralogist, v. 53, no. 1–2, p. 38–87.

Zartman, R. E., and Gallego, M. D., 1979, USGS(D)-ORA-301 [Sample 142], *in* Marvin, R. F., and Dobson, S. W., 1979, Radiometric ages: Compilation B, U.S. Geological Survey: Isochron/West, no. 26, p. 19.